

HYDROCARBON CONTAMINATION EVALUATION OF RIVER SEDIMENT
FROM THE LOWER FOX RIVER, WISCONSIN

A Thesis

by

CHASE SAMUEL BREWSTER

Submitted to the Office of Graduate and Professional Studies
Texas A&M University
in partial fulfillment of the requirements for the degree of

MASTER OF SCIENCE IN PUBLIC HEALTH

Chair of Committee,
Committee Members,
Head of Department,

Thomas J. McDonald
Leslie Cizmas
Bruce Herbert
Virender K. Sharma

August 2015

Major Subject: Environmental Health

Copyright 2015 Chase Samuel Brewster

ABSTRACT

The Lower Fox River is a thirty-nine mile section which supports approximately 270,000 rural inhabitants across eighteen counties, 303,000 metropolitan residents in Green Bay and Appleton, Wisconsin, and several large industrial complexes such as paper mills and power plants. The purpose of this study was twofold, a) to characterize aliphatic and aromatic hydrocarbon distribution and concentration in the Lower Fox River and b) to identify the sources of hydrocarbon contamination.

To quantify hydrocarbon contamination and distribution, nine cores were sampled downstream of the DePere Dam. Samples were analyzed for total organic carbon (TOC) using a Leco CR-412 total carbon analyzer and n-alkanes and polycyclic aromatic hydrocarbons using a gas chromatography - mass spectrometry (GC/MS).

Percent TOC values were between 0.73% and 19.9% with an average value of 6.79%. Total n-alkanes ranged from 3.96 $\mu\text{g/g}$ to 523 $\mu\text{g/g}$ and showed a strong presence of odd carbon-numbered n-alkane ratios (range of C25 to C35) which indicates the source input from terrestrial biomass. The mean polycyclic aromatic hydrocarbon (PAH) concentration was 24,800 ng/g. High molecular weight PAH (HWM PAH) concentrations dominated the distribution of hydrocarbon contaminants. River sediment samples nearest to the DePere dam contained the highest PAHs levels at 63,600 ng/g and 56,700 ng/g, respectively. Cross-plots of PAHs were used to compare diagnostic source ratios of: benzo[a]pyrene (BaA), chrysene (Chy), fluoranthene (Fl), pyrene (Py), anthracene (An), phenanthrene (Phe), indeno[1,2,3-cd]pyrene (PI), and

benzo[g,h,i]pyrene (BgP) by depth and area. PAH ratios varied slightly with the core depth. Deeper core sections indicated presence of biomass combustion while the upper core sections indicated combustion of both petroleum and biomass. PAH distribution was irrespective of sampling zones. PAH and n-alkane data established primary influxes from both natural and anthropogenic pyrogenic activities. A toxicological evaluation quotient (TEQ) was calculated for the Lower Fox River core sections revealing the most elevated PAH concentrations at 2295 ng/g-dry (649 ng/g-wet), 1695 ng/g-dry (898 ng/g-wet), and 2,438 ng/g-dry (829 ng/g-wet). Core section concentrations exceeded the Comprehensive Environmental Response, Compensation, and Liability Act (CERCLA) Method B cleanup level for benzo(a)pyrene of 137 ng/g. A secondary evaluation, using the Wisconsin Department of Natural Resources' (WDNR) threshold effect concentration (TEC), normalized sample concentrations to 1% TOC. After normalization, sample concentrations totaled 1520 ng/g-dry, 1073 ng/g-dry, and 492 ng/g-dry. PAH concentrations did not exceed WDNR TEC for PAHs at 1,610 ng/g at 1% TOC implying remediation is not presently required and river sediments currently have minimal adverse effects.

DEDICATION

This work is dedicated to my loving wife, Amanda Jo. Without her loving support, patience and encouragement; this manuscript would not be possible. Her knowledge and assistance with editing allowed us to suffer less together on those many sleepless nights. Amanda Jo, I love you with all my heart. Thank you for allowing me to achieve my dream.

I would also like to dedicate this to my family, especially my parents, Joseph and Toby Brewster. Without their love and compassion, I would not be where I am today.

To my chair of committee, mentor and friend, Dr. Thomas McDonald, thank you for the inspiration and the years of tolerance. I would not have taken these steps without your encouragement and support.

ACKNOWLEDGEMENTS

I would like to thank my committee chair Dr. McDonald, and my committee members Dr. Cizmas, and Dr. Herbert for their guidance and support throughout the course of this research.

I would like to thank Texas A&M University Health Science Center, School of Public Health faculty and staff for making my time at Texas A&M University a lasting and fulfilling experience.

I would like to thank B&B Laboratories for providing me with knowledge, instrumentation, supplies, and laboratory space. To Dr. James M. Brooks and Dr. Bernie B. Bernard, thank you for allowing me the time and space to accomplish my dreams. I want to extend my gratitude to Mrs. Yiwei Miao, who provided me with her knowledge in polycyclic aromatic hydrocarbons, understanding of chromatography, and the layout of ChemStation which can be rather intimidating; and Mr. Michael Gaskins, for assisting me with GC/MS injections and instrumentation insight.

Finally, I would like to Dr. Hilary Agbo, Mrs. Ame Brewster, Mr. Christopher Rohloff, and Mrs. Susan Wolff for their diligence in reviewing my manuscripts for errors and inconsistencies.

NOMENCLATURE

ALI	Aliphatic Hydrocarbons
An	Anthracene
AOC	Area of Concern
BaA	Benzo[a]anthracene
BaP	Benzo[a]pyrene
BgP	Benzo[g,h,i]perylene
Chy	Chrysene
CCC	Continuous Calibration Check
CERCLA	Comprehensive Environmental Response, Compensation, and Liability Act
Dupl.	Duplicate
Fl	Fluoranthene
GC/MS	Gas Chromatography - Mass Spectrometry
HMW	High Molecular Weight
ICal	Initial Calibration
LMW	Low Molecular Weight
mAn	Methylantracene
mPhe	Methylphenanthrene
MS	Matrix Spike
MSD	Matrix Spike Duplicate
NIST	National Institute of Standards and Technology

NRT	Natural Resource and Technology
PAH	Polycyclic Aromatic Hydrocarbon
PCBs	Polychlorinated Biphenyls
Pe	Perylene
Ph	Phytane
Phe	Phenanthrene
PI	Indeno[1,2,3-cd]pyrene
POPs	Persistent Organic Pollutants
Pr	Pristane
Py	Pyrene
QA	Quality Assurance
QC	Quality Control
SIM	Selective Ion Monitoring
SRM	Standard Reference Material
TALI	Total Aliphatic Hydrocarbons
TEC	Threshold Effect Concentration
TEQ	Toxicological Evaluation Quotient
TOC	Total Organic Carbon
TPAH	Total Polycyclic Aromatic Hydrocarbons
TPH	Total Petroleum Hydrocarbons
TRH	Total Resolved Hydrocarbons
UCM	Unresolved Complex Mixture

USEPA United States Environmental Protection Agency

WDNR Wisconsin Department of Natural Resources

TABLE OF CONTENTS

	Page
ABSTRACT	ii
DEDICATION	iv
ACKNOWLEDGEMENTS	v
NOMENCLATURE.....	vi
TABLE OF CONTENTS	ix
LIST OF FIGURES.....	xi
LIST OF TABLES	xii
1. INTRODUCTION.....	1
2. LITERATURE REVIEW.....	4
2.1. Polycyclic Aromatic Hydrocarbons	5
2.2. Saturated Hydrocarbons	11
3. OBJECTIVES	14
4. METHODS AND MATERIALS	16
4.1. Sampling.....	16
4.2. Sample Processing and Dry Weight Determination.....	18
4.3. Extraction Process	20
4.4. Total Organic Carbon Analysis.....	22
4.5. Gas Chromatography - Mass Spectrometry	23
4.6. Quality Assurance and Quality Control	24
4.7. Toxicological Evaluation	27
4.8. Diagnostic Comparisons	29
5. RESULTS AND DISCUSSION	32
5.1. Total Organic Carbon.....	32
5.2. Extracted Organic Material	32

5.3. Saturated Hydrocarbons	33
5.4. Polycyclic Aromatic Hydrocarbons	40
5.5. Toxicological Evaluation	58
6. CONCLUSIONS AND IMPLICATIONS OF RESEARCH.....	61
REFERENCES.....	64
APPENDIX A	68
APPENDIX B	102

LIST OF FIGURES

	Page
Figure 1 Lower Fox River, Green Bay, Wisconsin Sampling Location	3
Figure 2 Lower Fox River Sampling Areas and Core Sites	17
Figure 3 Total Petroleum Hydrocarbon Cross-plots	37
Figure 4 Total n-Alkanes versus Total Petroleum Hydrocarbons	39
Figure 5 Ring Distribution of PAHs as Percent Total PAHs by Core Section	41
Figure 6 Alkylated Methylphenanthrenes and 2-Methylanthracene	43
Figure 7 PAHs Diagnostic Cross-plots; Indications of PAH Source	48
Figure 8 Diagnostic Cross-plot of An/(An+Phe) versus Fl/(Fl+Py) by Depth	52
Figure 9 Diagnostic Cross-plot of An/(An+Phe) versus PI/(PI+BgP) by Depth	53
Figure 10 Diagnostic Cross-plot of An/(An+Phe) versus Fl/(Fl+Py) by Area	55
Figure 11 Diagnostic Cross-plot of An/(An+Phe) versus PI/(PI+BgP) by Area	57

LIST OF TABLES

		Page
Table 1	Sample Extract Parameters: PAH, ALI-TPH, and EOM Analysis	19
Table 2	Polycyclic Aromatic Hydrocarbon Ratios.....	30
Table 3	Aliphatic Hydrocarbon Ratios.....	30
Table 4	Other Diagnostic Ratios	31
Table 5	Distribution of Contaminants	34
Table 6	Methylphenanthrene and 2-Methylanthracene with Ratios.....	44
Table 7	PAH Diagnostic Ratios for Benzo[a]pyrene (BaA), Chrysene (Chy), Fluoranthene (Fl), Pyrene (Py), Anthracene (An), Phenanthrene (Phe), Indeno[1,2,3-cd]pyrene (PI), and Benzo[g,h,i]pyrene (BgP).....	46
Table 8	Diagnostic Cross-plot of Fl/(Fl+Py), An/(An+Phe), and PI/(PI+BgP) by Area	54
Table 9	Toxic Equivalency Factors for Lower Fox River Core Section FRDJ-SED-3-03-12 (Area 3)	59

1. INTRODUCTION

Polycyclic aromatic hydrocarbons (PAHs) are a group of ubiquitous environmental compounds with persistent toxic abilities known to bioaccumulate in the environment due to slow decomposition. PAHs are classified as persistent organic pollutants (POPs) by the United States Environmental Protection Agency (USEPA). POPs are defined as any chemical resistant to biodegradation which is produced intentionally or unintentionally for agricultural use, disease control, manufacturing, or industrial processes; or as a byproduct of industrial processes or combustion (i.e., automotive and factory exhaust) (USEPA 2014).

PAHs are a group of organic contaminants which are the result of incomplete combustion of organic materials (Ramírez et al. 2011). The toxic effects of PAHs on human health are known to include: mutagenicity, teratogenicity, immunogenicity, and carcinogenicity. PAHs such as benzo[a]pyrene can increase the risk of skin, lung, bladder, liver, and stomach cancers. Additionally, PAHs have been known to cross the placental boundary suggesting that a fetus is 10 times more vulnerable to PAH-induced DNA damage than the offspring's mother (Herbstman et al. 2012). Despite the associated dangers, several industrial processes produce PAHs and other hydrocarbons during manufacturing processes as a byproduct.

The purpose of this study is twofold, a) to characterize aliphatic and aromatic hydrocarbon distribution and concentration in the Lower Fox River and b) to identify the sources of hydrocarbon contamination through forensic fingerprinting of chemical

constituents. The Lower Fox River is a thirty-nine mile section located in east Wisconsin (**Figure 1**). Starting at the Menasha and Neenah channels, the Lower Fox River flows northeast where it discharges into the Green Bay and Lake Michigan basin. The watershed of the Lower Fox River supports approximately 270,000 rural inhabitants in eighteen counties, 303,000 metropolitan residents, and several large industrial complexes within the urban cities of Green Bay and Appleton (USEPA 2013). Despite the high probability of hydrocarbon contamination (Uhler et al. 2005), limited literature can be found on the distribution of hydrocarbons within the Lower Fox River. In order to identify the hydrocarbon levels and distribution, nine three-foot cores were collected from a river location. Cores were sampled below the DePere Dam to analyze for hydrocarbons with respect to location and depth.

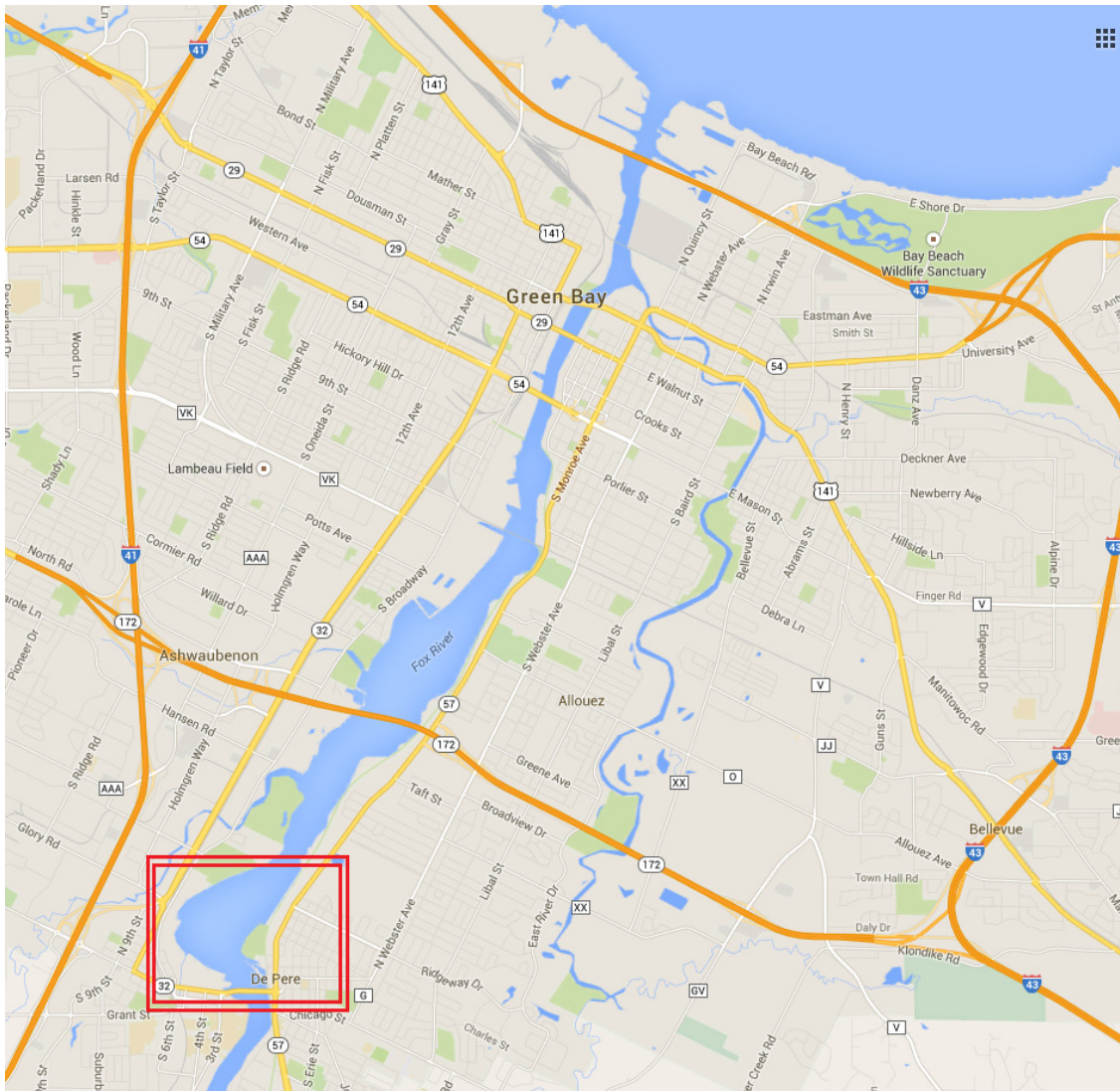


Figure 1: Lower Fox River, Green Bay, Wisconsin Sampling Location. (Google Maps 2015)

2. LITERATURE REVIEW

Due to the prevalent nature of PAH compounds and saturated hydrocarbons, identification of their sources can be difficult to determine, particularly adjacent to urban areas (Uhler et al. 2005). However, after the United States passed the Clean Water Act in 1972, the USEPA integrated aspects of hydrocarbon fingerprinting from geochemical exploration techniques. These techniques were modified specifically to assist in environmental monitoring and evaluation, and to establish a means to assess and remediate areas of concern (AOC) (Boehm et al. 1997). Hydrocarbon evaluations classify molecular and isotopic characteristics of pollutants within an AOC by examining the progression of weathering and the identification of hydrocarbon source (Boehm et al. 1997). Hydrocarbon contamination consists of complex mixtures of PAHs, saturated hydrocarbons, and polar compounds. Analysts can chemically fingerprint potential hydrocarbon sources by examining the concentration of individual hydrocarbon compounds present in organic material and their byproducts (Boehm et al. 1997 and Prince and Walters 2007). By evaluating the relative abundance of these compounds, differences and similarities can be identified among distinct fuels, refined products, manufactured products, and byproducts with respect to product-parent relationships (Boehm et al. 1997 and Uhler et al. 2005).

2.1. Polycyclic Aromatic Hydrocarbons

PAHs are a group of ubiquitous compounds generated by the incomplete combustion of refined fuel, coal, tar, oil, and other organic material. PAHs are known to be produced naturally by organic degradation, forest fires, and volcanic activities. However, anthropogenic production such as industrial emissions is the most common source of PAHs due to human utilization of petroleum products and combustion of organic matter (ATSDR 1995). PAHs are not found in the environment as individual compounds, but rather as mixtures consisting of at least two fused carbon-carbon rings with alternating double and single bonds (i.e., benzene rings) (Uhler et al. 2005). These arrangements can differ with alignment and number of rings. Naphthalene is the most basic PAH compound, consisting of two fused benzene rings.

2.1.1. Formation of PAHs

PAHs are classified as pyrogenic, petrogenic, or biogenic/diagenetic. Pyrogenic PAHs are the result of incomplete combustion of coal, petrochemicals, wood, and other organic materials at high temperatures over a short period of time. Due to this formation process, pyrogenic PAHs tend to have a source signature that contains predominantly higher molecular weight (HMW PAHs) and parent PAH analytes. Pyrogenic alkylated PAHs tend to decrease in abundance with respect to an increasing degree of alkylation (i.e., C0 (parent) > C1 > C2 > C3 > C4). In contrast to pyrogenic PAHs, petrogenic PAHs are the result of a lengthy application of low heat over millions of years. Petrogenic PAH sources primarily consist of lower molecular weight PAHs (LMW

PAHs) with little to no HMW PAHs. Petrogenic PAHs have a higher concentration of alkyl groups in comparison to the parent PAHs (Uhler et al. 2005). Anthropogenic activities such as automotive combustion and urbanization are the leading contributors to petrogenic and pyrogenic PAH contamination. Biogenic PAHs are produced by biological creation and degradation of organisms, a process also known as diagenesis (Uhler et al. 2005 and Bastami et al. 2014). Common biogenic PAHs, such as perylene, are found in sediments preceding anthropogenic activities. Perylene is a five-ringed PAH compound found in high concentrations in early stages of degradation in terrestrial soils, river and lake sediments, and anoxic marine environments and swamps. The concentration of perylene can be used as a parameter to determine diagenesis and flora influx (Iqbal, Overton, and Gisclair 2008a; Iqbal, Overton, and Gisclair 2008b; and Boehm et al. 1997). However, biogenic PAHs have also been discovered in more recent deposits due to industrial processes such as petroleum refining (Mount, Ingersoll, and McGrath 2003).

2.1.2. Degradation of PAHs

Sediments tend to show an even distribution of LMW PAHs to HMW PAHs over time in sedimentary deposition. However, due to high anthropogenic influxes, six-ring and five-ring PAHs have a higher abundance in soils and sediments in major rivers, urban areas, and industrial complexes when compared to LMW PAH abundance (i.e., 6-ring > 5-ring > 4-ring > 3-ring > 2-ring) (Iqbal, Overton, and Gisclair 2008b). Degraded samples with high concentrations of HMW PAHs relative to LMW PAHs are a potential

indication of pyrogenic activities but, this can also be an indication of highly degraded oils or high-rank coals (Yunker et al. 2002 and Liu et al. 2009). In contrast, samples with high concentrations of LMW PAHs are a potential indication of petrogenic incursion or low-ranking coal (Bence, Page, and Boehm 2007). Like petroleum, some coals are dominated by 2-ring PAHs which can lead to misidentification of contributing sources due to increased PAH and total petroleum hydrocarbon (TPH) concentrations (Uhler, Stout, and Douglas 2007).

Degradation of PAHs can be attributed to weathering, evaporation, microbial degradation, molecular reconfiguration, and photoreactivity. Analytes degrade following a reduction in concentration with an increase in alkylation state (Uhler et al. 2005). Chemically, parent and alkylated compounds can be a significant indication of source based on C0 (parent) - C1 - C2 - C3 - C4 characteristics and abundance. For example, biodegradation of crude oils and petrochemical products follow a typical degradation pattern with respect to molecular weight and structure (Bence, Page, and Boehm 2007). Parent PAH compounds degrade more rapidly in comparison to their alkylated counterparts (i.e., C0 > C1 > C2 > C3). The reduction of C0 - C2 indicates degradation in each PAH group as individual concentrations decrease in abundance (Prince and Walters 2007 and Bence, Page, and Boehm 2007).

2.1.3. Analytical Comparison of PAHs

The primary indicators of formation are individual PAH analyte concentrations. The understanding of formation parameters and degradation patterns allows the analyst

to chemically fingerprint potential sources based on their distinct compound signatures (Uhler et al. 2005). Diagnostic ratios of parent components can be used to interpret the characteristics of specific PAH isomers based on their stability and the temperature at which the analyte was created. The relative stability of isomers and their associated alkylated compounds provide a basis for high versus low heat ratio comparisons, which further provide an indication of formation based on their variation (Yunker et al. 2002). Concentrations of HMW PAHs such as fluoranthene, pyrene, benzopyrenes, indeno[1,2,3-c,d] pyrene, dibenzo[a,h]anthracene, and benzo[g,h,i]perylene are usually not detectable or only exist in low concentrations in petrogenic sources. However, petrogenic sources are dominated by lower molecular weight 2- and 3-ring PAHs (Uhler, Stout, and Douglas 2007). Because LMW PAHs are prevalent within both pyrogenic and petrogenic mixtures, the use of HMW PAH compounds are more viable for source identification (Uhler, Stout, and Douglas 2007).

2.1.3.1. Methylphenanthrene versus Methylanthracene

Methylphenanthrene versus methylanthracene (m/z 192) is a viable analytic comparison used to identify source. Methylphenanthrenes are formed over long periods of time (e.g., geological heating and time scale) (Uhler et al. 2007). In contrast, methylanthracenes are produced through rapid heating and are primarily found in pyrogenic materials, particularly 2-methylanthracene. Low-rank coals contain 2-methylanthracene, but as the coals increase in ranking the concentration of 2-methylanthracene is decreased in comparison to methylphenanthrenes. The absence or

low concentration of 2-methylanthracene is also typical in most crude oils when compared to the concentration of methylphenanthrenes. As a result, if the abundance of 2-methylanthracene is comparable to the abundance of methylphenanthrenes, the contamination is an indication of altered petrogenic source (e.g., combustion or refinement) (Wilhelms et al. 1998). Thus, the elevated presence of 2-methylanthracene in the cores or sediments would be a significant indication of a pyrogenic PAH source. Additionally, the presence of both stable and unstable methylphenanthrenes is an example of pyrogenic activity. Generally, the 3- and 2-methylphenanthrene isomers are more stable than 9-, 4-, and 1-methylphenanthrene. Thus, the lower the concentration of less stable methylphenanthrenes, the greater the likelihood of unrefined, aged fossil fuels (i.e., petrogenic incursion) (Uhler et al. 2007).

Another constituent of PAHs which can assist in the differentiation between natural and petrogenic PAH sources is perylene. Perylene is commonly recognized as a naturally occurring, diagenetic PAH. The relative abundance of perylene versus $\Sigma 5$ -ring PAHs can be used to distinguish between natural hydrocarbon contribution and petroleum contamination (Bence, Page, and Boehm 2007).

2.1.3.2. Diagnostic Ratios of PAHs

Considering that phenanthrene and anthracene (m/z 178) and fluoranthene and pyrene (m/z 202) have relatively the same stability and molecular mass/heat formation calculations, the comparative ratios of m/z 178 and m/z 202 can be used to interpret PAH source (Yunker et al. 2002). Cross-plotting PAHs is a typical oil geochemistry

method developed to identify PAH sources. Commonly, ratios such as anthracene / (anthracene + phenanthrene), indeno[1,2,3-c,d]pyrene / (indeno[1,2,3-c,d]pyrene + benzo[g,h,i]perylene), benzo[a]anthracene / (benzo[a]anthracene + chrysene), anthracene / (anthracene + chrysene), fluoranthene / (fluoranthene + pyrene) have been used to determine source.

Generally, an An / (An + Phe) ratio is used to distinguish between petroleum contamination (less than 0.1) or pyrogenic origin (greater than 0.1). Fl / (Fl + Py) and PI / (PI + BgP) ratios provide indications of fuel source. A value of less than 0.4 is consistent with petroleum pollution; between 0.4 and 0.5 is an indication of petroleum combustion (e.g., gasoline and diesel combustion); and greater than 0.5 signals biomass combustion (e.g., grasses, wood, or coal combustion) (Yunker et al. 2002). BaA / (BaA + Chy) ratio provides an understanding of coal variations. Comparatively, values less than 0.23 are an indication of low-weight coal combustion. By contrast, bituminous coal has a ratio greater than 0.29. The ratio of BaA / (BaA + Chy) can also be used to differentiate between a petrogenic source (less than 0.20) and a pyrogenic source (greater than 0.35) (Dvorská, Lammel, and Klánová 2011).

However, individual analyte ratios are poor indicators of mixed input sources (Bastami et al. 2014). Despite the attempt to isolate the primary source of PAHs, single ratios can overlap restricting the analyst's ability to distinguish between biomass and petroleum combustion. For instance, Fl / (Fl + Py) between 0.20 - 0.50 could include indications of gasoline (0.44) and diesel combustion (0.20 - 0.58), wood combustion (0.41 - 0.67), transit runoff from road dust and automotive/diesel oils (0.30 - 0.37), and

roadway tunnel exhaust (0.41 - 0.49) (Yunker et al. 2002). By implementing a cross-plot comparison, multiple single indicators are cross referenced within the same graph which provides a more thorough interpretation. By comparing $An / (An + Phe)$ versus $Fl / (Fl + Py)$, the two ratios depict a better understanding of primary and secondary PAH sources. The cross-plot of $BaA / (BaA + Chy)$ versus $Fl / (Fl + Py)$ compares two sets of ratios to determine whether the source is pyrogenic or petrogenic. The cross-plot of $BaA / (BaA + Chy)$ versus $Fl / (Fl + Py)$ can also compare individual fuel signatures (i.e., gasoline or combusted gasoline, coal or combusted coal). Because of this comparable overlap, comprehensive evaluation can specify the individual fuel source (i.e., gasoline or combusted gasoline, coal or combusted coal) (Bastami et al. 2014).

2.2. Saturated Hydrocarbons

Alkanes are a specific class of saturated hydrocarbons, also known as saturated aliphatics (ALI), found in sap, wax, and as a major component of fossil fuels. Alkane characteristics, specifically normal alkanes (n-alkanes), provide a valuable tool for evaluating potential sources and degradation progression (Wang et al. 2007). For example, a predominance of odd carbon-numbered n-alkanes within the range of C25 to C35 can be an indication of both terrestrial flora and microalgae input (Lichtfouse et al. 1994). Due to the physical properties of n-alkanes, degradation occurs more rapidly in comparison to the heavier unsaturated and ringed hydrocarbons. The light weight n-alkanes, n-C1 through n-C12 aliphatics, are most commonly volatilized or removed by water flow. As degradation continues, even the heavier n-alkanes begin to break down

(Wang et al. 2007). Because hydrocarbons in the environment are subjected to weathering, aliphatic fingerprinting can be limited in resolution and accuracy.

2.2.1. Degradation of ALI

Accordingly, the loss of individualization of n-alkanes, along with other resolved hydrocarbons, causes an increase in unresolved complex mixture (UCM). The UCM is comprised of degraded hydrocarbons and bioresistant compounds within organic mixtures such as PAHs and polar compounds. Therefore, the larger the UCM the higher the degradation which can account for all of the total UCM mass or less than half the total mass of detected hydrocarbons (Prince and Walters 2007). UCM in comparison to n-alkanes can only provide an understanding of hydrocarbon abundance with respect to the complex mixture and the progression of biodegradation (Boehm et al. 1997). The UCM concentration, in comparison to total concentration of n-alkanes or PAHs, can establish a trend of degradation and an evaluation of contribution to the overall contaminant mixture. This alteration of the hydrocarbon complex limits saturated hydrocarbons to a general identification based on boiling point ranges, with respect to the remaining identifiable n-alkanes (Boehm et al. 1997).

2.2.2. Additional Diagnostic Ratios of ALI

Aliphatic hydrocarbons can be used to estimate a timeline of biodegradation. Isoprenoids such as pristane and phytane are more resistant to weathering than their n-alkane counterparts; thus, they provide an understanding of progression of degradation.

Pristane and phytane (i-C19 and i-C20) and their counterparts n-heptadecane and n-octadecane (n-C17 and n-C18) allow for the evaluation of coal and oil maturity, as well as the biodegradation progression (Shen and Huang 2007). Both n-C17/Pristane (n-C17/Pr) and n-C18/phytane (n-C18/Ph) ratios have been widely used as evaluation tools in the assessment of oil biodegradation. The n-C17/Pr and n-C18/Ph ratios provide a significant assessment tool in evaluating the biodegradation progression based on the significant loss or conversion of the n-alkane precursors. The pristane/Phytane (Pr/Ph) ratio can be used as an indication of organic origins and formation conditions. The Pr/Ph ratio helps to identify marine, organic-rich sediments, marine oils, or the combustion of marine oils and sediments under anoxic conditions with a ratio value of less than 0.8. The Pr/Ph ratio can also indicate terrestrial organic matter under oxic conditions with a ratio value greater than 3 and bituminous coals and terrestrial oils ranging from 5 to 10. However, a Pr/Ph ratio of 1.0 should be interpreted cautiously, biological influences such as pristane and phytane precursors can easily influence the Pr/Ph ratio (Powell 1998, Peters and Walters 2005, and Haven et al. 1988).

C30-hopane is a conservative analyte used to assess the biodegradation process of oil spills (Prince and Walters 2007, and Mills et al. 1999). C30-hopane can be used to evaluate degradation within the sediments, oils, coals, and other source materials serving as an indicator throughout the bioremediation process. The relative abundance of C30-hopane versus PAHs within the cores and locations can indicate levels and progression of biodegradation at each location and depth.

3. OBJECTIVES

Sediment samples will be evaluated based on the hydrocarbon concentration relative to the time of historical distribution (based on section depth). The evaluation of core samples from the Lower Fox River will quantitatively focus on hydrocarbon concentrations within river sediment to provide distinctive fingerprinting that can be used in evaluating the potential discharge source(s). The objectives of this thesis are to:

- 1) Determine hydrocarbon distribution and concentration with respect to core location and section depth. The AOC consists of the lower dam reservoir and undredged river sediment. The analysis of the collected cores could provide insight about possible upstream contributions, the redistribution of downstream sediment due to dam operations and flooding, and the potential direction of hydrocarbon source input.

- 2) Evaluate the toxicity of hydrocarbon analytes within sediment (i.e., parent and alkylated constituents). A toxicology report by the U.S. Department of Health and Human Services (USDHHS), Agency for Toxic Substances and Disease Registry (ATSDR) in 1995 *Toxicological Profile for Polycyclic Aromatic Hydrocarbons*, report number 1995-639-298 defines the following seven PAHs categorized as class B2 human carcinogens: benz[a]anthracene, benzo[a]pyrene, benzo[b]fluoranthene, benzo[k]fluoranthene, chrysene, dibenzo[a,h]anthracene,

and indeno[1,2,3-c,d]pyrene (ATSDR 1995). Analysis of 88 PAH analytes, which includes seven carcinogenic PAH components, will be quantified using Gas Chromatography-Mass Spectrometry (GC/MS) Selective Ion Monitoring (SIM).

- 3) Determine hydrocarbon source through forensic fingerprinting of the chemicals within sediment in the Lower Fox River. Quantified hydrocarbon analytes will be used to generate histograms and cross-plots in order to determine potential hydrocarbon source input.

4. METHODS AND MATERIALS

Sediment samples were provided by a third party group from Wisconsin, Natural Resource Technologies (NRT). These samples were collected upstream from US Paper and Georgia-Pacific paper mills within the metropolitan area of Green Bay, Wisconsin. To ensure good representation of hydrocarbon input, sample sites were selected in areas that had not been influenced by discharge zones. In the lower quadrant, sampling areas such as US Paper Mills and Georgia-Pacific were avoided due to the potential high concentration of hydrocarbon refuse. Dredging was conducted in the lower river quadrant to remove high concentrations of polychlorinated biphenyls (PCBs) from 2009 through 2012 in order to fulfill the Fox River remedial action (RA) requirements set by USEPA. Viable sampling locations were selected in areas that had not been dredged.

4.1. Sampling

Cores were obtained from a sampling zone below the DePere Dam and consisted of three different sampling areas (e.g., area 1, area 2, and area 3) (**Figure 2**). Three cores were collected from each area of interest using a vibracore system. Each core collected had to surpass the required minimum length of three feet four inches. If the core length was not satisfactory, the sample was discarded and the disposable core liner was replaced. The core liner was then rinsed with river water prior to relocation and further sample acquisition.

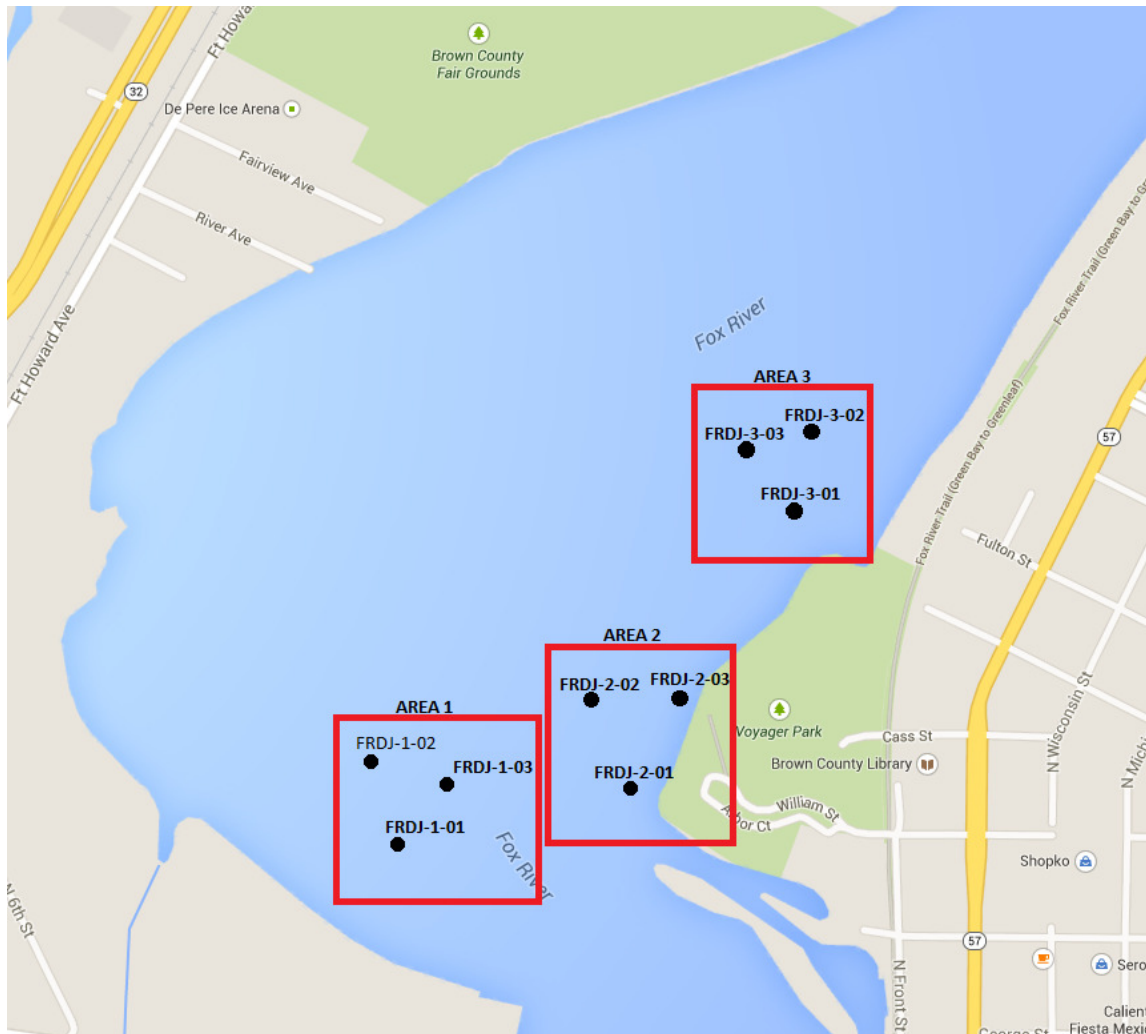


Figure 2: Lower Fox River Sampling Areas and Core Sites. (Google Maps 2015)

The purpose of these core samples was to establish current and historical input of anthropogenic and natural hydrocarbons, concentration, and source input. Cores were divided into three, one-foot sections and labeled "Fox River Department of Justice (FRDJ) - Matrix (SED) -"area#"-"core#"-"section starting inch mark" (i.e., area 1, core 1 top section = ID: FRDJ-SED-1-01-01). If the collected core was longer than three feet

and four inches the remainder was labeled '3T'. Each section was placed into a gallon Ziploc bag and labeled by: core identifier, section number, site location, and collection date. Samples were frozen and shipped via FedEx. Samples were received by the laboratory on 26 July 2012. Custody seals were present and intact upon receipt, and chain of custody (CoC) records accompanied each cooler. The coolers did not contain a temperature blank; however, the internal temperatures of the coolers ranged from -0.2 - 0.0°C, well within the acceptable range for sediments of $4^{\circ}\text{C} \pm 2^{\circ}\text{C}$. Samples were stored in a -20°C freezer prior to analysis.

4.2. Sample Processing and Dry Weight Determination

Samples were homogenized prior to subsampling. Pre-cleaned sixteen ounce clear jars were used for the 'wet' sample aliquot and pre-cleaned eight ounce clear jars were used for 'dry' aliquot. The original sample and 'wet' aliquot were then returned for archive in a -20°C freezer. Wet weight determination was obtained by pre-weighing a 57mm aluminum pan (recorded), and weighing approximately one gram of sample into the pan. Samples were then dried at 105°C and checked twice over the next two days (recorded) (**Table 1**). After percent moisture was determined, a subsample of each sample was placed in a 40°C forced-air oven until dry. Due to the polar nature of the extraction solvent, dichloromethane (DCM), water within the samples is removed prior to extraction. Samples were then pulverized using a mortar and pestle.

Table 1: Sample Extract Parameters: PAH, ALI-TPH, and EOM Analysis. % dry weight, and % wet weights with no wet weight, % dry weight, or % wet weight is available for FRDJ-SED2-03A-01U.

Sample Name	Sample Dry Weight (g)	Sample Wet Weight (g)	% Dry	% Moisture
FRDJ-SED-1-01-01	15.1	24.4	38	62
FRDJ-SED-1-01-12	15.0	24.6	38	62
FRDJ-SED-1-01-23	15.0	34.8	30	70
FRDJ-SED-1-02-01	15.0	32.7	32	68
FRDJ-SED-1-02-12	15.1	41.1	27	73
FRDJ-SED-1-02-23	15.1	46.6	24	76
FRDJ-SED-1-03-01	15.0	56.6	21	79
FRDJ-SED-1-03-12	15.0	39.0	28	72
FRDJ-SED-1-03-23	15.2	31.9	32	68
FRDJ-SED-2-01-01	15.0	35.5	30	70
FRDJ-SED-2-01-12	15.1	31.8	32	68
FRDJ-SED-2-01-23	15.2	40.0	28	72
FRDJ-SED-2-02-01	15.0	36.2	29	71
FRDJ-SED-2-02-12	15.1	40.0	27	73
FRDJ-SED-2-02-23	15.1	35.1	30	70
FRDJ-SED-2-02-3T	15.1	38.1	28	72
FRDJ-SED-2-03A-01	15.2	19.5	44	56
FRDJ-SED-2-03A-12	15.0	28.4	35	65
FRDJ-SED-2-03A-23	15.1	17.1	47	53
FRDJ-SED-2-03A-3T	15.0	25.1	37	63
FRDJ-SED-3-01-01	15.1	7.90	66	34
FRDJ-SED-3-01-12	15.1	16.2	48	52
FRDJ-SED-3-01-23	15.1	5.60	73	27
FRDJ-SED-3-01-3T	15.1	10.7	59	41
FRDJ-SED-3-02-01	15.0	27.2	36	64
FRDJ-SED-3-02-12	15.2	15.8	49	51
FRDJ-SED-3-02-23	15.1	13.8	52	48
FRDJ-SED-3-02-3T	15.1	5.50	73	27
FRDJ-SED-3-03-01	15.1	50.8	23	77
FRDJ-SED-3-03-12	15.0	28.9	34	66
FRDJ-SED-3-03-23	15.2	8.10	65	35
FRDJ-SED-3-03-3T	15.0	18.0	45	55
FRDJ-SED-2-03A-01U	0.80	N/A	N/A	N/A

4.3. Extraction Process

Using a top loading balance, 15 grams of dry sediment were weighed into a stainless steel extraction cell (**Table 1**). 100 μ l of PAH and aliphatic (ALI) surrogates were added to each sample prior to extraction. PAH-saturated biomarker surrogate contained naphthalene-d8, acenaphthene-d10, phenanthrene-d10, chrysene-d12, perylene-d12, and 5 β (H)-cholane. ALI surrogate contained n-dodecane-d26, n-eisocane-d42, and n-triacontane-d62. Quality control samples (method blank, matrix spike, matrix spike duplicate, and laboratory duplicate sample) and National Institute of Standards and Technologies (NIST) SRM 1941b were also prepared with the appropriate surrogate and spike volumes. Using an Automated Solvent Extractor (Automated Solvent Extractor 200, Thermo Scientific Dionex, CA) samples were extracted using 100% DCM (>99.8% purity chromatography grade, ECD Millipore Corporation, Darmstadt, Germany) at 100°C and 1500 PSI into pre-cleaned 60 mL collection vials. Extracts were concentrated to 3-5 mL using a hot water concentration bath. Copper was used to remove sulfur. Extracts were then transferred into Kuderna-Danish (K-D) concentration tubes and the copper and vial were rinsed with DCM a minimum of three times to remove any residual extract. K-D tubes were returned to a water bath to reduce the extract volume to 3 mL.

4.3.1. Extracted Organic Material Determination

Extracted Organic Material (EOM) determination was obtained by verifying each sample at a volume of 3 mL. VWR 2.4 cm glass microfiber filters were placed in a 40°C oven on solvent cleaned stainless steel screens. Accuracy and range were verified by checking a DCM solvent blank. A filter was pre-weighed on a microbalance, with sensitivity to approximately 0.001 mg and the initial weight was recorded. The filter was placed in a 40°C oven and 100 µl of DCM was applied to the filter. The filter remained in the oven for two minutes after which the filter was then weighed a second time, verifying a weight equal to 0.000 mg. An EOM standard was used to check high range by pre-weighing a filter. The initial weight was recorded. The filter was placed in the 40°C oven and 100 µl of oil solution was applied to the filter. The filter remained in the oven for two minutes and the filter was weighed a second time, verifying a weight equal to 10.000 mg ± 0.500. Each extracted sample was processed accordingly. The method blank was verified with required criteria of 0.000 mg + 0.003. EOMs were calculated using **Equation 1**. Duplicate relative percent difference (RPD) was recorded to within 25%.

$$\text{(Equation 1) } EOM (\mu\text{g/g}) = [(We \times Vf) / (Ws \times Va)] \times (1000\mu\text{g} / 1\text{mg})$$

Where: *We* is the residual weight of EOM aliquot (mg), *Ws* is sample weight (g), and *Vf* is volume of sample extract (3000 µL), and *Va* is volume of aliquot (100 µL).

4.3.2. Sample Cleanup and Final Concentration

To remove interferences such as pigments, sulfur oxide residuals, and large non-polar residues, samples were passed through silica gel, alumina, copper, and sodium sulfate. Extracts were run through a 6 mL solid phase extractor column (Resprep Normal Phase SPE Cartridge 6 mL 1000 mg silica, Restek, Bellefonte, PA) layered with one gram of alumina, one gram of silica gel, one centimeter of sodium sulfate, and one centimeter of copper. Using a vacuum pump system, the extract was processed through the cleanup column followed by 40 - 50 mL of DCM. Extracts were collected in pre-cleaned 60 mL collection vials. Filtered extracts were concentrated to 3 - 5 mL using a hot water concentration bath and transferred to K-D tubes. K-D tubes were returned to the water bath to reduce the extract volume to 800 μ L. Internal Standards were added to each sample. PAH-saturated biomarker internal standards were fluorene-d10, pyrene-d10, and benzo[a]pyrene-d12. ALI internal standards were n-hexadecane-d34 and 5 α -androstane. Extracts were adjusted to a final volume of 1 mL and then transferred to graduated 2 mL amber vials. Extracts that contained high EOM concentrations were adjusted by dilution using dichloromethane before GC/MS analysis. Additional surrogates and internal standards were added based on dilution factors.

4.4. Total Organic Carbon Analysis

TOC analysis is used to evaluate the percent of organic carbon in soils and sediment samples. Organic carbon input is generated by several sources: hydrocarbons, coals, vegetation (humic acid), microorganisms, and anthropogenic input. TOC is

determined using a carbon analyzer (CR-412 Total Carbon Analyzer, Leco, St. Joseph, MI). NRT sediment samples were dried at 105°C to remove interstitial water. Dry sediment was then weighed at 350 mg into carbon-free, tared ceramic crucibles. A diluted phosphoric acid solution (50% by volume ratio) was added to remove any inorganic carbon within the material, such as calcium carbonate (CaCO₃) within the material. Samples were then returned to the oven for a minimum of 16 hours to remove the excess water. Following quality assurance (QA) and quality control (QC) criteria, method blanks, SRMs, duplicates and continuous calibration checks (CCC) were used to ensure quality and accuracy. Each sample was individually analyzed at 1350°C for a maximum duration of 180 seconds. The Leco CR-412 produced results in percent carbon (%C) based on sample weight and response (area times peak). Data was converted into an Excel report file calculating milligrams of carbon based on percent carbon and sample mass.

4.5. Gas Chromatography - Mass Spectrometry

After final concentration was attained, extracts were analyzed for PAH and aliphatic hydrocarbon concentrations using a HP5890 gas chromatograph (HP5890, Hewlett Packard Company, Wilmington, DE) coupled with an Agilent 5972 mass spectrometer (Agilent 5972, Agilent Technologies, Santa Clara, CA). A HP-5MS capillary column (Agilent HP-5MS 60 m long with an interior diameter of 0.25 mm and 0.25 µm film thickness, Agilent Technologies, Santa Clara, CA) was used to chromatographically separate PAHs and n-alkanes analytes. The initial temperature of

the injection port was held at 285°C, vaporizing the injected extract prior to entering the capillary column. The oven was initially set to 60°C. After injection, the oven was programmed to increase in temperature at a rate of 7°C/min until it reached the final holding temperature of 310°C with a final holding time of 22 minutes. Aliphatic hydrocarbons (ALI) were determined using full scan mode. Full scan utilizes computer libraries to compare unknown analyte spectrums within the entire range of ions generated, providing information to resolve or confirm peaks qualitatively, pattern recognition, and structural elucidation (Wang et al. 2007). Full scan was used to identify ALI concentrations such as n-C9 through n-C44 (including isoprenoids: i-C13, i-C14, i-C15, and i-C18), and determine total resolved hydrocarbons (TRH), total petroleum hydrocarbons (TPH), and unresolved complex mixture (UCM). Selected ion monitoring mode (SIM) was used to identify and quantify PAH components. The use of SIM enables the determination of analytes of interests and improves the ability to measure highly specific compounds that occur at lower concentrations within the extract. Data generated by GC/MS was quantified using the ChemStation program (ChemStation software, Agilent Technologies, Santa Clara, California).

4.6. Quality Assurance and Quality Control

Quality assurance (QA) and quality controls (QC) were in place to verify and determine recovery losses, potential contamination carry-over, and sample adjustments during the extraction and instrumentation process. To establish retention times, NIST SRM 1941b, Organics in Marine Sediment was used. To ensure data reliability and

integrity, quality control measures were followed. The GC/MS quality control measures included: a system tune, six-level initial calibration (ICal), independent calibration verification solution (ICV), continuing calibration checks (CCC), reference oils (SRM 1582, and SRM1779), method blank, matrix spike (MS) and matrix spike duplicate (MSD), and duplicate sample (Dupl.). Extract concentration (C_e) was calculated based on:

$$\text{(Equation 2)} \quad C_e = ((AA) \times (CeIS)) / ((A_{IS}) \times (RRF_I))$$

where: Aa = analyte area, $CeIS$ = concentration of internal standard added to the extract ($\mu\text{g/mL}$), A_{IS} = area of internal standard, and RRF_I = relative response factor of initial calibration. Actual concentration (C) of extract is then calculated as

$$\text{(Equation 3)} \quad C = C_e \times (V_e / W) \times DF$$

where: V_e = final volume of the extract (mL), W = original dry weight of the extract (g), and DF = dilution factor.

QA and QC are important during the quantification stage; however, it is important to note the limitations of QA and QC in this project. The ICal analytes were quantified to within 25% of actual analyte values for PAH and ALI analysis. CCC values provided a periodic check amid the instrument analysis for consistency. It also provided

a range of 50 - 200% of internal standard response for individual samples to be compared. Analyte concentrations were based on internal and surrogate recoveries and were adjusted based on these recovery percentages.

MS and MSD samples exceeded the fifty-times known recovery values due to dilutions and high hydrocarbon concentrations for both analyses. Adjustments did not account for spiking solutions, which caused diluted MS and MSD responses to be unreliable. However, due to the high concentrations of hydrocarbon analytes within the samples, the ability to extract analytes of interest with efficiency was not impacted. Duplicates were quantified to within 20% relative difference; however, seven total analytes were outside the 20% relative difference and above the minimum detection limit.

SRM1941b was quantified only for PAH analysis providing retention times for analytes not contained within the ICal and CCC solutions. Four analytes were outside the 50% recovery window for PAH extractions. SRM1941b does not contain certified aliphatic reference values, thus SRM1941b was not quantified for aliphatic hydrocarbons. For SRM2779, all aliphatic analytes were within 50% of known value, with the exception of six analytes (n-C9, n-C10, n-C11, n-C12, n-C13, i-C12, and i-C13). For PAH analysis, three analytes were outside 50% recovery and above the minimum detection limit for both PAH extraction sets. SRM2779 was used to define analytic retention times for aliphatics and assess the quantification process for both analyses. The limited recoveries of the more volatile analytes did not impede the quality of the data due to the limited presence of the six outlying analytes within the sample

extracts. SRM1582 was quantified for only the PAH analysis. All analytes were within 50% of known values above the minimum detection limit. Method blanks were monitored for potential contamination that occurred during the extraction process. GC/MS analyses determined that the method blank contained analyte concentrations exceeding three times the minimal detection limit within the second extraction set (NRT0017 through NRT0032). In contrast to the concentration levels in the samples, the contamination levels seen in the method blank would not impact the sample data concentrations.

4.7. Toxicological Evaluation

PAHs are generated by both natural and anthropogenic processes and are not found in the environment as individual compounds, but rather as mixtures (ATSDR 1995). Humans and wildlife are rarely exposed to individual analytes, but rather to the potentially harmful mixtures which generate acute, chronic, individual, synergistic, and antagonistic responses (USEPA 2003b). As a result of human activities both intentional and unintentional, PAH mixtures are released into the environment and pose potential toxicological risks. These risks can be assessed by using the equilibrium partitioning sediment benchmark toxic unit (ESBTU), toxic evaluation factors (TEF), and TEQ to better understand the hazardous levels posed by mixtures within an AOC (USEPA 2003a and USEPA 2003b).

The equilibrium partitioning sediment benchmark (ESB) evaluation was used to account for the presence of benthic organisms and varying biological availability of

chemicals in the sediment. However, ESB calculations are limited because they do not take into account the antagonistic, additive, or synergistic effects potentially caused by PAH mixtures or bioaccumulation transfer (USEPA 2003a). Due to these limitations, a TEF toxicity evaluation was used to conduct an evaluation of seven carcinogenic and ten non-carcinogenic analytes in the river sediment. TEFs are conservative estimations based on scientific judgment with respect to uncertainties of the analyte specific potency relative to the toxicity of an index chemical (Reeves et al. 2001 and USEPA 2003b). Analytes are prioritized based on the potential harm posed by an individual PAH present in the medium. PAHs are evaluated based on their relative potency with respect to benzo[a]pyrene, the index chemical for PAHs. Analytes, which are classified as carcinogens, receive higher TEF values compared to non-carcinogens (i.e., 1.0, 0.1, or 0.01) (Nisbet and Lagoy 1992).

The toxic equivalency quotient (TEQ) and analyte concentrations (ng/g) determine the level of toxicity within the core sediment with respect to benzo[a]pyrene potency (1.0) (Wickliffe et. al 2014, Nisbet and Lagoy 1992 and Eguvbe et al. 2014). Because dibenzo(a,h)anthracene potency is intensified when in the presence of benzo[a]pyrene, as is the case with most PAH mixtures, the conservative TEF value of 5.0 is used (Nisbet and Lagoy 1992). The concentration of the individual PAHs (C) are multiplied by the TEF to normalize the concentration of the analyte in terms of benzo[a]pyrene equivalence. TEQ is calculated by summing the benzo[a]pyrene equivalency values and the sum of potential toxicity within the present mixture (**Equation 4**). This value can be used to evaluate benzo[a]pyrene dose response data and

can be used to address the potential risk of exposures to mixtures of benzo[a]pyrene and PAHs with respect to the individual concentration of analytes (Nisbet and Lagoy 1992). TEQs can also be used to describe the risk posed by an AOC and to identify potential high risk areas in the AOC.

(Equation 4) $TEQ = \sum_{n=1}^n (C \times TEF)$

4.8. Diagnostic Comparisons

After extraction and quantification, histograms, single ratio, and cross-plots were used to identify potential source of hydrocarbon contamination. Chromatography profiles with m/z responses provided an understanding of these sources (i.e., m/z 178, m/z 191, and m/z 202). Fingerprint profiles of the suspected source in the samples were examined graphically by reviewing PAH concentrations of parent and alkylation abundance to display their relative slope (decrease, increase, or bell-shaped). Diagnostic ratios were used to identify a probable match (Dević and Jovančićević 2008). PAH diagnostic ratios of PAHs (**Table 2**) were used to determine petrogenic or pyrogenic sources and potential input sources (Short et al. 1998 and Crane 2014). Diagnostic ratios of n-Alkanes (**Table 3**) were used to determine potential environmental and anthropogenic sources. Other diagnostic ratios (**Table 4**) were used to determine the total contribution of hydrocarbons within the extracts with respect to other organic materials and degradation.

Table 2: Polycyclic Aromatic Hydrocarbon Ratios

Diagnostic PAH Ratios				
<i>PAHs</i>	<i>Abbreviation</i>	<i>PAHs</i>	<i>Abbreviation</i>	<i>Formula</i>
Fluoranthene	Fl	Pyrene	Py	Fl / (Fl + Py)
Phenanthrene	Phe	Anthracene	An	Phe / An
Phenanthrene	Phe	Anthracene	An	Phe / (An + Phe)
Benzo[a]anthracene	BaA	Chrysene	Chy	BaA / (BaA + Chy)
Indeno[1,2,3-cd]pyrene	PI	Benzo[g,h,i]perylene	BgP	PI / (PI + BgP)
2-methylanthracene	2-mAn	2-methylphenanthrene	2-mPhe	2-mAn / 2-mPhe
Perylene	Pe	Σ5-ring PAHs	Σ5-ring PAHs	Pe / Σ5-ring PAHs
Sum 2-3 ring PAHs	ΣLMW PAHs	Sum 4-6 ring PAHs	ΣHMW PAHs	ΣLMW / ΣHMW
9-, 4-, and 1-methylphenanthrene	1-,4-,9-mPhe	3- and 2-methylphenanthrene	3-,2-mPhe	1,4,9-mPhe / 3-,2-mPhe

Table 3: Aliphatic Hydrocarbon Ratios

Diagnostic n-Alkanes Ratios				
<i>n-Alkane</i>	<i>Abbreviation</i>	<i>n-Alkane</i>	<i>Abbreviation</i>	<i>Formula</i>
odd-numbered n-Alkanes (n-C19 through n-C39)	odd n-C	even-numbered n-Alkanes (n-C20 through n-C40)	even n-C	odd n-C / even n-C
Phytane	Ph	Pristane	Pr	Ph / Pr
Total Petroleum Hydrocarbons	TPH	Total n-Alkanes	ALI	TPH / ALI
n-Heptadecane	n-C17	Pristane	Pr	n-C17 / Pr
n-Octadecane	n-C18	Phytane	Ph	n-C18 / Ph
Total Petroleum Hydrocarbons (Log10)	log TPH	Total Resolved Hydrocarbons (Log10)	log TRH	log TPH / log TRH

Table 4: Other Diagnostic Ratios

Other Diagnostic Ratios				
<i>Name</i>	<i>Abbreviation</i>	<i>Name</i>	<i>Abbreviation</i>	<i>Formula</i>
Total Petroleum Hydrocarbons (log10)	log TPH	Extracted Organic Material (log10)	log EOM	log TPH / log EOM
Total Polycyclic Aromatic Hydrocarbons	TPAH	Total Organic Carbon	TOC	TPAH / TOC
Total n-Alkanes	ALI	Total Organic Carbon	TOC	ALI / TOC
Total Polycyclic Aromatic Hydrocarbons	TPAH	Extracted Organic Material	EOM	TPAH / EOM
Total Aliphatic Hydrocarbons	TALI	Extracted Organic Material	EOM	TALI / EOM
C30 Hopane	C30	Total Petroleum Hydrocarbons	TPH	C30 / TPH

TOC provides an indication of nonspecific organic influx by a weight/weight (mg/g) ratio and a percent carbon value. PAH/TOC or n-alkane/TOC ratios can be used to determine the input of PAHs or n-alkanes with respect to the total organic concentration. Low ratio values are an indication of low PAH or n-alkane contribution to the total organic carbon.

To calculate UCM, total petroleum hydrocarbon (TPH) and total resolved hydrocarbon (TRH) concentration values are needed. TRH concentration should always be higher than the total n-alkane concentration because TRH includes all peak values, which are individualized, not solely the selected n-alkane analytes. TPH is the sum of all peak area above the baseline of the chromatograph. TPH concentrations should always be less than EOM concentrations because of sample clean-up. TPH concentration includes the TRH and UCM, which are the bioresistant compounds of the organic mixture, and thus, UCM equals the difference between TPH and TRH.

5. RESULTS AND DISCUSSION

5.1. Total Organic Carbon

TOC analysis provides an indication of nonspecific organic influx based on a sum concentration of all organic carbon molecules within a given sample (i.e., milligrams of carbon detected within grams of the sample). High TOC ratios and percentages are typically an indication of large organic influx such as biomass, petrochemicals, coal, or other hydrocarbon based constituents (i.e., PAHs, n-alkanes, etc.). As shown in **Table 5**, the NRT total organic carbon data averaged 6.8% TOC (excluding FRDJ-SED-2-03A-01U). The graphite-like material removed from core section FRDJ-SED-2-03A-01 (denoted as FRDJ-SED-2-03A-01U) was 85.2% TOC. Cores sections ranged from 0.7% TOC (FRDJ-SED-3-01-23) to 19.9% TOC (FRDJ-SED-2-03A-23). FRDJ-SED-2-03A-23 contained significant amounts of the graphite-like material which may explain the high carbon values found in this sample. Core sections were averaged to obtain a TOC measurement for each core. Total organic carbon data per core ranged from 10.9% TOC (FRDJ-1-03) to 2.0% TOC (FRDJ-3-01).

5.2. Extracted Organic Material

Extracted organic material (EOM) determination is the concentration of measurable organic matter extracted from a know weight of material. EOM analysis provides an ug/g concentration value which can be used to prepare adjustments preventing column overload for better peak resolution. EOMs also provide an

understanding of chromatography responses of unknown sample contamination such as EOM versus hydrocarbon contribution. And finally, EOMs can justify results of low or high UCM, TPH, TRH, and PAH concentrations versus unknown sample contamination levels. EOM results are unfiltered extract values, whereas final extracts are filtered and potentially diluted. EOM determination of core data averaged 5663 $\mu\text{g}/\text{dry g}$, as shown in **Table 5**. The graphite-like material removed from core section FRDJ-SED-2-03A-01U was 286 $\mu\text{g}/\text{dry g}$. Sample extracts were less than 0.08% organic by weight.

5.3. Saturated Hydrocarbons

Core sediments were analyzed using GC/MS. Aliphatic hydrocarbon (n-alkanes and isoprenoids) data was adjusted according to dilution factors and surrogate corrected to 100% recovery. As shown in **Table 5**, total n-alkanes range from 3.96 $\mu\text{g}/\text{g}$ (FRDJ-SED-3-02-3T) to 523 $\mu\text{g}/\text{g}$ (FRDJ-SED-1-03-23). The predominant aliphatic hydrocarbons in the samples were pristane, phytane, n-C27 and n-C29. Aliphatic odd:even ratio depicted a strong presence of odd carbon-numbered n-alkanes ratios (range of C25 to C35), with one exception--FRDJ-SED-2-03A-3T (**Appendix B**). The strong presence of odd carbon numbered n-alkanes within the range of C25 to C35 is an indication of terrestrial plant waxes and microalgae (Lichtfouse et al. 1994). However, FRDJ-SED-2-03A-3T contained an elevated concentration of n-C24 contributed by an unknown source. If n-C24 was excluded from the FRDJ-SED-2-03A-3T data, the ratio value would increase from 0.78 to 1.92, more closely resembling the other extract ratios.

Table 5: Distribution of Contaminants

Sample Name	Σ Alkanes ($\mu\text{g/g}$)	Σ PAHs ($\mu\text{g/g}$)	Σ LMW-PAH ($\mu\text{g/g}$)	Σ HMW-PAH ($\mu\text{g/g}$)	UCM (mg/g)	TOC (%)	EOM (mg/g)
FRDJ-SED-1-01-01	29.2	26.4	4.11	22.3	0.914	6.82	3.86
FRDJ-SED-1-01-12	39.2	18.4	3.70	14.2	1.68	7.18	6.47
FRDJ-SED-1-01-23	57.3	37.7	9.16	27.8	2.05	7.38	6.58
FRDJ-SED-1-02-01	46.1	19.6	4.48	14.3	2.08	7.89	8.60
FRDJ-SED-1-02-12	62.1	21.5	6.54	14.2	2.02	6.97	7.00
FRDJ-SED-1-02-23	83.5	25.0	7.30	15.6	3.58	8.15	9.61
FRDJ-SED-1-03-01	117	52.7	11.8	38.8	3.16	11.5	11.9
FRDJ-SED-1-03-12	86.5	60.4	9.57	50.2	3.15	11.7	9.28
FRDJ-SED-1-03-23	69.8	36.3	6.80	28.8	3.25	9.64	8.84
FRDJ-SED-2-01-01	33.9	22.8	3.84	18.8	1.02	6.95	5.24
FRDJ-SED-2-01-12	58.6	22.2	5.74	15.7	2.25	6.20	6.18
FRDJ-SED-2-01-23	60.2	20.1	6.63	12.0	2.83	7.18	8.36
FRDJ-SED-2-02-01	42.2	27.0	5.18	21.6	1.48	8.69	7.16
FRDJ-SED-2-02-12	53.2	39.0	7.40	31.3	2.09	9.61	5.88
FRDJ-SED-2-02-23	52.8	26.3	6.12	19.3	1.86	6.73	6.76
FRDJ-SED-2-02-3T	46.8	23.2	5.29	16.9	2.27	7.13	8.73
FRDJ-SED-2-03A-01	11.7	15.8	1.98	13.9	0.648	3.77	3.56
FRDJ-SED-2-03A-12	29.8	25.0	3.96	20.7	1.64	5.93	4.95
FRDJ-SED-2-03A-23	66.7	48.7	9.86	38.1	3.01	19.9	7.96
FRDJ-SED-2-03A-3T	85.4	40.0	7.17	31.7	4.08	8.19	11.4
FRDJ-SED-3-01-01	6.80	5.59	0.991	4.62	0.299	1.42	0.751
FRDJ-SED-3-01-12	14.5	2.61	0.474	2.35	0.295	3.41	0.731
FRDJ-SED-3-01-23	3.51	0.463	0.135	0.346	0.148	0.730	0.423
FRDJ-SED-3-01-3T	7.22	0.861	0.129	0.705	0.209	2.48	1.04
FRDJ-SED-3-02-01	26.6	25.7	3.95	21.4	1.51	6.57	5.69
FRDJ-SED-3-02-12	15.4	7.75	1.43	6.20	0.816	3.65	1.96
FRDJ-SED-3-02-23	10.7	4.27	0.718	3.64	0.329	3.57	1.21
FRDJ-SED-3-02-3T	3.96	0.245	0.067	0.155	0.141	0.842	0.484
FRDJ-SED-3-03-01	43.2	28.2	8.44	18.9	1.72	7.62	8.66
FRDJ-SED-3-03-12	46.3	53.4	10.3	42.0	2.18	8.59	7.90
FRDJ-SED-3-03-23	7.70	6.38	1.24	5.13	0.462	2.25	1.40
FRDJ-SED-3-03-3T	16.4	17.5	3.54	14.0	0.947	7.17	2.71
FRDJ-SED-2-03A-01U	43.6	34.7	17.6	15.2	3.05	85.2	0.286

Pristane/phytane ratios varied from 0.88 to 1.50, with an outlier at 6.67 (FRDJ-SED-2-03A-12), and a mean of 1.30. With the pristane/phytane ratios close to 1.0, pristane and phytane contributions may be a result of microbial activities in the river (Powell 1998, Peters and Walters 2005, and Haven et al. 1988). However, the abrupt changes in concentrations of pristane and phytane with an equivocal ratio may also indicate presence of diffused residual petroleum in limited or degraded form, such as those contained in surface runoff (Hamilton and Cline 1981). The n-C17/Pr ratios range from 0.29 to 2.33 with a mean of 0.88. The n-C18/Ph ratios range from 0.11 to 4.20 with a mean of 0.65. Both n-C17/Pr and n-C18/Ph indicate biodegradation of the hydrocarbon substrate with ratios less than 1.

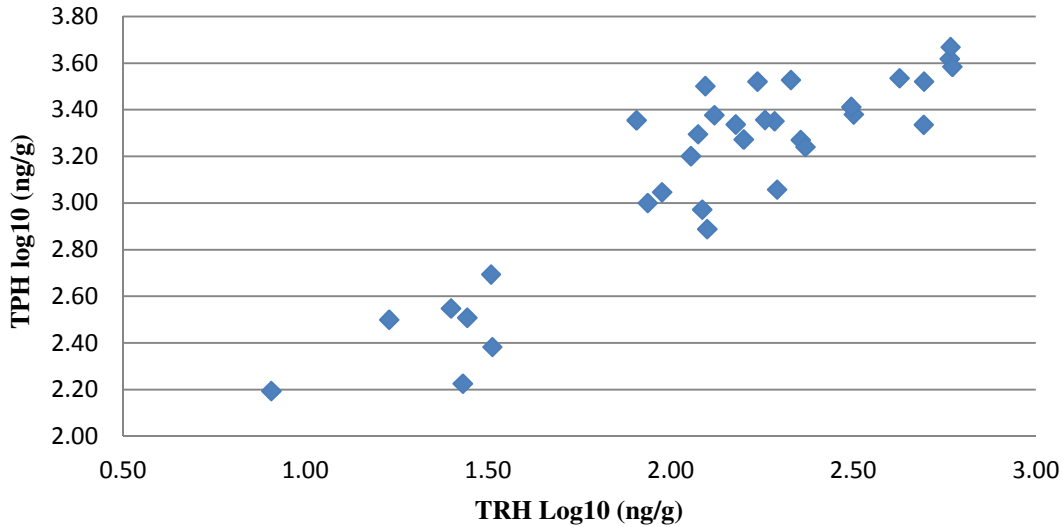
TPH and TRH were compared by normalizing the large range of response values using a logarithmic scale (\log_{10}). This comparison provided an indication of weathered versus non-weathered saturated hydrocarbon influx. Because the concentration of TRH, with respect to TPH, shows linearity, hydrocarbon degradation is consistent throughout (**Figure 3a**). The large variation in TPH and TRH concentrations depicted in **Table 5** indicates low concentrations of resolved hydrocarbons are present within the more bioresistant organic substrate (i.e., limited biodegradation). Similarly, C30-hopane concentration versus TPH can be used to interpret degradation of hydrocarbons (**Figure 3b**). A detectable linear trend provides an understanding of the current distribution and concentrations, or status, of hydrocarbon contamination with respect to C30-hopane. To determine organic influx, particularly petroleum incursion, EOM was compared to the

UCM concentration (**Figure 3c**). When the UCM concentrations were cross-plotted with EOM concentrations, the plot showed a linear correlation.

UCM versus EOM depicted a relatively low percentage of hydrocarbon-based material present in comparison to the total extracted material (**Figure 3c**). UCM concentrations accounted for approximately 33% of total EOM extracted indicating a large deposition of non-specific, non-petroleum based organic material within the sampling areas.

EOM concentrations were also cross-plotted with TPH to compare total extractable material versus degraded and non-degraded hydrocarbons within the extractable range (**Figure 3d**). After EOM and TPH were normalized using a log₁₀ base comparison, the plot provided an observation of a potential contribution of hydrocarbon-based contamination within the overall organic substrate. Log₁₀ EOM versus log₁₀ TPH shows all core sections to have almost identical contributions of hydrocarbon-based composition with limited petroleum influx.

TPH vs TRH



C30-Hopane vs TPH

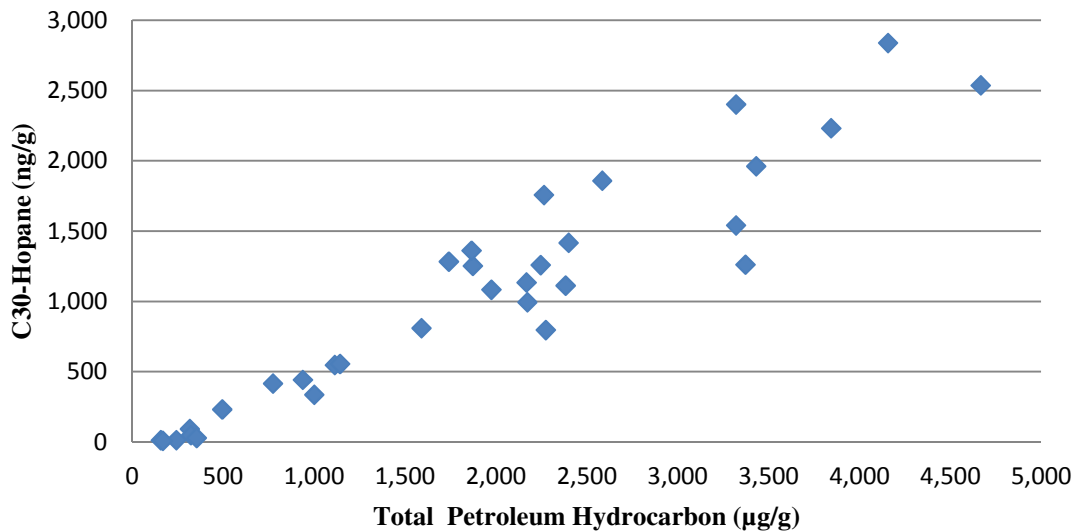
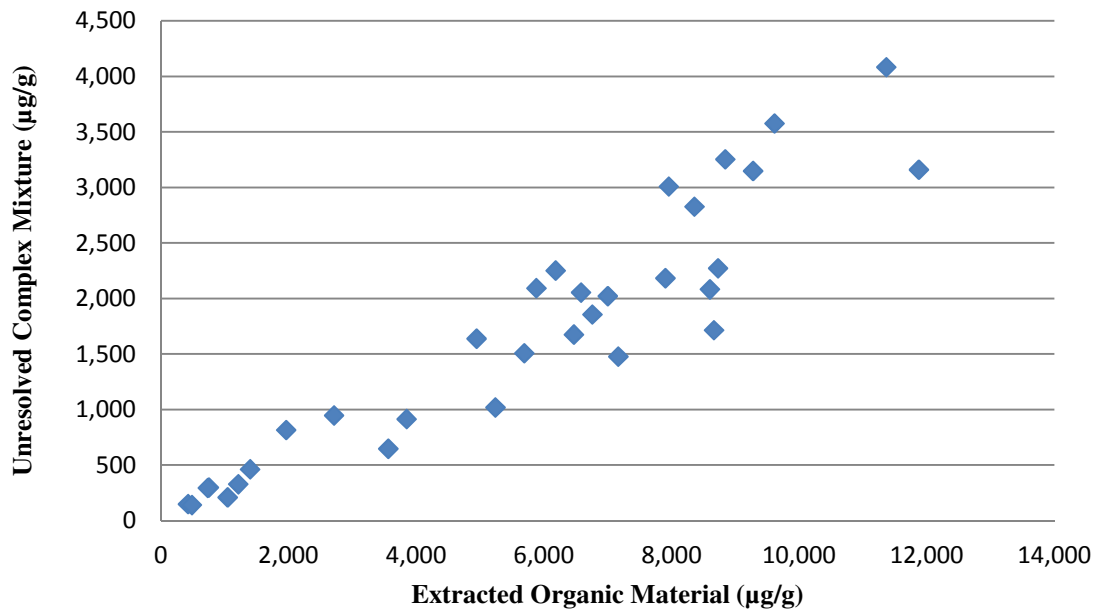


Figure 3: Total Petroleum Hydrocarbon Cross-plots. Figure 3 depicts petroleum hydrocarbon abundance versus distribution and degradation. (Figure 3a) Total Residual Hydrocarbon (TRH) versus Total Petroleum Hydrocarbon (TPH), (Figure 3b) C30-hopane versus TPH, (Figure 3c) Unresolved Complex Mixture (UCM) versus extracted organic material (EOM) and (Figure 3d) EOM versus TPH. Cross-plots depict degradation, abundance, and trends; assisting in deciphering hydrocarbon influx source(s).

UCM vs EOM



EOM vs TPH

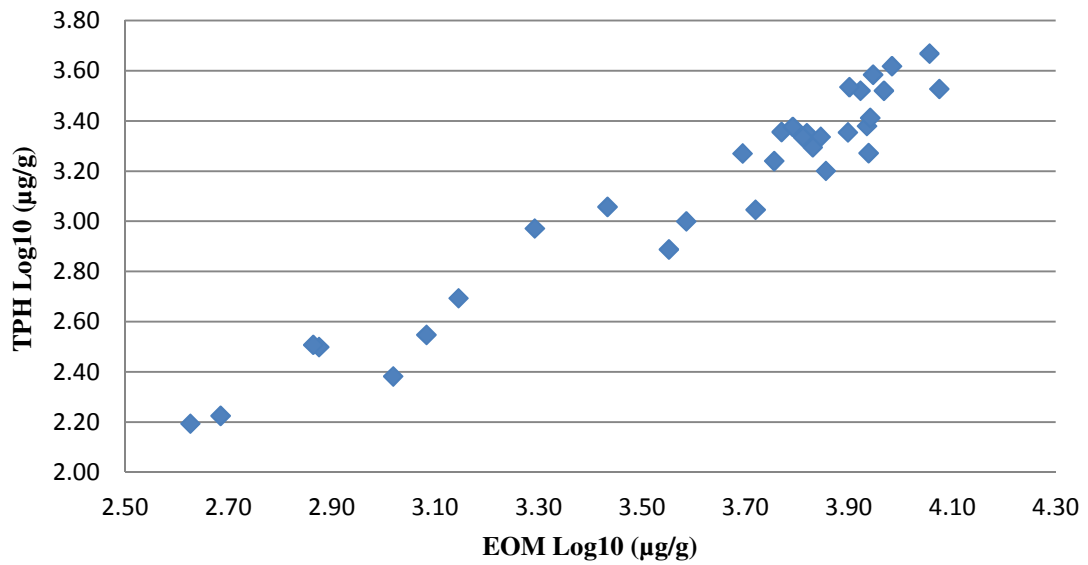


Figure 3: Continued

Total n-alkanes and identified TRH analytes provided a specialized tool in source identification. Although n-alkanes are subjected to weathering, the retained concentrations of identifiable n-alkanes provide an understanding of influx source. As shown in **Figure 4**, total n-alkane concentrations within the core sections vary with TPH concentration. The linearity of the total n-alkanes versus TPH depicts limited degradation of the n-alkanes.

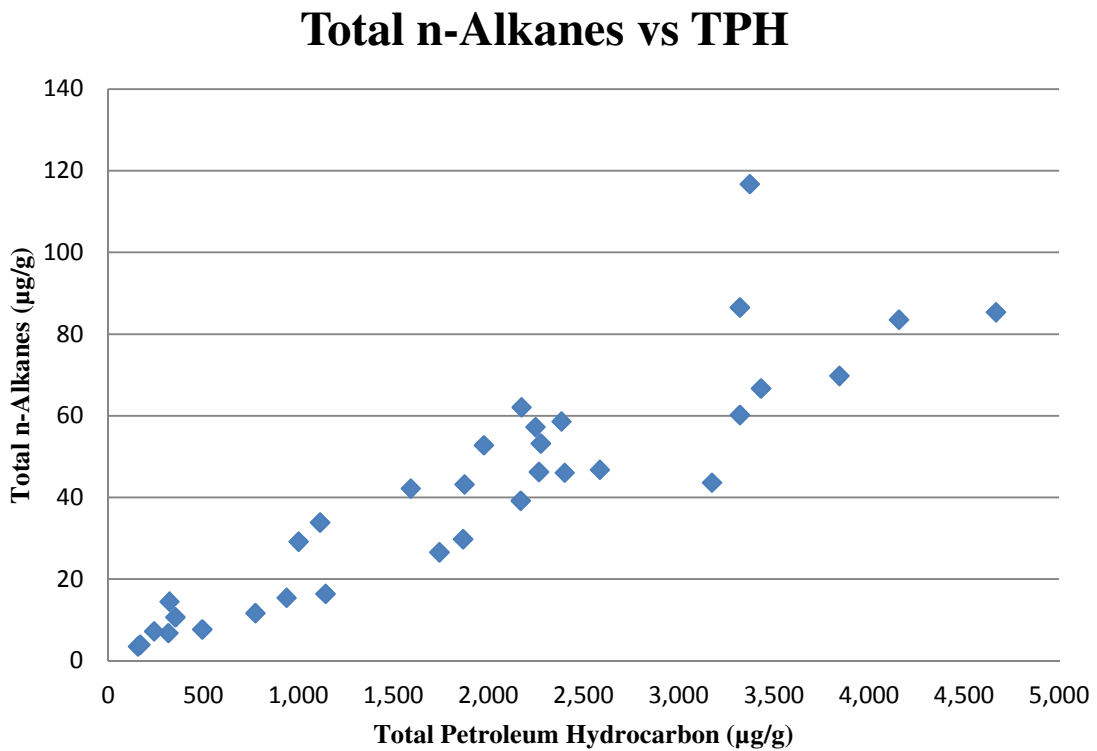


Figure 4: *Total n-Alkanes versus Total Petroleum Hydrocarbons.* Figure 4 depicts the abundance of total n-alkanes versus TPH indicating limited degradation

5.4. Polycyclic Aromatic Hydrocarbons

The PAH data was adjusted according to dilution factors and surrogate corrected to 100% recovery. The predominant PAH analytes were: chrysenes, pyrene, fluoranthene, and C4-phenanthrenes/anthracenes. The mean total PAH concentration was 24,800 ng/g with FRDJ-SED-1-03-12 and FRDJ-SED-1-03-01 sections showing the highest concentrations at 63,600 ng/g and 56,700 ng/g, respectively. Both sections represent core FRDJ-SED-1-03 in the upper twenty-three inches. Core FRDJ-SED-3-01 subsections were the lowest values with a range of 519.3 ng/g to 5,802 ng/g. The mean values for the seven PAHs classified as B2 carcinogens present in the river sediment were: benzo[a]anthracene (540 ng/g), benzo[a]pyrene (426 ng/g), benzo[b]fluoranthene (484 ng/g), benzo[k]fluoranthene (157 ng/g), chrysene (660 ng/g), dibenzo[a,h]anthracene (107 ng/g), and indeno[1,2,3-c,d]pyrene (249 ng/g), which equaled 10% of the total PAH concentration. Cores FRDJ-SED-1-03, FRDJ-SED-2-03A, and FRDJ-SED-2-02 contain the highest concentration of PAHs with respect to the upper three sections (see **Table 5**, page 34). FRDJ-SED-1-03, FRDJ-SED-2-03A, and FRDJ-SED-2-02 collection areas were located closest to the DePere Dam, upstream from the US Paper Mills and Georgia Pacific. Subsequently, the lowest PAH concentrations were located furthest downstream of the DePere Dam at FRDJ-SED-3-01 and FRDJ-SED-3-02. PAH concentrations were highest closest to the center of the river and lowest towards the shore.

Core sections show an uneven distribution of LMW PAHs to HMW PAHs (**Table 5**, page 34 and **Figure 5**). HMW PAHs were predominant over LMW PAHs with

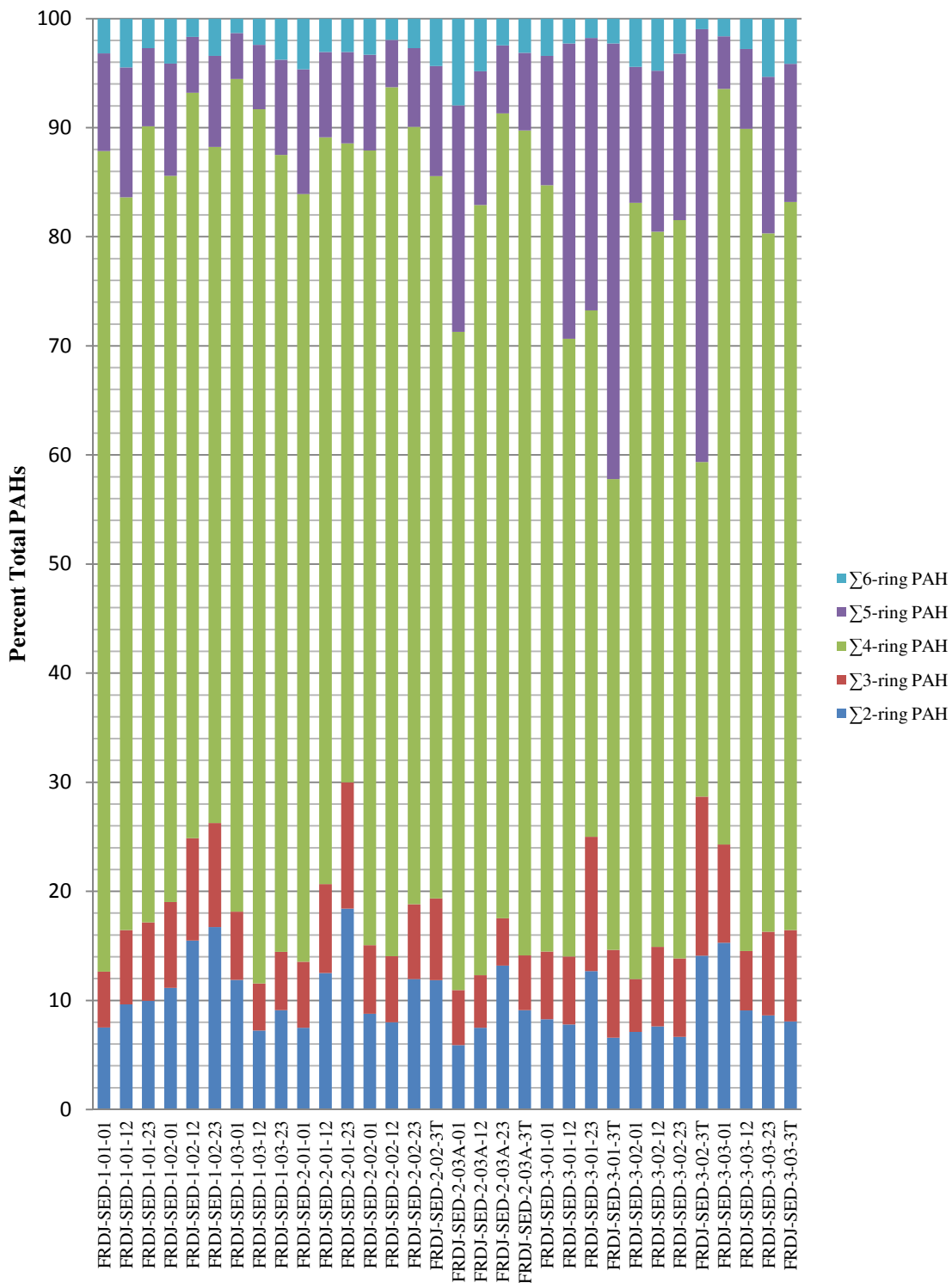


Figure 5: Ring Distribution of PAHs as Percent Total PAHs by Core Section.

high concentrations of C0, C1, and C2 alkylated analytes indicating pyrogenic activities (**Appendix A**). LMW PAH and HWM PAH analytes are both depicted as a downward slope to bell-shape curve with C2 as the predominant alkylation (e.g., C2-Fluoranthenes/Pyrenes). The elevated presence of parent PAH analytes is an indication of recent deposition of pyrogenic PAH contamination. The high concentration of HMW PAHs such as 4-ring, 5-ring and 6-ring PAHs is typical of an urban region. C2 abundance, with respect to other alkylation levels, is an indication of combustion of both petroleum (LMW) and biomass (HMW) (Wagener et al. 2010). C2- and C3-anthracene/phenanthrene concentrations suggest an incursion of petrogenic residues in addition to pyrogenic PAH, typical of urban runoff (Uhler et al. 2005).

The presence and abundance of 2-methylanthracene (m/z 192) in comparison with methylphenanthrenes can indicate refined petrochemicals (e.g., combustion or byproducts) (Wilhelms et al. 1998). This presence of 2-methylanthracene in the cores is an indication of a pyrogenic PAH source (**Figure 6** and **Table 6**). Further, the presence of both stable and unstable methylphenanthrenes is another example of pyrogenic activities. Generally, 3- and 2-methylphenanthrene isomers are more stable than 9-, 4-, and 1-methylphenanthrene. Therefore, the higher concentration of less stable methylphenanthrene isomers is an indication of pyrogenesis. The sample extracts contained significant concentrations of 2-methylanthracene and 9-, 4-, and 1-methylphenanthrenes, with respect to 3- and 2-methylphenanthrene.

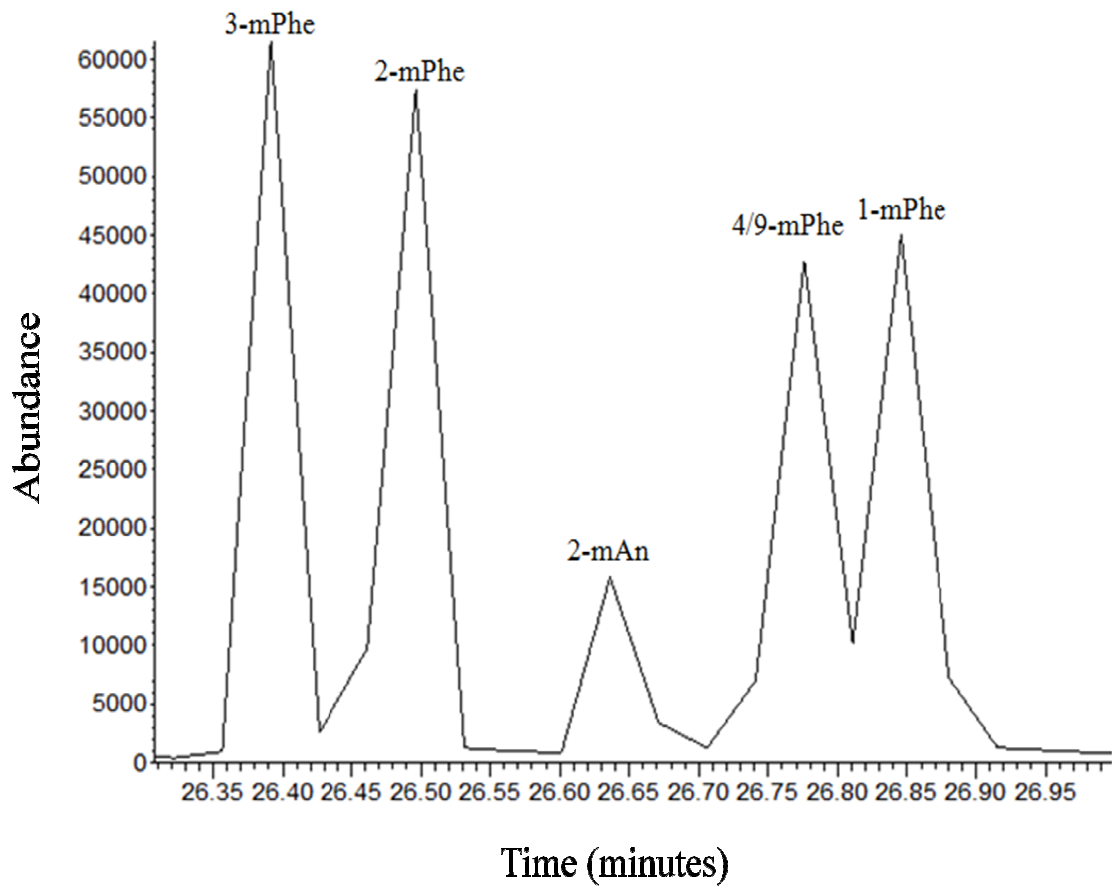


Figure 6: *Alkylated Methylphenanthrenes and 2-Methylanthracene.* Analytes in **Figure 6** are from FRDJ-SED-3-03-23 chromatograph. Presence of alkylated unstable 9-, 4-, and 1-methylphenanthrene and 2-methylanthracene (m/z 192) depict pyrogenic sources.

Table 6: Methylphenanthrene and 2-Methylantracene with Ratios

Sample Name	2-mPhe (µg/g)	2-mAn (µg/g)	2-mAn/ 2-mPhe	9-,4-,1-Phe (µg/g)	3-,2-Phe (µg/g)	9-,4-,1-Phe/ 3-,2-Phe
FRDJ-SED-1-01-01	332.8	97.67	0.29	452.9	594.7	0.76
FRDJ-SED-1-01-12	211.2	48.55	0.23	271.1	402.7	0.67
FRDJ-SED-1-01-23	560.3	78.44	0.14	506.8	910.8	0.56
FRDJ-SED-1-02-01	238.8	50.23	0.21	293.0	459.1	0.64
FRDJ-SED-1-02-12	298.9	78.50	0.26	364.9	515.7	0.71
FRDJ-SED-1-02-23	310.3	38.95	0.13	354.8	561.7	0.63
FRDJ-SED-1-03-01	606.2	89.36	0.15	819.9	1001	0.82
FRDJ-SED-1-03-12	789.6	96.14	0.12	930.1	1295	0.72
FRDJ-SED-1-03-23	455.5	76.40	0.17	592.6	880.1	0.67
FRDJ-SED-2-01-01	314.1	73.08	0.23	370.2	494.6	0.75
FRDJ-SED-2-01-12	335.5	56.13	0.17	338.6	519.3	0.65
FRDJ-SED-2-01-23	276.6	48.64	0.18	303.9	509.9	0.60
FRDJ-SED-2-02-01	364.7	74.53	0.20	436.8	588.4	0.74
FRDJ-SED-2-02-12	450.2	79.50	0.18	536.5	712.9	0.75
FRDJ-SED-2-02-23	369.6	67.22	0.18	393.0	606.5	0.65
FRDJ-SED-2-02-3T	315.3	49.75	0.16	354.9	559.5	0.63
FRDJ-SED-2-03A-01	124.7	42.36	0.34	210.3	262.7	0.80
FRDJ-SED-2-03A-12	280.9	52.40	0.19	411.1	585.2	0.70
FRDJ-SED-2-03A-23	434.5	66.49	0.15	753.8	912.4	0.83
FRDJ-SED-2-03A-3T	360.4	62.20	0.17	485.5	674.1	0.72
FRDJ-SED-3-01-01	96.91	24.09	0.25	130.2	155.1	0.84
FRDJ-SED-3-01-12	31.59	10.98	0.35	63.48	55.71	1.14
FRDJ-SED-3-01-23	6.031	6.333	1.05	6.831	9.454	0.72
FRDJ-SED-3-01-3T	5.828	5.070	0.87	15.59	12.60	1.24
FRDJ-SED-3-02-01	278.2	61.31	0.22	428.4	572.8	0.75
FRDJ-SED-3-02-12	85.69	28.80	0.34	154.8	177.1	0.87
FRDJ-SED-3-02-23	58.24	24.46	0.42	109.9	101.4	1.08
FRDJ-SED-3-02-3T	1.705	4.624	2.71	1.897	3.475	0.55
FRDJ-SED-3-03-01	470.6	102.5	0.22	525.1	764.8	0.69
FRDJ-SED-3-03-12	891.2	106.5	0.12	878.9	1381	0.64
FRDJ-SED-3-03-23	104.1	27.83	0.27	164.4	201.3	0.82
FRDJ-SED-3-03-3T	259.4	100.3	0.39	478.9	539.1	0.89
FRDJ-SED-2-03A-01U	669.3	331.2	0.49	1440.2	1687	0.85

Perylene is a constituent of PAH mixtures which can assist in the differentiation between natural and anthropogenic PAH sources. The abundance of $\Sigma 5$ -ring PAHs with respect to perylene concentration indicates pyrogenesis. When perylene is compared to total PAHs, the provenance of perylene within sediments is identified as diagenetic when the ratio is larger than 0.1 (Readman et al. 2002). Perylene concentration within sampling area 3, with respect to total PAHs, exceeds 0.1. This indicates that the perylene source for area 3 is predominantly biogenic. The abundance of perylene elsewhere, less than 0.1, is an indication of pyrolytic contribution of PAHs.

The $An / (An + Phe)$ ratio is used to distinguish between petrogenic (less than 0.1) or pyrogenic origin (greater than 0.1) (Yunker et al. 2002 and Bastami et al. 2014). The majority of sections contained a ratio greater than 0.1 indicating a pyrogenic source (**Table 7**). The $Fl / (Fl + Py)$ ratio provides an indication of source (**Table 7**). Sample extracts contained a $Fl / (Fl + Py)$ ratio with a range of 0.32 -0.62 and a mean of 0.46. The majority of the sample ratios fell between 0.4 - 0.5, indicating a mixture of combusted and non-combusted petrol fuels in conjunction with biomass combustion and degradation (Yunker et al. 2002 and Bastami et al. 2014).

Table 7: PAH Diagnostic Ratios for Benzo[a]pyrene (BaA), Chrysene (Chy), Fluoranthene (Fl), Pyrene (Py), Anthracene (An), Phenanthrene (Phe), Indeno[1,2,3-cd]pyrene (PI), and Benzo[g,h,i]pyrene (BgP)

Sample Name	BaA/(BaA+Chy)	Fl/(Fl+Py)	An/(Phe+An)	PI/(PI+BgP)
FRDJ-SED-1-01-01	0.44	0.47	0.20	0.44
FRDJ-SED-1-01-12	0.42	0.54	0.16	0.34
FRDJ-SED-1-01-23	0.47	0.34	0.14	0.30
FRDJ-SED-1-02-01	0.42	0.52	0.14	0.30
FRDJ-SED-1-02-12	0.44	0.34	0.10	0.30
FRDJ-SED-1-02-23	0.43	0.49	0.12	0.27
FRDJ-SED-1-03-01	0.49	0.35	0.14	0.32
FRDJ-SED-1-03-12	0.46	0.36	0.15	0.30
FRDJ-SED-1-03-23	0.45	0.50	0.16	0.28
FRDJ-SED-2-01-01	0.44	0.41	0.17	0.42
FRDJ-SED-2-01-12	0.44	0.37	0.14	0.34
FRDJ-SED-2-01-23	0.44	0.53	0.09	0.30
FRDJ-SED-2-02-01	0.47	0.38	0.17	0.39
FRDJ-SED-2-02-12	0.44	0.40	0.16	0.35
FRDJ-SED-2-02-23	0.47	0.32	0.14	0.30
FRDJ-SED-2-02-3T	0.45	0.50	0.14	0.31
FRDJ-SED-2-03A-01	0.46	0.60	0.17	0.45
FRDJ-SED-2-03A-12	0.41	0.47	0.13	0.30
FRDJ-SED-2-03A-23	0.38	0.46	0.10	0.29
FRDJ-SED-2-03A-3T	0.48	0.51	0.14	0.33
FRDJ-SED-3-01-01	0.55	0.37	0.19	0.41
FRDJ-SED-3-01-12	0.52	0.41	0.13	0.38
FRDJ-SED-3-01-23	0.38	0.44	0.08	0.30
FRDJ-SED-3-01-3T	0.44	0.56	0.13	0.39
FRDJ-SED-3-02-01	0.40	0.50	0.15	0.35
FRDJ-SED-3-02-12	0.48	0.57	0.16	0.45
FRDJ-SED-3-02-23	0.53	0.37	0.17	0.46
FRDJ-SED-3-02-3T	0.40	0.62	0.10	0.39
FRDJ-SED-3-03-01	0.44	0.36	0.12	0.34
FRDJ-SED-3-03-12	0.45	0.33	0.13	0.31
FRDJ-SED-3-03-23	0.49	0.56	0.19	0.44
FRDJ-SED-3-03-3T	0.51	0.58	0.21	0.49
FRDJ-SED-2-03A-01U	0.38	0.53	0.09	0.38

The BaA / (BaA + Chy) ratio can also be used to indicate a petrogenic or a pyrogenic source (**Table 7**). The BaA / (BaA + Chy) ratios range from 0.38- 0.55 with a mean of 0.45 indicating pyrogenic sources (greater than 0.35) (Dvorská, Lammel, and Klánová 2011). This range could indicate pyrogenic combustions of coals, biomass, and petrol fuels with a potential mixture of lubricants and road runoff. PI / (PI + BgP) ratios provide an indication of source (**Table 7**). The PI / (PI + BgP) ratio has a range of 0.27 - 0.49 with a mean 0.35, which indicates pyrogenic combustion, automotive residues, and road runoff (Yunker et al. 2002 and Bastami et al. 2014). However, similar to BaA / (BaA + Chy) ratio, the PI / (PI + BgP) ratio range can include multiple potential sources.

To identify potential PAH sources, PAH analyte ratios were plotted using a typical oil geochemistry correlation cross-plot. By comparing An / (An + Phe) versus Fl / (Fl + Py), a better understanding of primary and secondary PAH sources is achieved (**Figure 7**). This cross-plot indicates a complexity of parameters with multiple PAH contributions from the surrounding environment. The core sections are comprised of organic sediments mixed with different PAH constituents from different sources. These disparate sources can be identified as pyrogenic with values representing the combustion of petroleum and combustion of biomass.

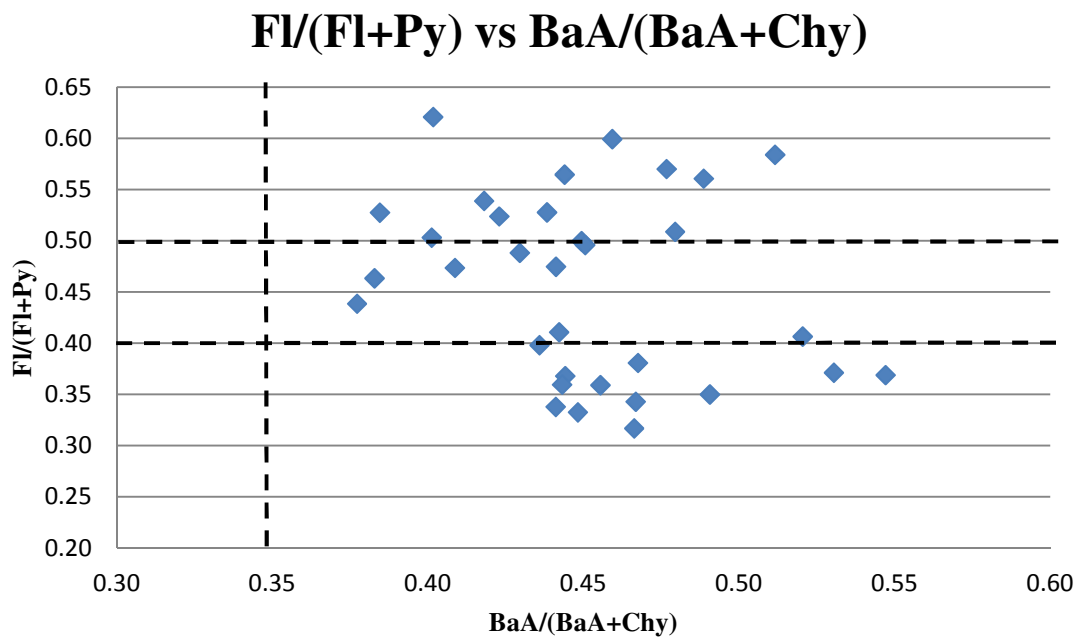
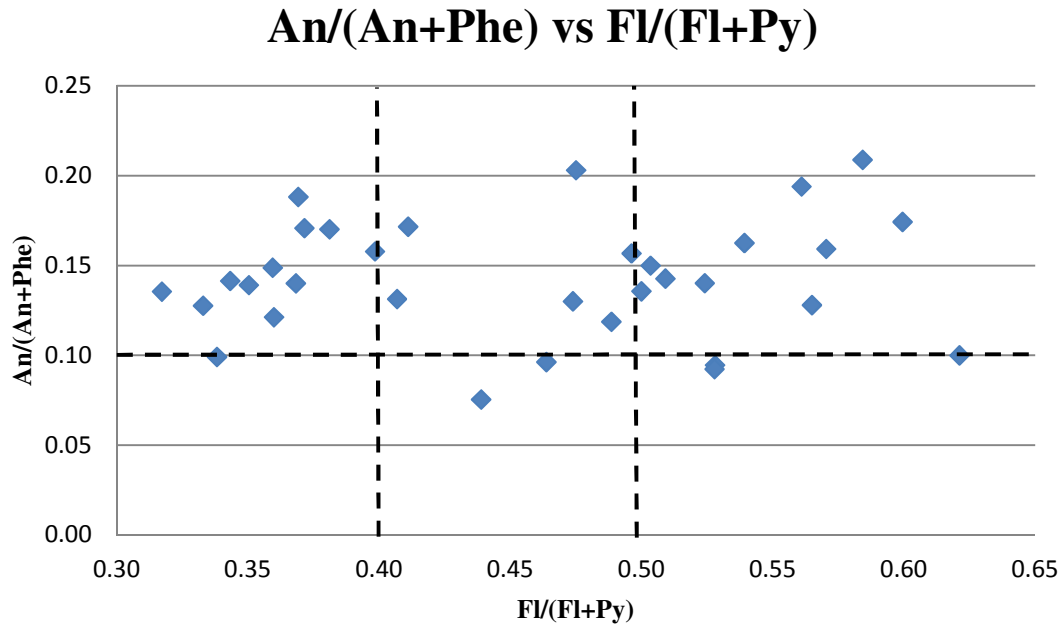
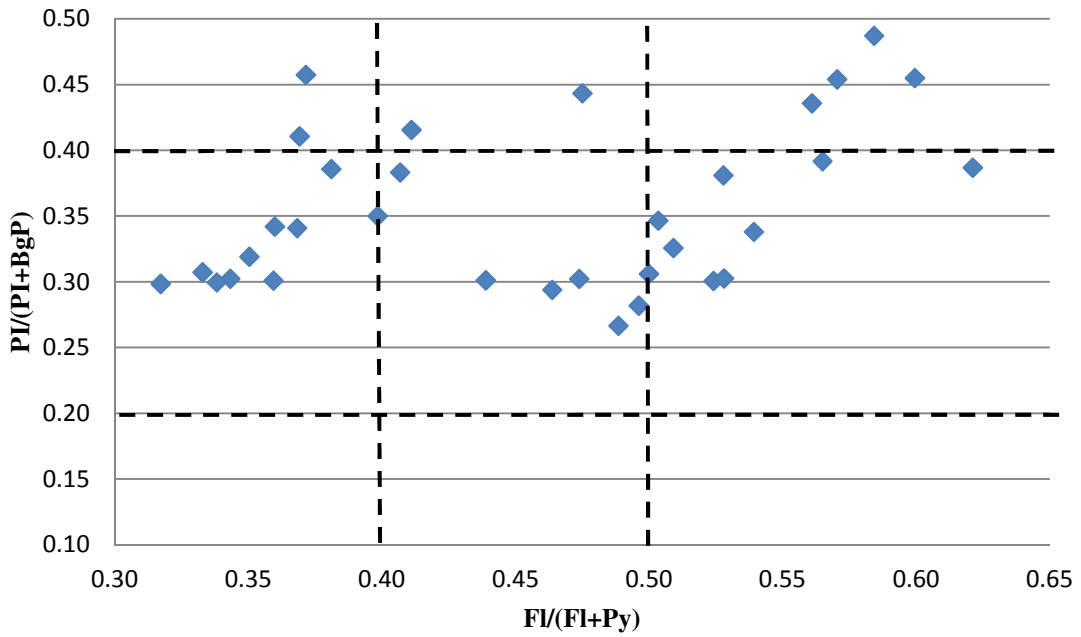


Figure 7: PAH Diagnostic Cross-plots; Indications of PAH Source. An / (An + Phe) ratio <0.1 petrogenic or >0.1 pyrogenic. Fl / (Fl + Py) ratio <0.4 petrogenic; 0.4 - 0.5 petroleum combustion (e.g., combustion engines, and furnaces); >0.5 biomass combustion (e.g., grasses, wood, or coal combustion). BaA / (BaA + Chy) ratio can <0.2 petrogenic or >0.35 pyrogenic. PI / (PI + BgP) ratio <0.2 petrogenic; 0.4 - 0.5 petroleum combustion; and >0.5 biomass combustion.

PI/(PI+BgP) vs FI/(FI+Py)



PI/(PI+BgP) vs BaA/(BaA+Chy)

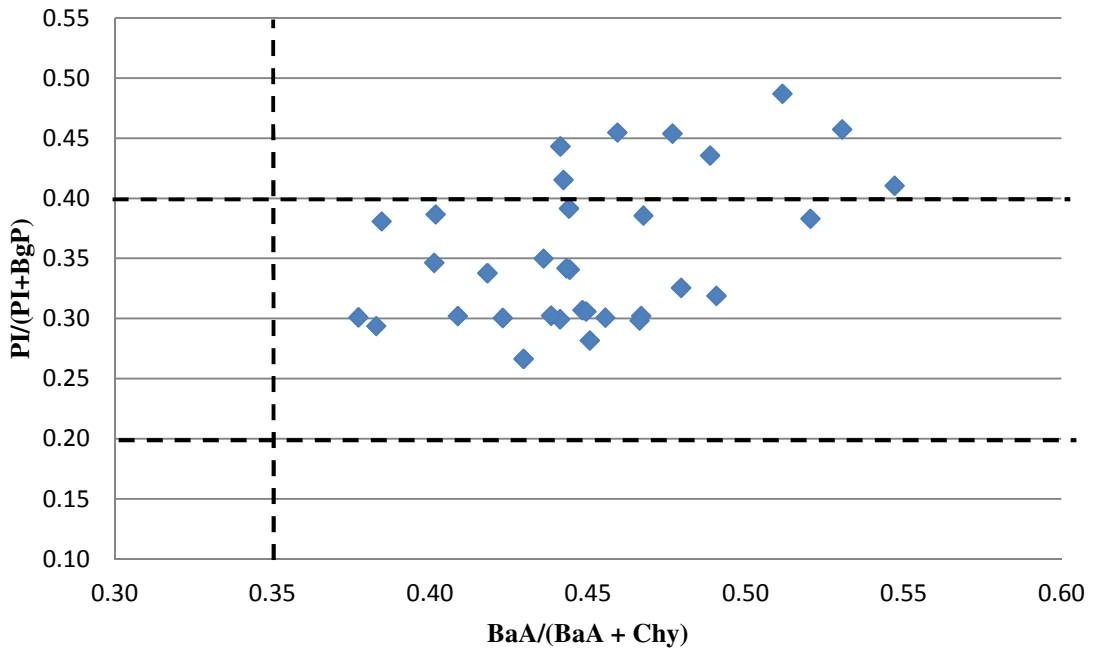


Figure 7: Continued

$Fl / (Fl + Py)$ versus $BaA / (BaA + Chy)$ were compared (**Figure 7**) to differentiate combustion of different biomass materials (Bastami et al. 2014). This contrast provided an indication of the type of biomass that has been combusted (e.g., coal, wood, or grasses). However, despite an attempt to isolate the primary source of PAHs through combustion, distribution indicates some petroleum combustion. Biomass and coal ranges (0.35 - 0.77) for $Fl / (Fl + Py)$ and $BaA / (BaA + Chy)$ overlap: gasoline (0.44) and diesel (0.20 - 0.58) combustion, roadway runoff and automotive/diesel oils (0.30 - 0.37), and roadway tunnel exhaust (0.41-0.49) (Yunker et al. 2002). This overlap limits the ability to identify a single source influx.

$PI / (PI + BgP)$ versus $Fl / (Fl + Py)$ compares potential source PAHs with similar ranges (Bastami et al. 2014). **Figure 7** shows $PI / (PI + BgP)$ ratio and $Fl / (Fl + Py)$ ratio indicates multiple sources of PAH influx. However, both ratios identify petroleum combustion and biomass combustion as main contributors. $PI / (PI + BgP)$ versus $BaA / (BaA + Chy)$ was used to compare fossil fuel types. The cross-plots provide an understanding of coal grades and fuel variations. The cross-plot of $PI / (PI + BgP)$ versus $BaA / (BaA + Chy)$, as with $An / (An + Phe)$ versus $Fl / (Fl + Py)$, indicates a complexity of sediments containing various PAH constituents from different pyrogenic sources, including the combustion of higher ranking coals and petroleum.

To understand the distribution and concentration of hydrocarbon sources, core sections were grouped by depth and location. PAH analytes were cross-plotted based on depth. $An / (An + Phe)$ versus $Fl / (Fl + Py)$ and $An / (An + Phe)$ versus $PI / (PI + BgP)$ display a deposition of PAH residues within the Lower Fox River sediments (**Figure 8**

and **Figure 9**). These cross-plots visually indicate that over a period of time, changes in PAH source input have occurred, with a shift from biomass combustion in the lower core sections to more petroleum combustion and automotive discharge in the upper two core sections.

PAH analytes were cross-plotted based on sampling area. $An / (An + Phe)$ versus $Fl / (Fl + Py)$ and $An / (An + Phe)$ versus $PI / (PI + BgP)$ show differences in PAH source (**Figure 10**, **Figure 11**, and **Table 8**). Area 1 and area 2 display lower ratio groupings with a higher density of points in the petroleum combustion zone. However, in area 2, some presence of biomass combustion is observed. Area 3 displays more source diversity, with $Fl / (Fl + Py)$ and $PI / (PI + BgP)$ ratios between 0.2 and 0.4 and some distributions greater than 0.4. All areas contain outliers below the $Fl / (Fl + Py)$ 0.4 intercept; however, this does not indicate petroleum incursion. The residual PAHs are more consistent with diesel combustion (0.20 - 0.58) from automotives in the metropolitan area with respect to $PI / (PI + BgP)$ ratios. This area comparison indicates that over the course of the river, changes in PAH source input occurs with a shift from upstream petroleum combustion and automotive discharge to an even distribution of both petroleum combustion and biomass combustion downstream.

An/(An+Phe) vs Fl/(Fl+Py)

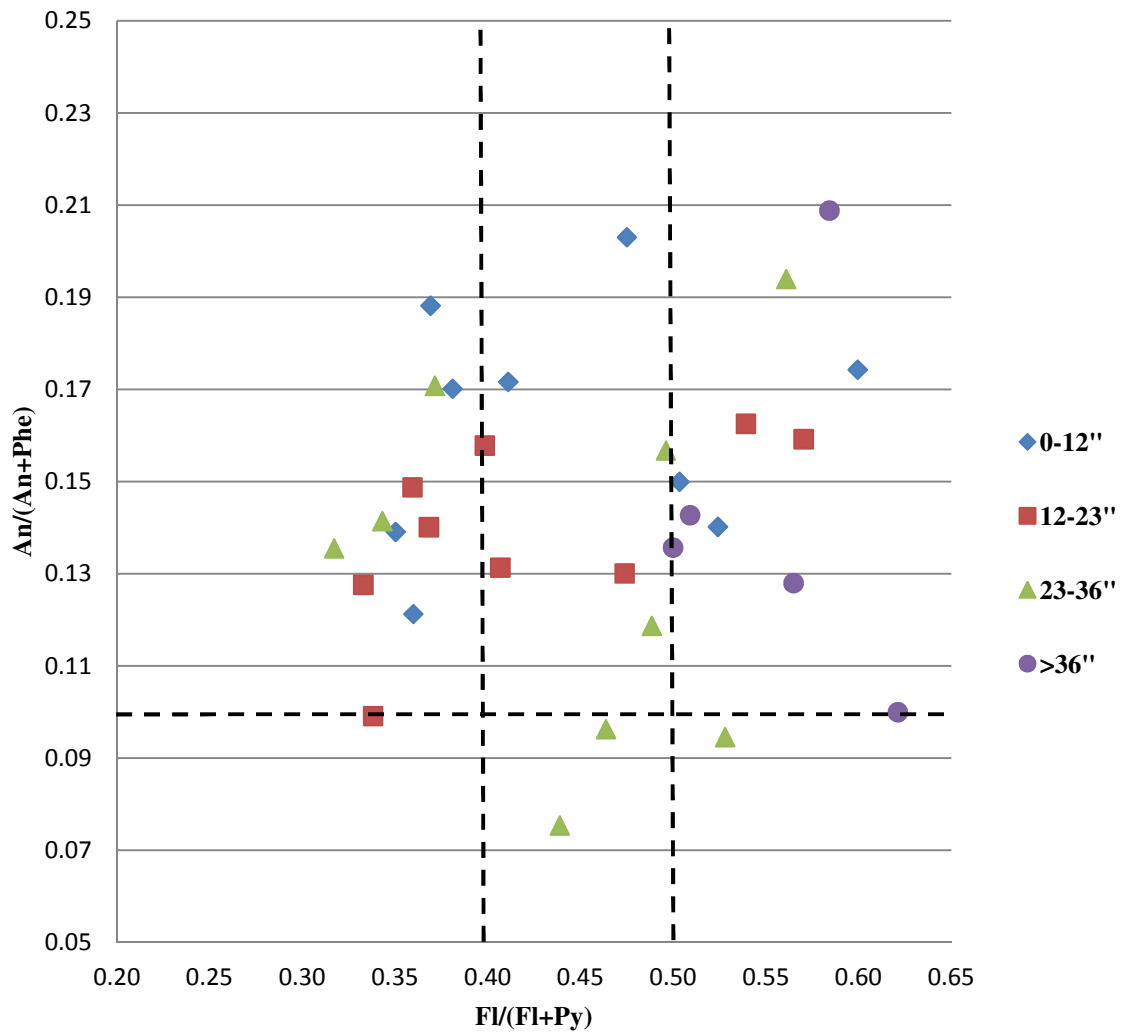


Figure 8: Diagnostic Cross-plot of An/(An+Phe) versus Fl/(Fl+Py) by Depth. 0-12", 12-23", 23-36", and >36" sectional depths. An / (An + Phe) ratio <0.1 petrogenic or >0.1 pyrogenic. Fl / (Fl + Py) ratio <0.4 petrogenic; 0.4 - 0.5 petroleum combustion (e.g., combustion engines, and furnaces); >0.5 biomass combustion (e.g., grasses, wood, or coal combustion).

An/(An+Phe) vs PI/(PI+BgP)

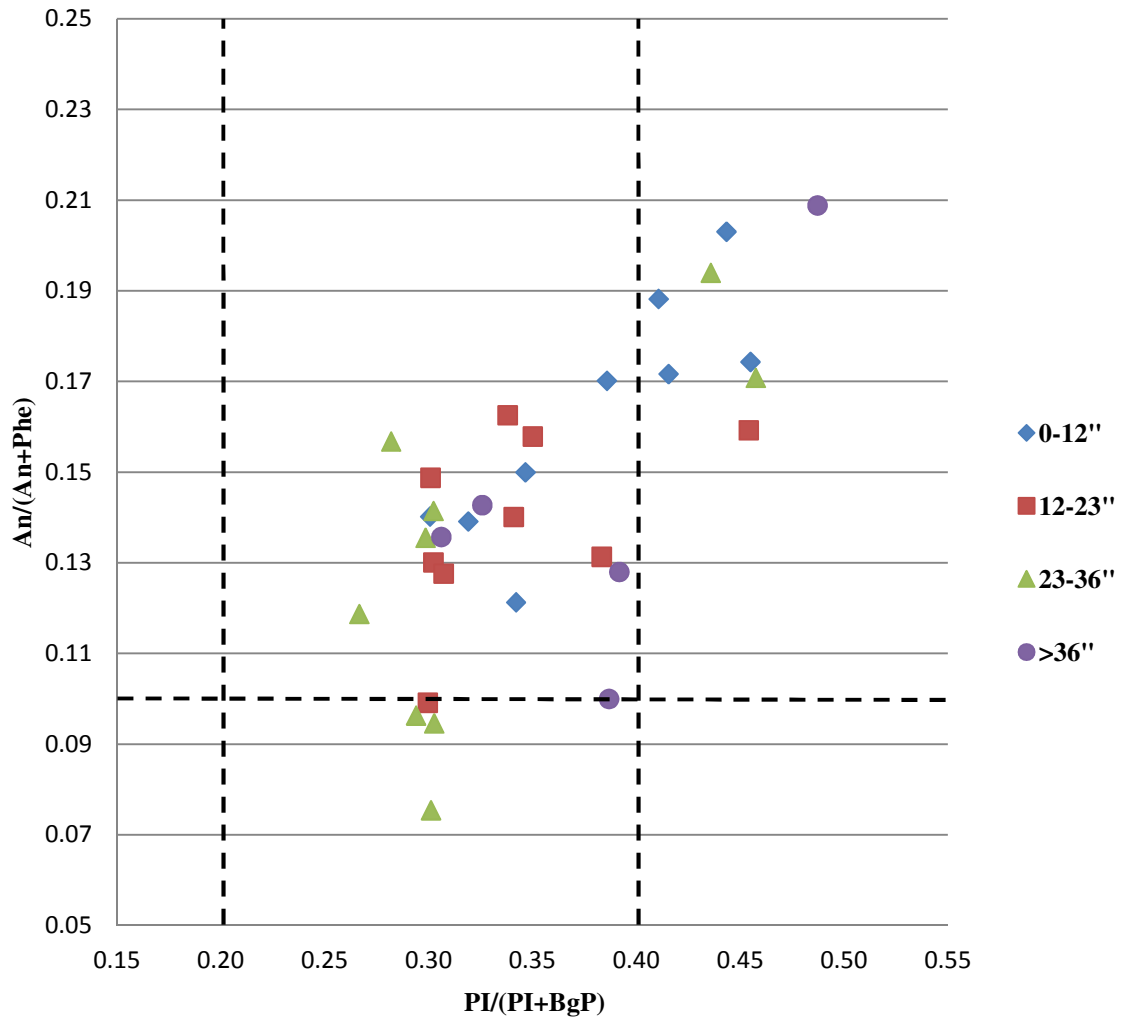
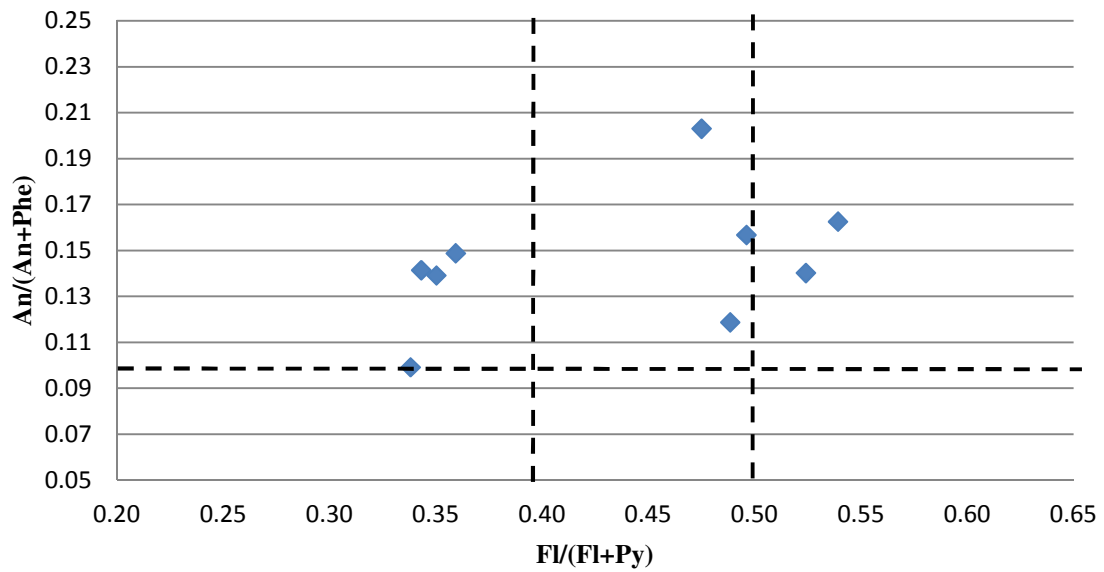


Figure 9: Diagnostic Cross-plot of An/(An+Phe) versus PI/(PI+BgP) by Depth. 0-12", 12-23", 23-36", and >36" sectional depths. An / (An + Phe) ratio <0.1 petrogenic or >0.1 pyrogenic. PI / (PI + BgP) ratio <0.2 petrogenic; 0.4 - 0.5 petroleum combustion; and >0.5 biomass combustion.

Table 8: Diagnostic Cross-plot of $Fl/(Fl+Py)$, $An/(An+Phe)$, and $PI/(PI+BgP)$ by Area

Sample Name	Flu/(Flu+Py)	An/(Phe+An)	PI/(PI+BgP)
Area 1			
FRDJ-SED-1-01-01	0.47	0.20	0.44
FRDJ-SED-1-01-12	0.54	0.16	0.34
FRDJ-SED-1-01-23	0.34	0.14	0.30
FRDJ-SED-1-02-01	0.52	0.14	0.30
FRDJ-SED-1-02-12	0.34	0.10	0.30
FRDJ-SED-1-02-23	0.49	0.12	0.27
FRDJ-SED-1-03-01	0.35	0.14	0.32
FRDJ-SED-1-03-12	0.36	0.15	0.30
FRDJ-SED-1-03-23	0.50	0.16	0.28
Area 2			
FRDJ-SED-2-01-01	0.41	0.17	0.42
FRDJ-SED-2-01-12	0.37	0.14	0.34
FRDJ-SED-2-01-23	0.53	0.09	0.30
FRDJ-SED-2-02-01	0.38	0.17	0.39
FRDJ-SED-2-02-12	0.40	0.16	0.35
FRDJ-SED-2-02-23	0.32	0.14	0.30
FRDJ-SED-2-02-3T	0.50	0.14	0.31
FRDJ-SED-2-03A-01	0.60	0.17	0.45
FRDJ-SED-2-03A-12	0.47	0.13	0.30
FRDJ-SED-2-03A-23	0.46	0.10	0.29
FRDJ-SED-2-03A-3T	0.51	0.14	0.33
Area 3			
FRDJ-SED-3-01-01	0.37	0.19	0.41
FRDJ-SED-3-01-12	0.41	0.13	0.38
FRDJ-SED-3-01-23	0.44	0.08	0.30
FRDJ-SED-3-01-3T	0.56	0.13	0.39
FRDJ-SED-3-02-01	0.50	0.15	0.35
FRDJ-SED-3-02-12	0.57	0.16	0.45
FRDJ-SED-3-02-23	0.37	0.17	0.46
FRDJ-SED-3-02-3T	0.62	0.10	0.39
FRDJ-SED-3-03-01	0.36	0.12	0.34
FRDJ-SED-3-03-12	0.33	0.13	0.31
FRDJ-SED-3-03-23	0.56	0.19	0.44
FRDJ-SED-3-03-3T	0.58	0.21	0.49

Area 1



Area 2

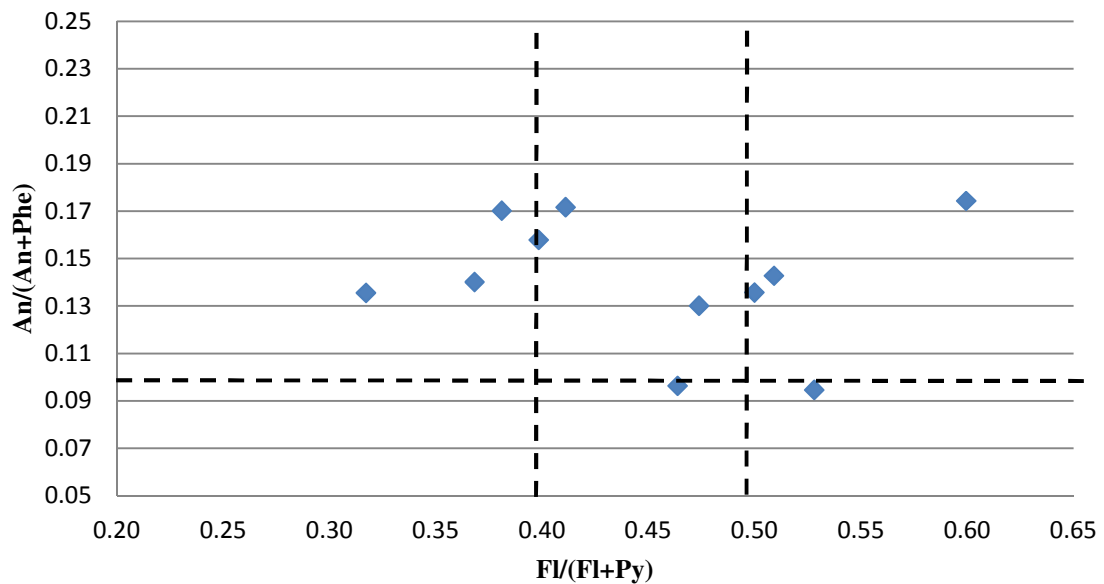


Figure 10: Diagnostic Cross-plot of $An/(An+Phe)$ versus $Fl/(Fl+Py)$ by Area. Figure 10 display PAH sources based on regional input. $An / (An + Phe)$ ratio <0.1 petrogenic or >0.1 pyrogenic. $Fl / (Fl + Py)$ ratio <0.4 petrogenic; $0.4 - 0.5$ petroleum combustion (e.g., combustion engines, and furnaces); >0.5 biomass combustion (e.g., grasses, wood, or coal combustion).

Area 3

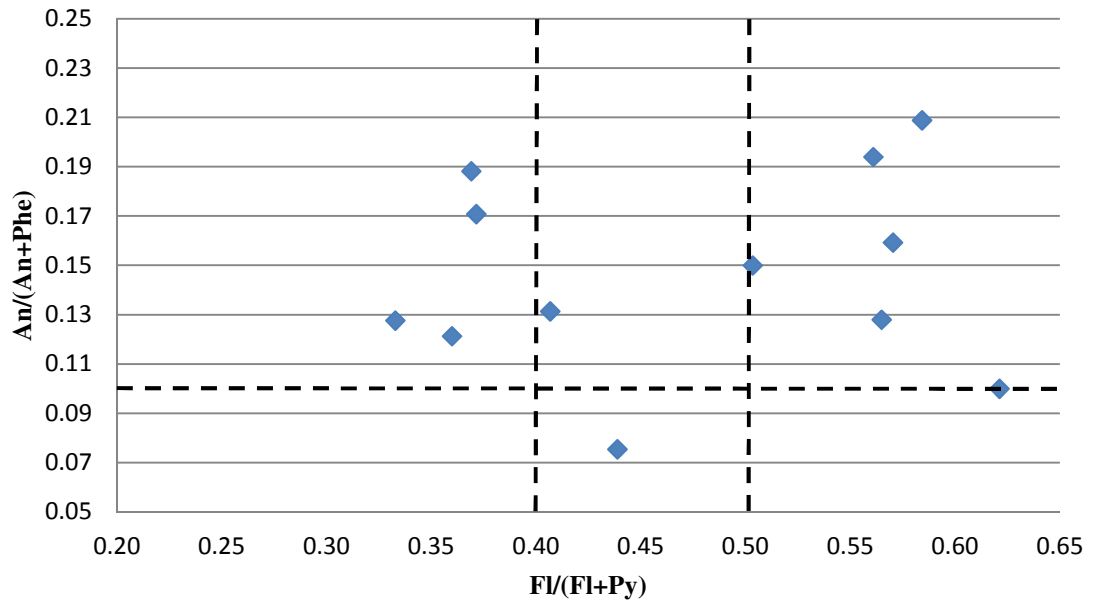


Figure 10: Continued.

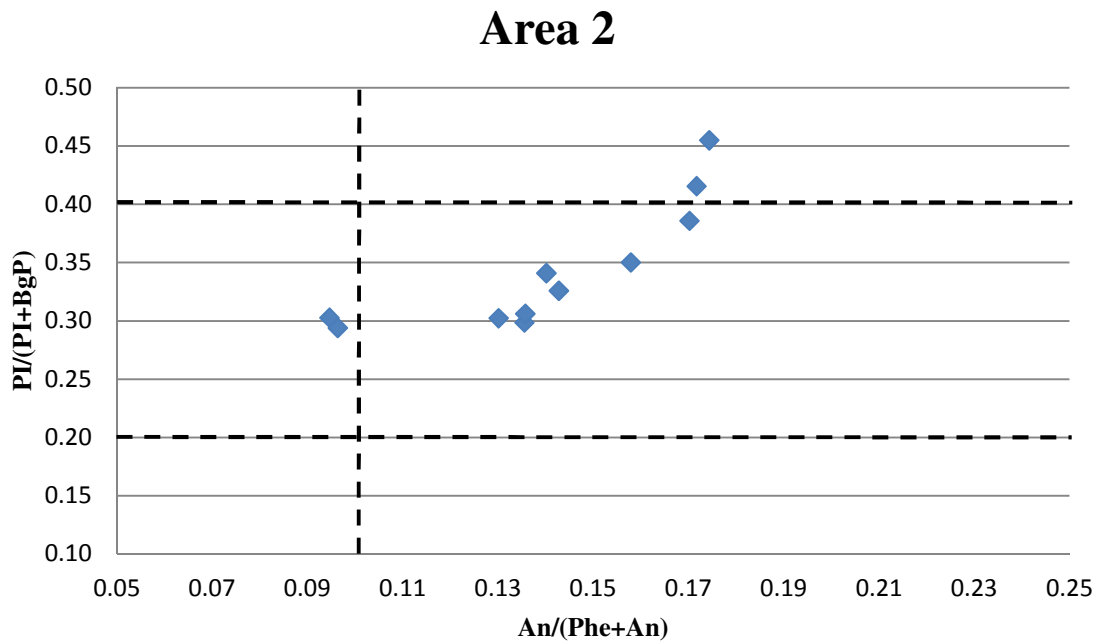
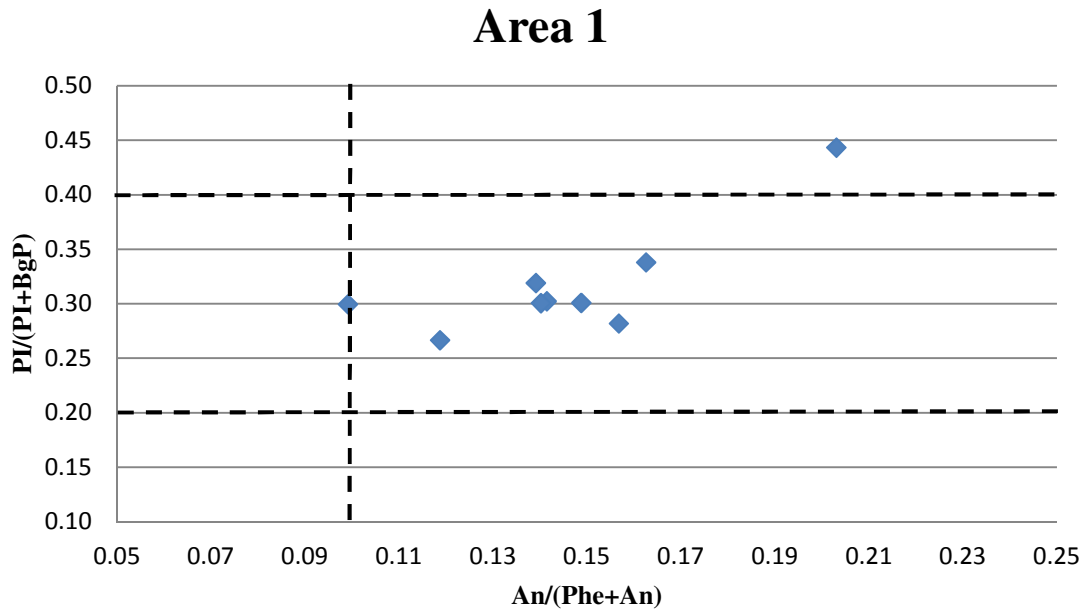


Figure 11: Diagnostic Cross-plot of $An/(An+Phe)$ versus $PI/(PI+BGP)$ by Area. Figure 11 display PAH sources based on regional input. $An / (An + Phe)$ ratio <0.1 petrogenic or >0.1 pyrogenic. $PI / (PI + BgP)$ ratio <0.2 petrogenic; $0.4 - 0.5$ petroleum combustion; and > 0.5 biomass combustion.

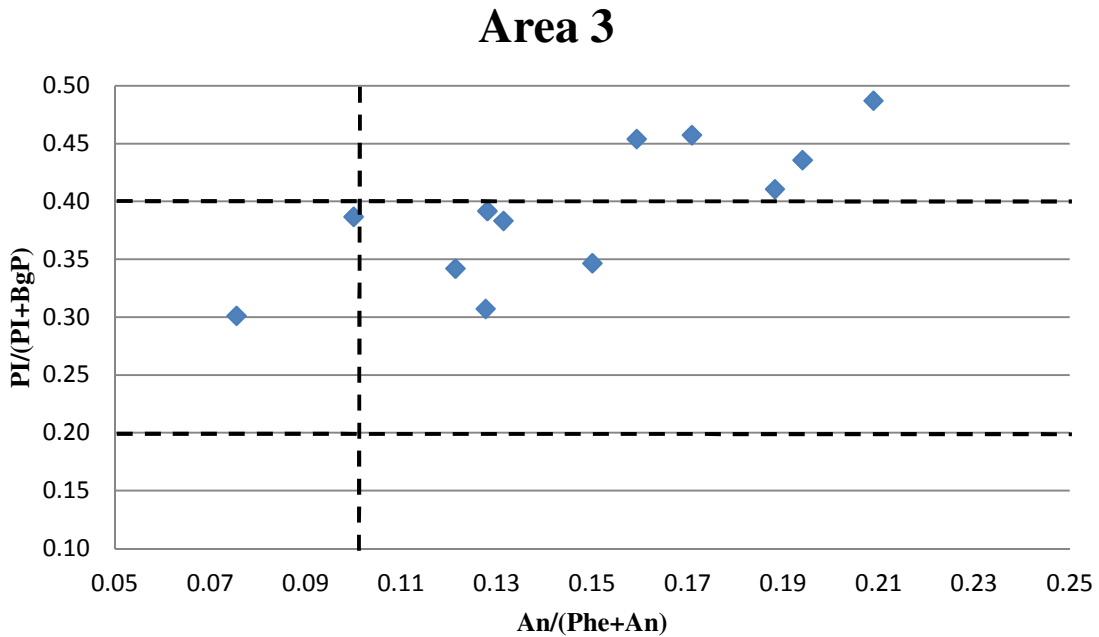


Figure 11: Continued

5.5. Toxicological Evaluation

A TEF toxicity evaluation was conducted for seven carcinogenic and ten non-carcinogenic analytes for core section FRDJ-SED-3-03-12 (**Table 9**). The benzo[a]pyrene equivalency quotient was summed for these seventeen analytes, totaling 2,435 ng/g-dry. The calculated carcinogenic potency of dibenzo[a,h]anthracene and benzo[a]pyrene are 46.6% and 39.4% of the PAH concentrations within core section FRDJ-SED-3-03-12.

In accordance with the Wisconsin governmental standards issued by the Wisconsin Department of Natural Resources, the PAH concentrations are normalized to 1% TOC for PAHs of interest (WDNR 2003). After normalization the new PAH value is 1,520 ng/g-dry at 1% TOC.

Table 9: Toxic Equivalency Factors for Lower Fox River Core Section FRDJ-SED-3-03-12 (Area 3)

PAHs of Interest	Sediment Concentration (ng/g dry)	Toxic Equivalency Factor (TEF)	Benzo(a)pyrene Equivalent Quotient (ng/g dry wt.)	Sediment Concentration at 1% TOC (ng/g dry wt.) [TOC = 8.6%]
Dibenzo(a,h)anthracene	213.8	5.0	1,069	24.86
Benzo(a)pyrene	904.9	1.0	904.9	105.2
Benz(a)anthracene	1,279	0.1	127.9	148.8
Benzo(b)fluoranthene	802.6	0.1	80.26	93.32
Benzo(k,j)fluoranthene	317.8	0.1	31.78	36.96
Chrysene/Triphenylene	1,575	0.1	157.5	183.2
Indeno(1,2,3-c,d)pyrene	447.2	0.1	44.72	51.99
Anthracene	225.5	0.01	2.255	26.22
Benzo[g,h,i]perylene	1,008	0.01	10.08	117.2
Acenaphthene	87.36	0.001	0.0874	10.16
Acenaphthylene	140.5	0.001	0.1405	16.34
Flroranthene	1,020	0.001	1.020	118.6
Fluorene	207.5	0.001	0.2075	24.13
2-Methylnaphthalene	630.4	0.001	0.6304	73.30
Naphthalene	627.3	0.001	0.6273	72.95
Phenanthrene	1,541	0.001	1.541	179.2
Pyrene	2,044	0.001	2.044	237.7
Sum of 17 PAHs	12,860		2,435	1,520

Subsequently, TEF values were also calculated for core sections from area 1 and area 2 which contained high PAH concentrations. FRDJ-SED-1-03-12 (area 1) and FRDJ-SED-2-03A-23 (area 2) TEF values were 2,294 ng/g-dry (1,073 ng/g-1% TOC) and 1,694 ng/g-dry (491.8 ng/g-1% TOC), respectively. These three core sections exceed the Comprehensive Environmental Response, Compensation, and Liability Act (CERCLA) Method B cleanup level for benzo(a)pyrene of 137 ng/g. However, based on normalization to 1% TOC, the cores do not exceed the Wisconsin Department of Natural Resources' (WDNR) threshold effect concentration (TEC) for PAHs which is 1,610 ng/g at 1% TOC.

6. CONCLUSIONS AND IMPLICATIONS OF RESEARCH

Extracts of the NRT core sections contained signatures of parent and alkylated PAHs. The source of PAH influx is primarily pyrogenic with a complex mixture of coal, biomass, and petroleum combustion residuals. All core sections contained an elevated concentration of chrysenes, pyrenes, fluoranthenes, and C4-phenanthrenes/anthracenes -- classic indicators of conifer trees, coal tar, industrial manufacturing, transportation, and paper mill refuse (Koistinen et al. 1998). PAH ratios suggest a correlated high influx of petroleum combustion and biomass combustion sources which are indicated by the distribution of HMW PAHs and cross-plots of anthracene / (anthracene + phenanthrene), indeno(1,2,3-c,d)pyrene / (indeno(1,2,3-c,d)pyrene + benzo(g,h,i)perylene), benzo[a]anthracene / (benzo[a]anthracene + chrysene), anthracene / (anthracene + chrysene), and fluoranthene / (fluoranthene + pyrene).

The presence of C0, C1, and C2 alkylated analytes are a strong indication of combustion with a limited degree of degradation. Total carbon, EOM, and saturated hydrocarbon data supports the PAH data indicating high inputs of organic substrate with odd-numbered n-alkanes suggesting terrestrial or aquatic plant origin.

The TEQ of PAH concentrations within the river sediments (area 1, area 2 and area 3) exceed the CERCLA Method B levels of 137 ng/g due to high influxes of the seven PAHs classified as B2 carcinogens present in the river sediment:

benzo[a]anthracene, benzo[a]pyrene, benzo[b]fluoranthene, benzo[k]fluoranthene, chrysene, dibenzo[a,h]anthracene, and indeno[1,2,3-c,d]pyrene, as well as non-

carcinogens such as phenanthrene, pyrene, and naphthalenes. However, based on normalization to 1% TOC the cores do not exceed the WDNR threshold effect concentration (TEC) for PAHs.

To prevent concentrations from exceeding the TEC, continual monitoring and further research of PAH concentrations is required. Future sample collections should allow for a comparison to this research. This study incorporates biomarker fingerprinting, source identification, and toxicological evaluation tools to investigate hydrocarbon concentrations within the Lower Fox River sediments. The use of this research may provide useful and relevant information in similar environments and situations with samples containing unknown concentrations of hydrocarbon contamination.

To better understand past, present, and future distribution-accumulation of hydrocarbons within the Lower Fox River, additional sampling is required. Runoff from urban and rural roadways, diesel and gasoline combustion engines, household heating, and commercial-industrial byproducts accumulate within Lower Fox River sediments. Future monitoring is needed to examine the extent of the incursion and toxicological effects posed by hydrocarbon concentrations within the Lower Fox River basin. Future sample collections would allow for a comparison of PAHs, ALI, UCM, TPH, and C30-hopane concentrations to this research in order to gain insight into hydrocarbon migration, influx, accumulation, degradation and depletion within the Lower Fox River.

Based on this research, the following recommendations are proposed: 1) Future confirmation analysis of river sediments within the Lower Fox River; and 2) More stringent efforts are needed to reduce or prevent hydrocarbon contamination from entering and accumulating in Lower Fox River sediments. Due to the limited literature available, these recommendations are based on a single coring event. In order to establish and confirm a trend, future analysis and continual monitoring of the Lower Fox River basin is necessary. Runoff, refuse, discharge, and spills should be monitored and remediated. Efforts by the state of Wisconsin to establish additional measures would help to reduce hydrocarbon accumulation within the Lower Fox River remediation zone which is currently focused on PCB contamination.

REFERENCES

- Bastami, K. D., Afkhami, M., Ehsanpour, M., Mohammadizadeh, M., Haghparast, S., Soltani, F., et al. 2014. Polycyclic Aromatic Hydrocarbons in the Coastal Water, Surface Sediment and Mullet *Liza Klunzingeri* from Northern part of Hormuz Strait (Persian Gulf). *Marine Pollution Bulletin*, 76: 411-416.
- Bence, A., Page, D., and P. Boehm. 2007. Advances in Forensic Techniques for Petroleum Hydrocarbons: The *Exxon Valdez* Experience. *Oil Spill Environmental Forensics: Fingerprinting and Source Identification*, 449-487. Amsterdam: Elsevier/Academic Press.
- Boehm, P., Douglas, G., Burns, W., Mankiewicz, P., Page, D., and A. Bence. 1997. Application of Petroleum Hydrocarbon Chemical Fingerprinting and Allocation Techniques after the Exxon Valdez Oil Spill. *Marine Pollution Bulletin*, 34: 599-613.
- Crane, J. 2014. Source Apportionment and Distribution of Polycyclic Aromatic Hydrocarbons, Risk Considerations, and Management Implications for Urban Storm Water Pond Sediments in Minnesota, USA. *Archives of Environmental Contamination and Toxicology*, 66: 176-200.
- Dević, G., and B. Jovančićević. 2008. The Diagenesis of Plant Lipids during the Formation of the Krepoljin Coal Basin (Serbia) - Using Multivariate Statistical Analysis in the Saturated Biomarkers. *Acta Geologica Sinica - English Edition*, 82: 1168-1178.
- Dvorská, A., Lammel, G., and J. Klánová. 2011. Use of diagnostic ratios for studying source apportionment and reactivity of ambient polycyclic aromatic hydrocarbons over Central Europe. *Atmospheric Environment*, 45: 420-427.
- Egubbe, P., Iwegbue, C., Ogala, J., Nwajei, G., and S. Egboh. 2014. Distribution of Polycyclic Aromatic Hydrocarbons (PAHs) in Sediment Cores of Selected Creeks in Delta State, Nigeria. *Environmental Forensics*, 15: 121-133.
- Google Maps. (2015). [Wisconsin] [Street map]. Retrieved from <https://www.google.com/maps/place/Wisconsin/@44.7862968,-89.8267049,7z/data=!3m1!4b1!4m2!3m1!1s0x52a8f40f9384e3af:0xf2d5d5b8f88649d6>
- Hamilton, S. and J. Cline. 1981. Hydrocarbons Associated with Suspended Matter in the Green River, Washington. NOAA Technical Memorandum ERL PMEL-30, Boulder, Colorado: U.S. Dept. of Commerce, National Oceanic and Atmospheric Administration, Environmental Research Laboratories.

- Haven, H., Rullkötter, J., De Leeuw, J., and J. Damsté. 1988. Pristane/Phytane Ratio as Environmental Indicator. *Nature*, 333: 604-604.
- Herbstman, J., Tang, D., Zhu, D., Qu, L., Sjödin, A., Li, Z., Camann, D., and F. Perera. 2012. Prenatal Exposure to Polycyclic Aromatic Hydrocarbons, Benzo[a]pyrene–DNA Adducts, and Genomic DNA Methylation in Cord Blood. *Environmental Health Perspectives*, 120: 733-738.
- Iqbal, J., Overton, E., and D. Gisclair. 2008a. Polycyclic Aromatic Hydrocarbons in Louisiana Rivers and Coastal Environments: Source Fingerprinting and Forensic Analysis. *Environmental Forensics*, 9: 63-74.
- Iqbal, J., Overton, E., and D. Gisclair. 2008b. Sources of Polycyclic Aromatic Hydrocarbons in Louisiana Rivers and Coastal Environments: Principal Components Analysis. *Environmental Forensics*, 9: 310-319.
- Koistinen, J., Lehtonen, M., Tukia, K., Soimasuo, M., Lahtiperä, M., and A. Oikari. 1998. Identification of Lipophilic Pollutants Discharged from a Finnish Pulp and Paper Mill. *Chemosphere*, 37: 219–235.
- Lichtfouse, É., Derenne, S., Mariotti, A., and C. Largeau. 1994. Possible algal origin of long chain odd n-alkanes in immature sediments as revealed by distributions and carbon isotope ratios. *Organic Geochemistry*, 22: 1023-1027.
- Liu, W. X., Dou, H., Wei, Z. C., Chang, B., Qiu, W. X., Liu, Y., et al. 2009. Emission Characteristics of Polycyclic Aromatic Hydrocarbons from Combustion of Different Residential Coals in North China. *Science of the Total Environment*: 407, 1436-1446.
- Mills, M., McDonald, T., Bonner, J., Simon, M., and R. Autenrieth. 1999. Method for Quantifying the Fate of Petroleum in the Environment. *Chemosphere*: 39, 2563-2582.
- Mount, D., Ingersoll, C., and J. McGrath. 2003. "Approaches to Developing Sediment Quality Guidelines for PAHs." In *PAHs: an ecotoxicological perspective*, Douben, P. E., 331-355. Chichester: Wiley.
- Nisbet, I. and P. Lagoy, 1992. Toxic Equivalency Factors (TEFs) for Polycyclic Aromatic Hydrocarbons (PAHs). *Regulatory Toxicology and Pharmacology*, 16: 290-300. Lincoln, Massachusetts: I.C. T. Nisbet & Company.
- Peters, K., and C. Walters. 2005. "Non-biomarker maturity parameters." In *The Biomarker Guide*. 2nd ed., 1155. Cambridge, UK: Cambridge University Press.
- Powell, T. 1988. Pristane/Phytane Ratio as Environmental Indicator. *Nature*, 333: 604-604.

- Prince, R. and C. Walters. 2007. Biodegradation of Oil Hydrocarbons and Its Implications for Source Identification. *Oil Spill Environmental Forensics: Fingerprinting and Source Identification*, 349-379. Amsterdam: Elsevier/Academic Press.
- Ramírez, N., Cuadras, A., Rovira, E., Marcé, R., and F. Borrull. 2011. Risk Assessment Related to Atmospheric Polycyclic Aromatic Hydrocarbons in Gas and Particle Phases near Industrial Sites. *Environmental Health Perspectives*, 119: 1110-1116.
- Readman, J., Fillman, G., Tolosa, I., Bartocci, J., Villeneuve, J., Catinni, C., Mee, L., 2002. Petroleum and PAH contamination in the Black Sea. *Marine Pollution Bulletin*, 44: 48–62.
- Reeves, W., Barhoumi, R., Burghardt, R., Lemke, S., Mayura, K., McDonald, T., Phillips, T., and K. Donnelly. 2001. Evaluation of Methods for Predicting the Toxicity of Polycyclic Aromatic Hydrocarbon Mixtures. *Environmental Science & Technology*, 35: 1630-636.
- Shen, J. and W. Huang. 2007. Biomarker Distributions as Maturity Indicators in Coals, Coaly Shales, and Shales From Taiwan. *Terrestrial Atmosphere Ocean Sciences*, 18: 739-755.
- Short, J., Kvenvolden, K., Carlson, P., Hostettler, F., Rosenbauer, R., and B. Wright. 1998. Natural Hydrocarbon Background in Benthic Sediments of Prince William Sound, Alaska: Oil vs Coal. *Environmental Science & Technology*, 33: 34-42.
- Uhler, A., Emsbo-Mattingly, S., Liu, B., Hall Jr., L., and D. Burton. 2005. An Integrated Case Study for Evaluating the Impacts of an Oil Refinery Effluent on Aquatic Biota in the Delaware River: Advanced Chemical Fingerprinting of PAHs. *Human and Ecological Risk Assessment*, 11: 771-836.
- Uhler, A., Stout, S., and G. Douglas. 2007. Chemical Heterogeneity in Modern Marine Residual Fuel Oils. *Oil Spill Environmental Forensics: Fingerprinting and Source Identification*, 327-348. Amsterdam: Elsevier/Academic Press.
- USDHHS (U.S. Department of Health and Human Services), ATSDR (Agency for Toxic Substances and Disease Registry). 1995. Toxicological Profile for Polycyclic Aromatic Hydrocarbons. 1995-639-298. Washington, D.C.: U.S. United States Government Printing Office.

USEPA (U.S. Environmental Protection Agency). 2003a. Implementation. In *Procedures for the derivation of equilibrium partitioning sediment benchmarks (ESBs) for the protection of benthic organisms: PAH mixtures*. By David J. Hansen et al. EPA-600-R-02-013, Washington D.C.: Office of Research and Development, National Health and Environmental Effects Research Laboratory, Atlantic Ecology Division.

USEPA (U.S. Environmental Protection Agency). 2003b. *Recommended Toxicity Equivalence Factors (TEFs) for Human Health Risk Assessments of 2,3,7,8-Tetrachlorodibenzo-p-dioxin and Dioxin-Like Compounds*. EPA-600-R-10-005, Washington D.C.: Risk Assessment Forum.

USEPA (U.S. Environmental Protection Agency). 2013. *Fox River NRDA/PCB releases, Wisconsin* (WI0001954841).

USEPA (U.S. Environmental Protection Agency), Office of International and Tribal Affairs. 2014. *Persistent Organic Pollutants: A Global Issue, A Global Response*.

Wagener, A., Hamacher, C., Farias, C., Godoy, J., and A. Scofield. 2010. Evaluation of Tools to Identify Hydrocarbon Sources in Recent and Historical Sediments of a Tropical Bay. *Marine Chemistry*, 121: 67-79.

Wang, Z., Yang, C., Fingas, M., Hollebone, B., Yim, U., and J. Oh. 2007. Petroleum Biomarker Fingerprinting for Oil Spill Characterization and Source Identification. *Oil Spill Environmental Forensics: Fingerprinting and Source Identification*, 73-146. Amsterdam: Elsevier/Academic Press.

Wilhelms, A., Telnæs, N., Steen, A., and J. Augustson. 1998. A Quantitative Study of Aromatic Hydrocarbons in a Natural Maturity Shale Sequence - The 3-Methylphenanthrene/Retene Ratio, a Pragmatic Maturity Parameter. *Organic Geochemistry*, 29: 97-105.

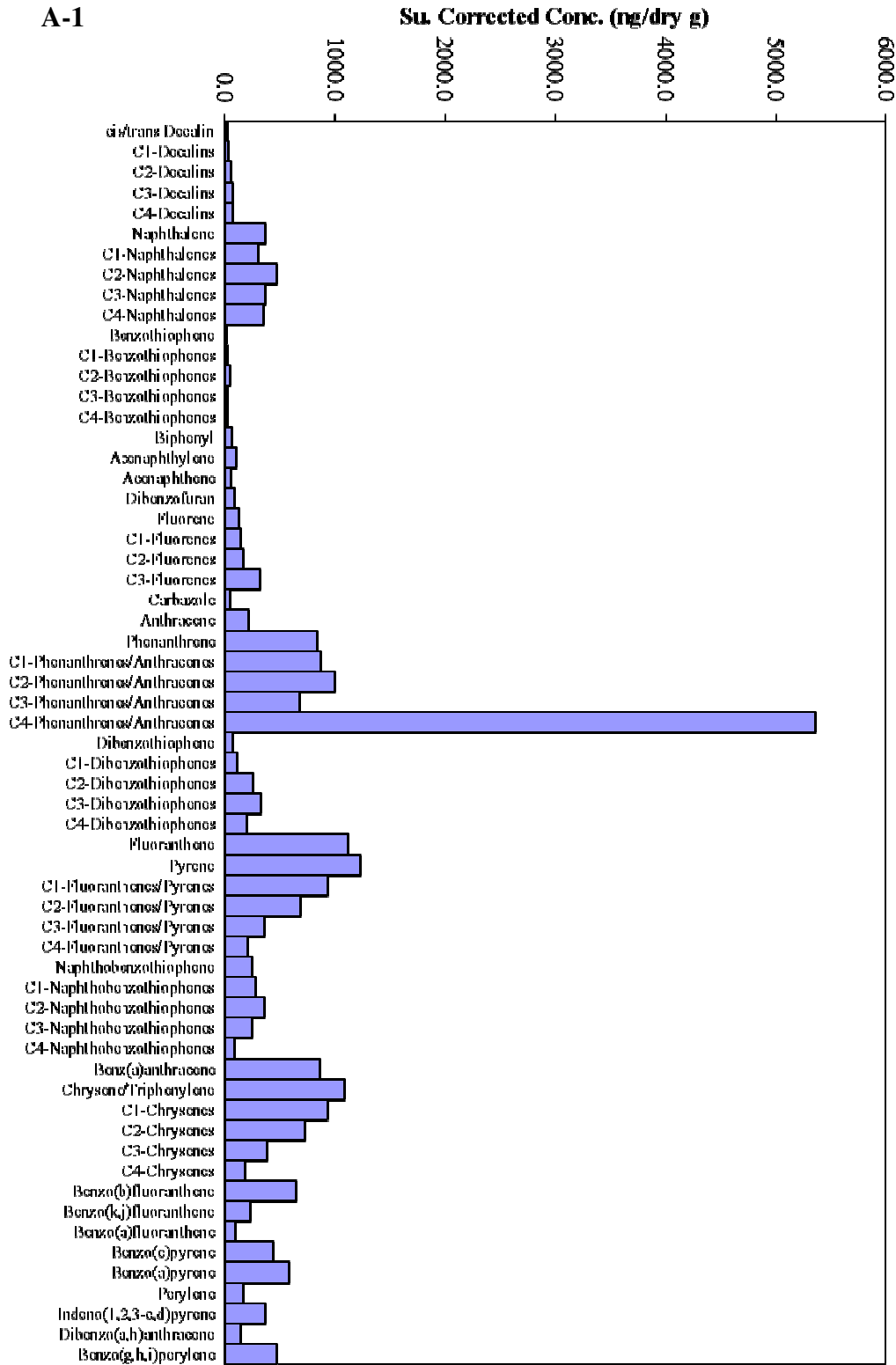
Wickliffe, J., Overton, E., Frickel, S., Howard, J., Wilson, M., Simon, B., et al. 2013. Evaluation of Polycyclic Aromatic Hydrocarbons Using Analytical Methods, Toxicology, and Risk Assessment Research: Seafood Safety after a Petroleum Spill as an Example. *Environmental Health Perspectives*: 122: 6-9.

WDNR (Wisconsin Department of Natural Resources). 2003. Consensus-Based Sediment Quality Guidelines Recommendations for Use & Application Interim Guidance. WT-732 2003. Madison, WI: Developed by the Contaminated Sediment Standing Team.

Yunker, M., Macdonald, R., Vingarzanc, R., Mitchell, R., Goyette, D., and S. Sylvestrec. 2002. PAHs in the Fraser River Basin: a Critical Appraisal of PAH Ratios as Indicators of PAH Source and Composition. *Organic Geochemistry*, 33: 489-515.

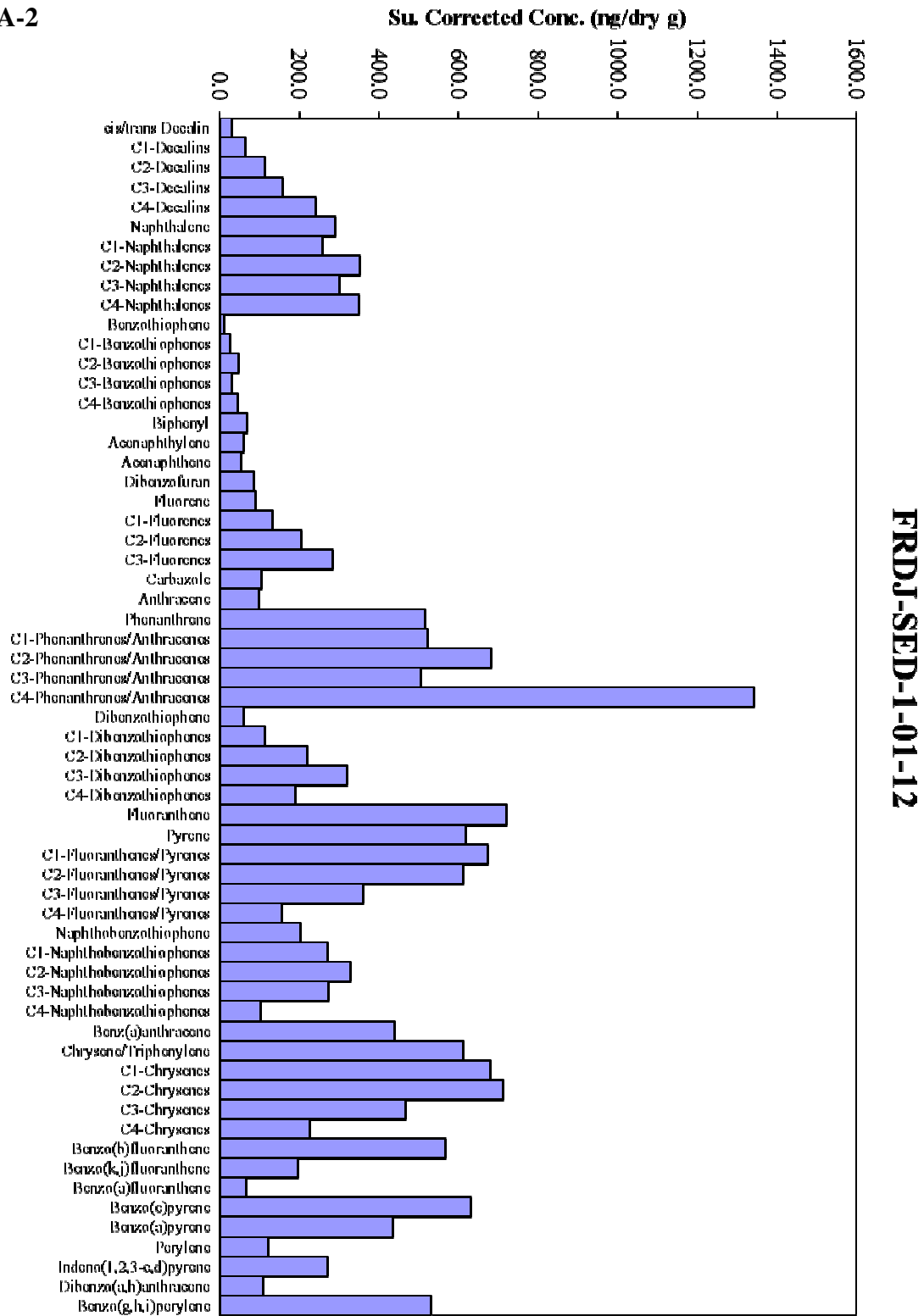
APPENDIX A

A-1

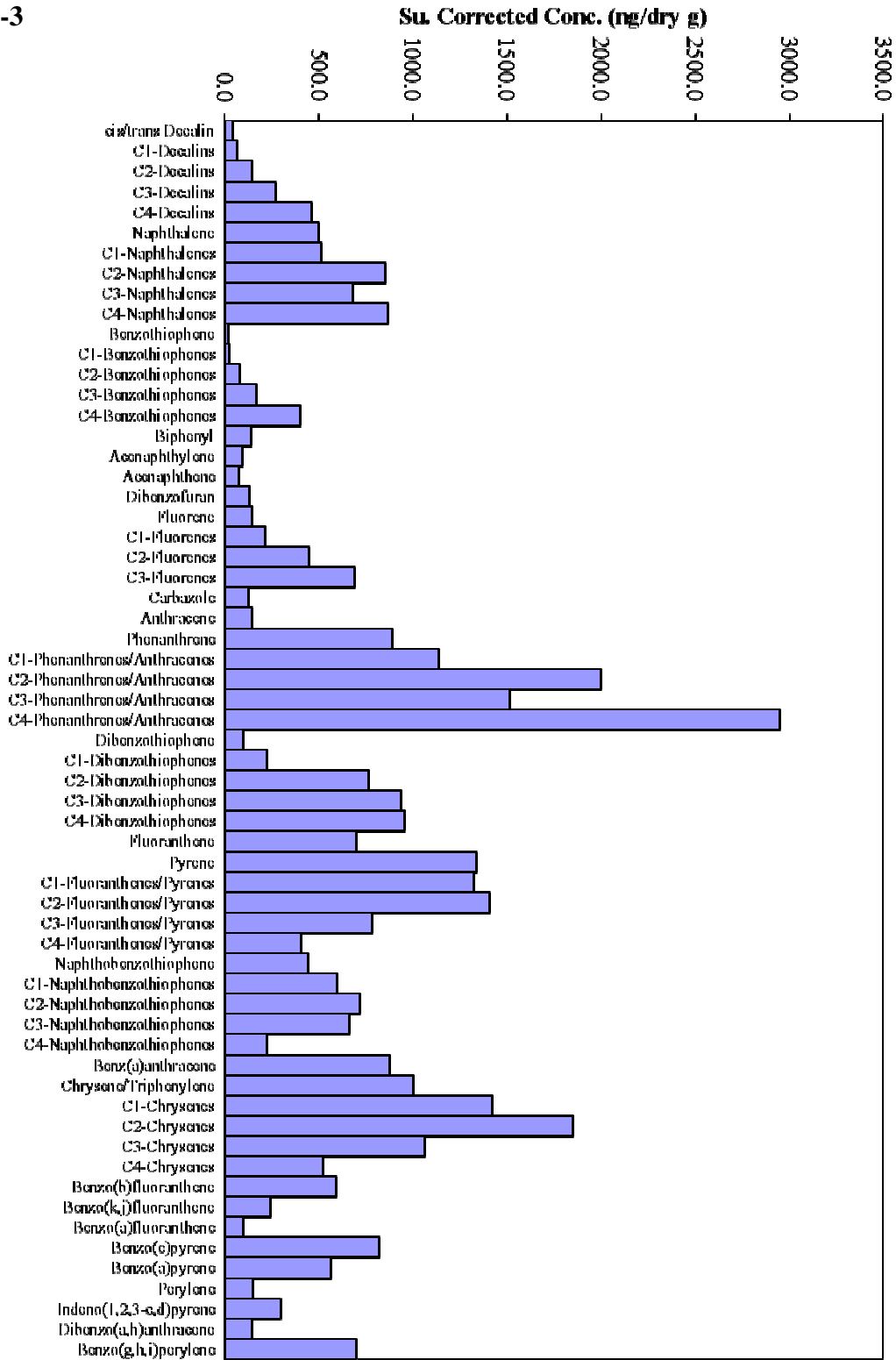


FRDJ-SED-1-01-01

A-2

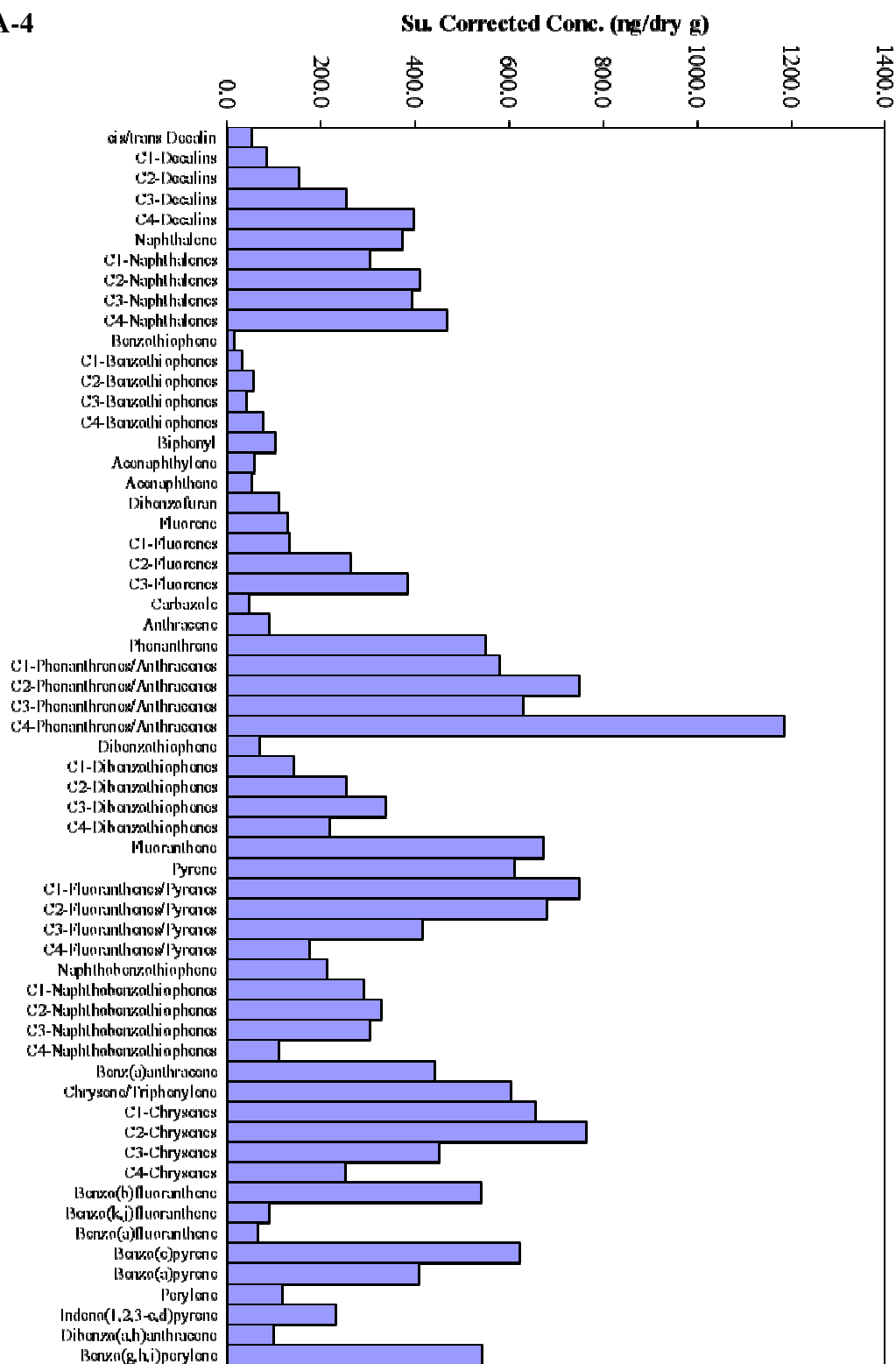


A-3



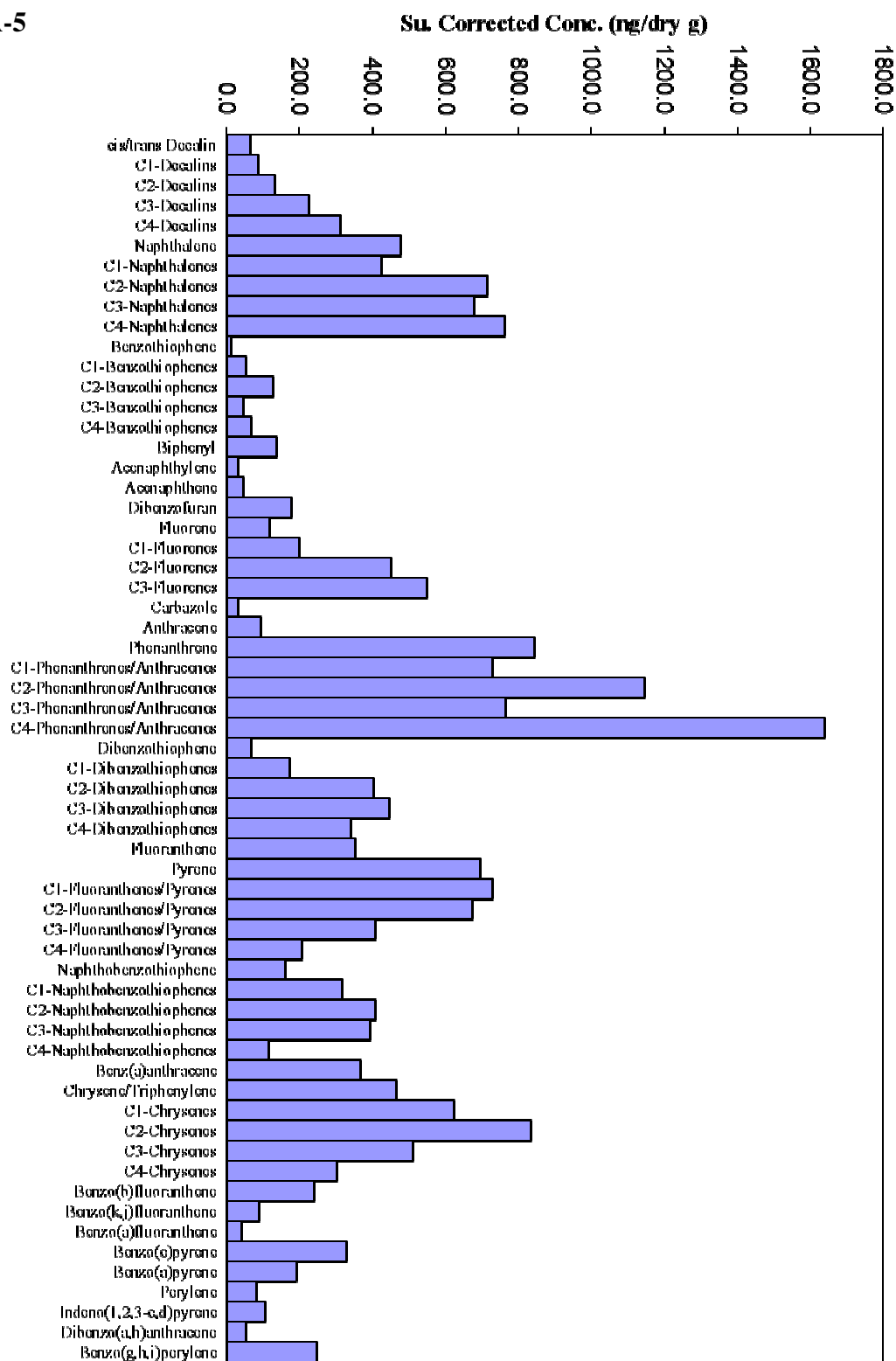
FRDJ-SED-1-01-23

A-4

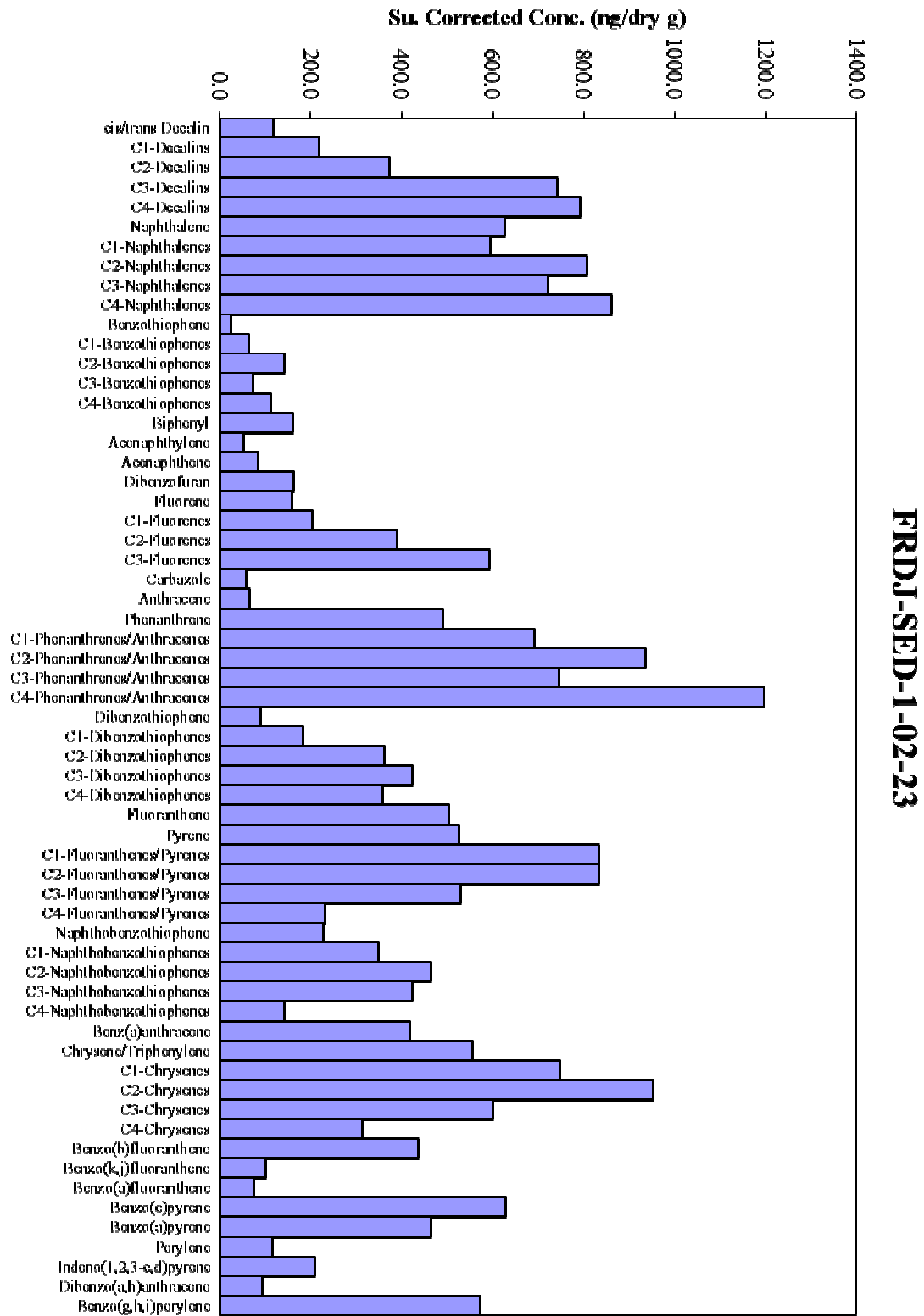


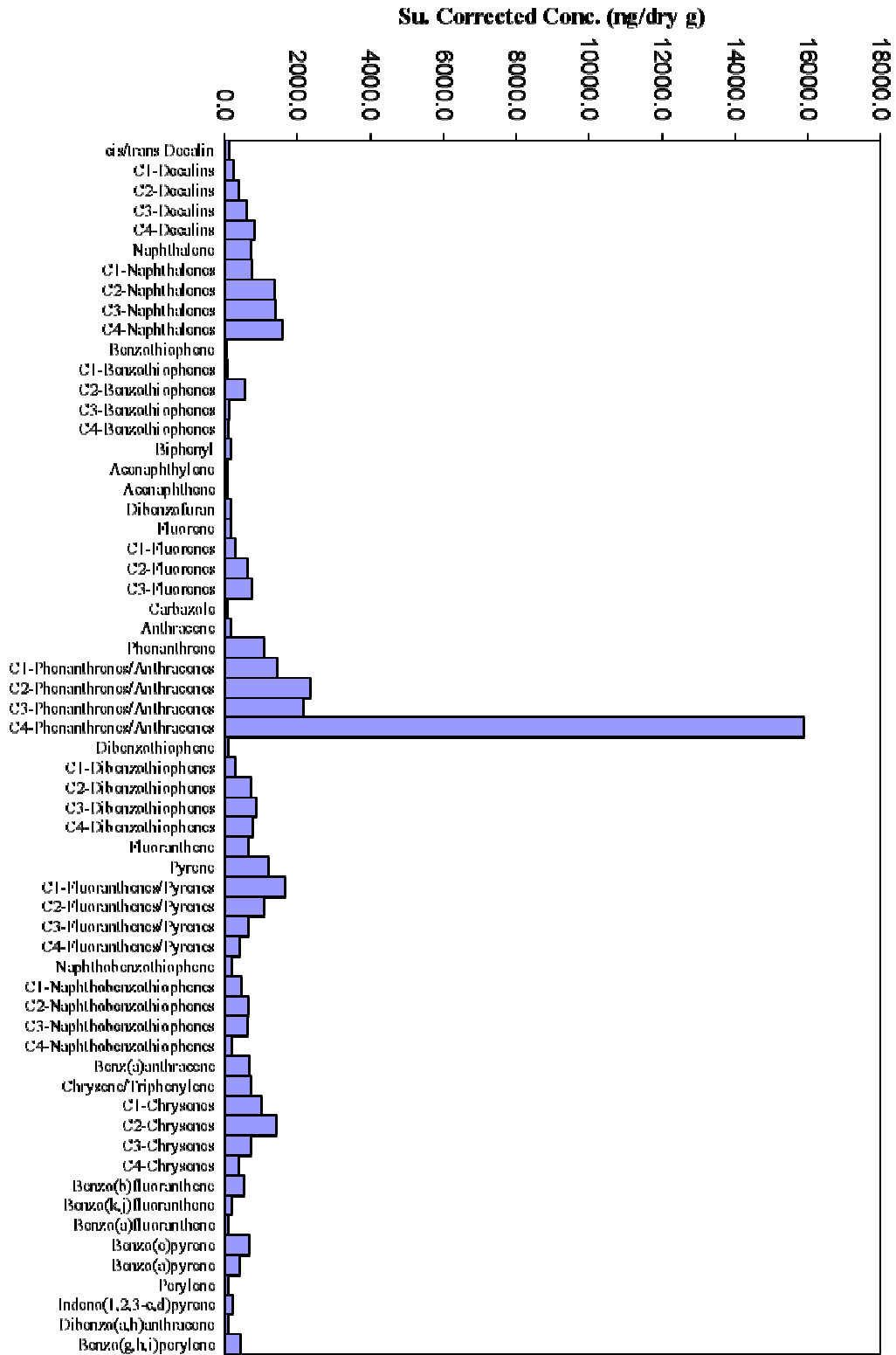
FRDJ-SED-1-02-01

A-5

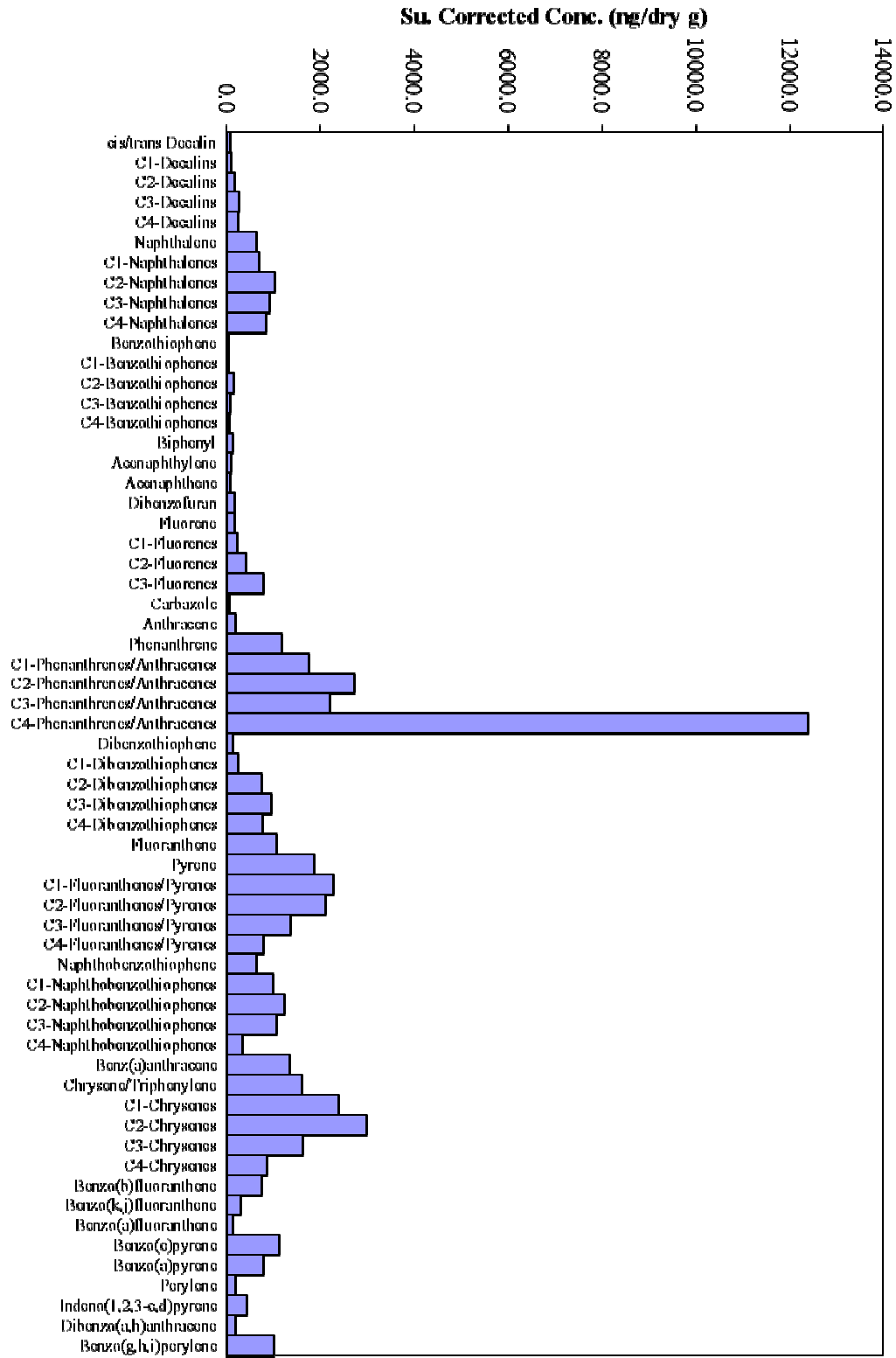


FRDJ-SED-1-02-12

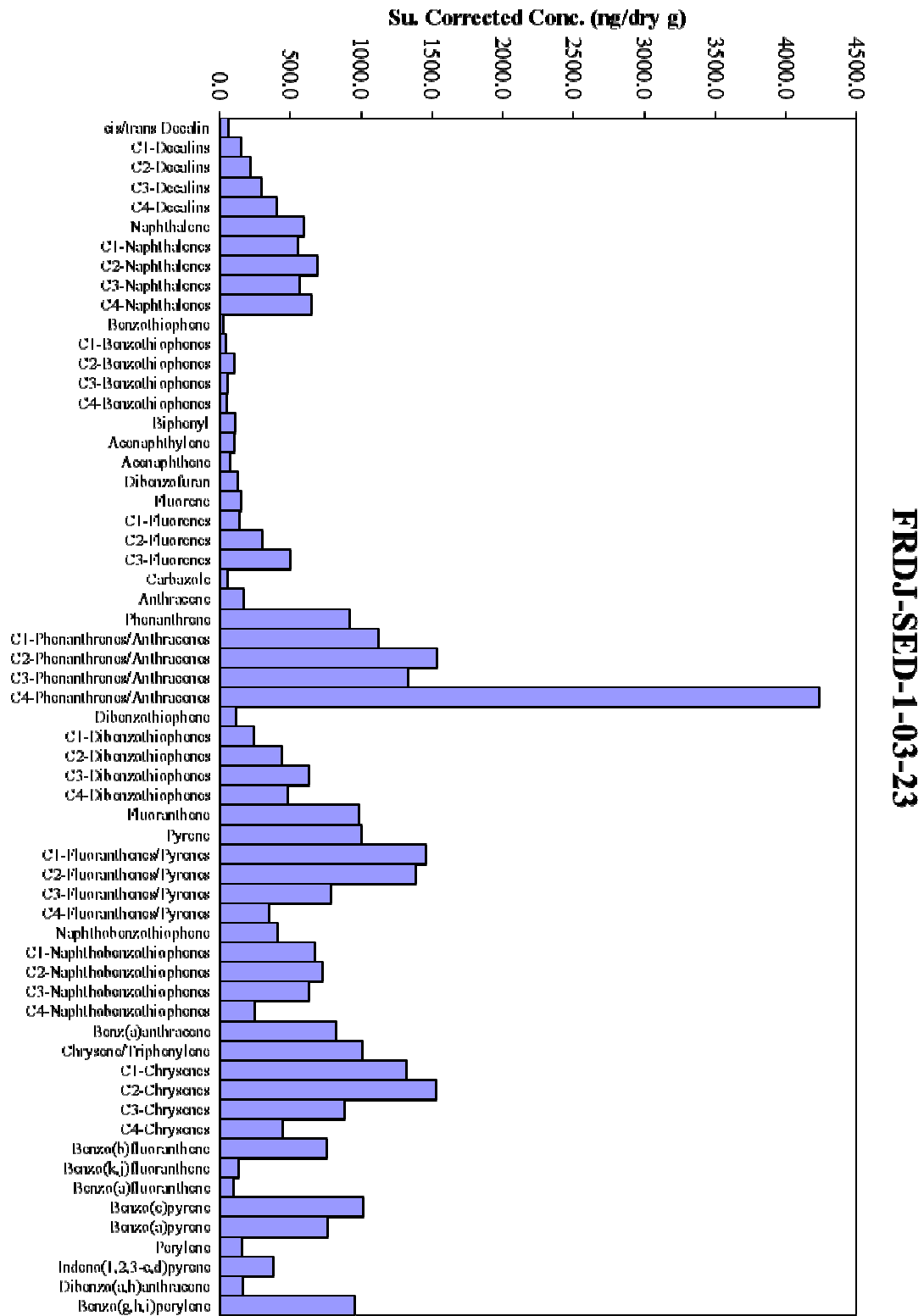


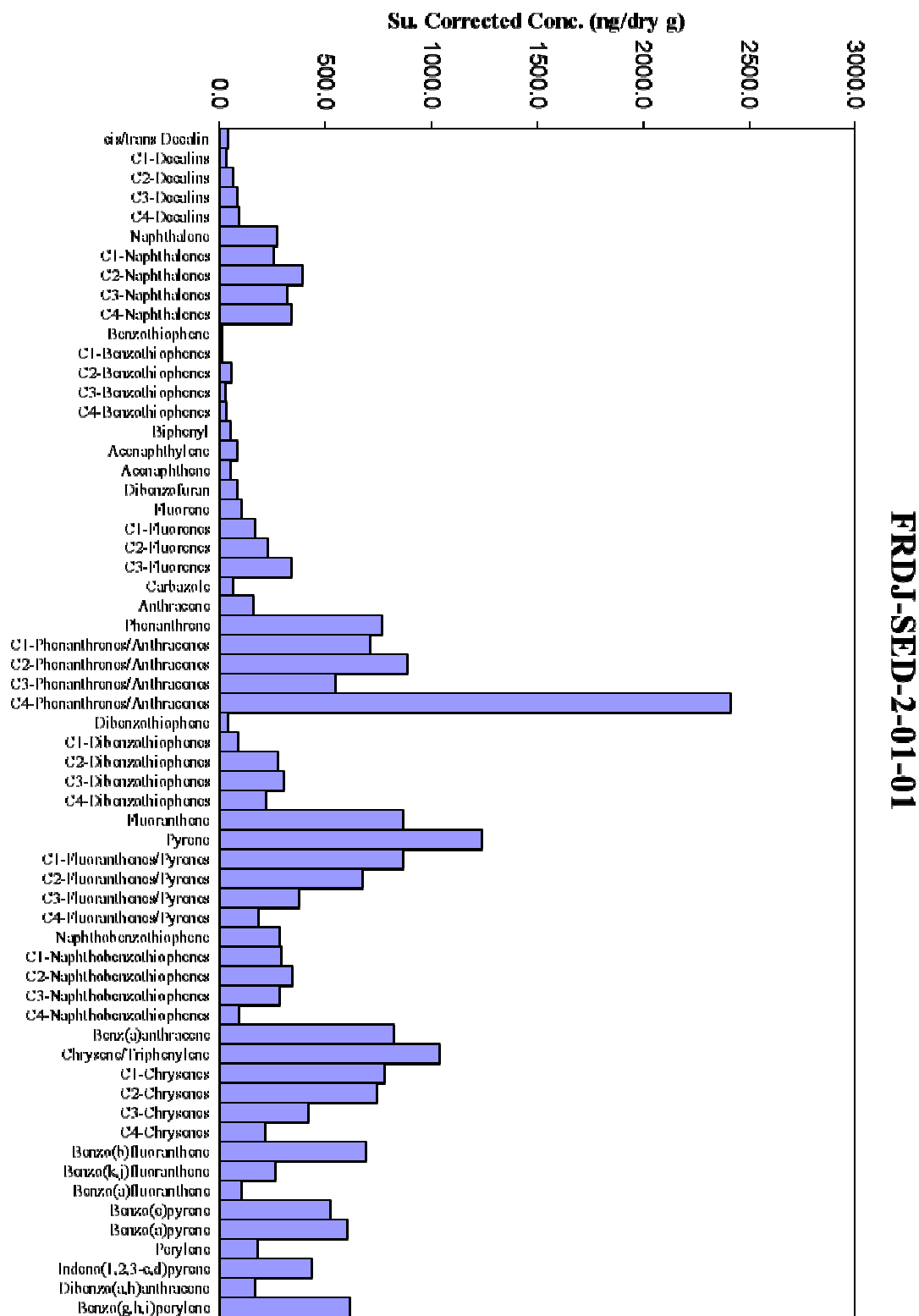


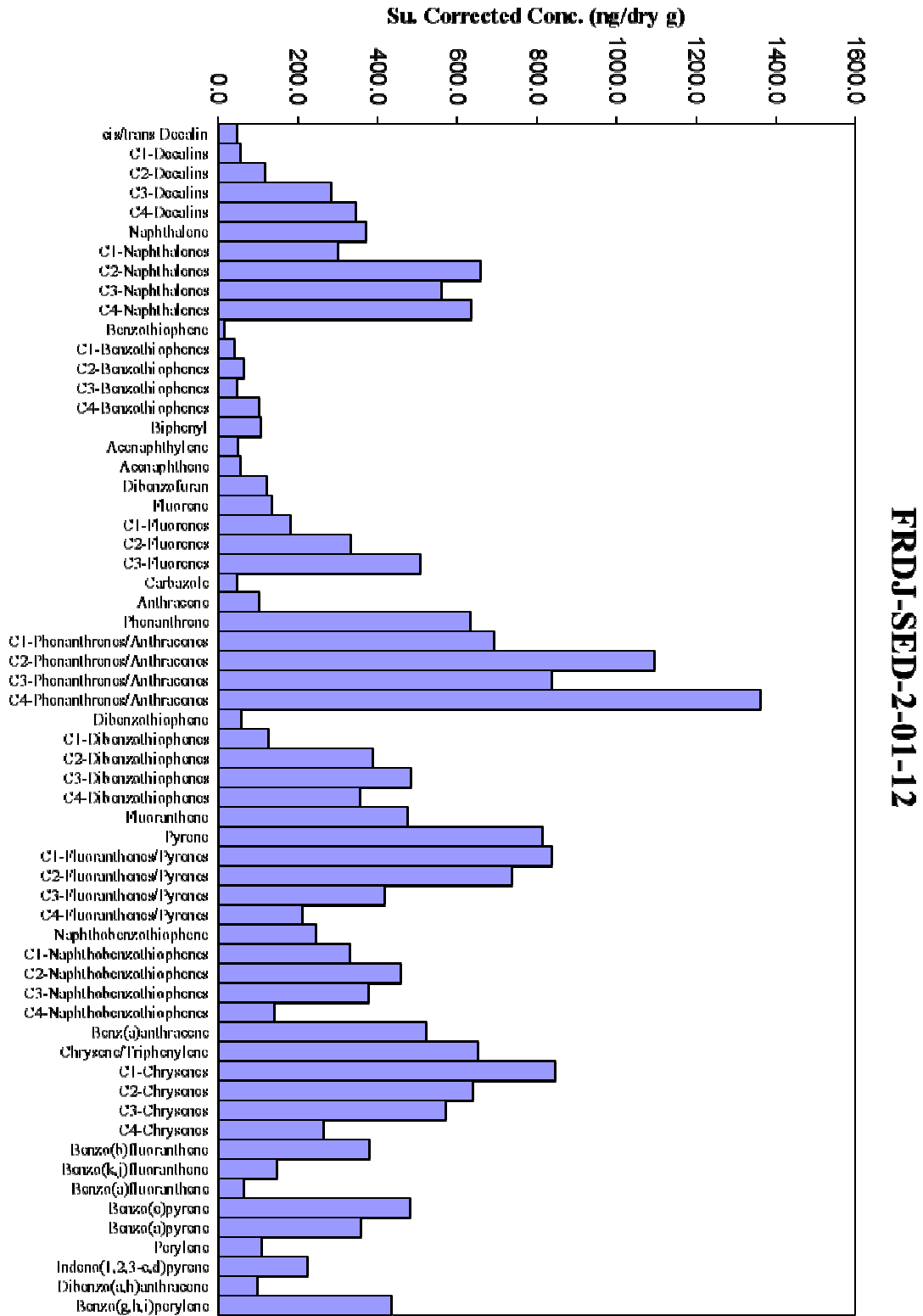
FRDJ-SED-1-03-01

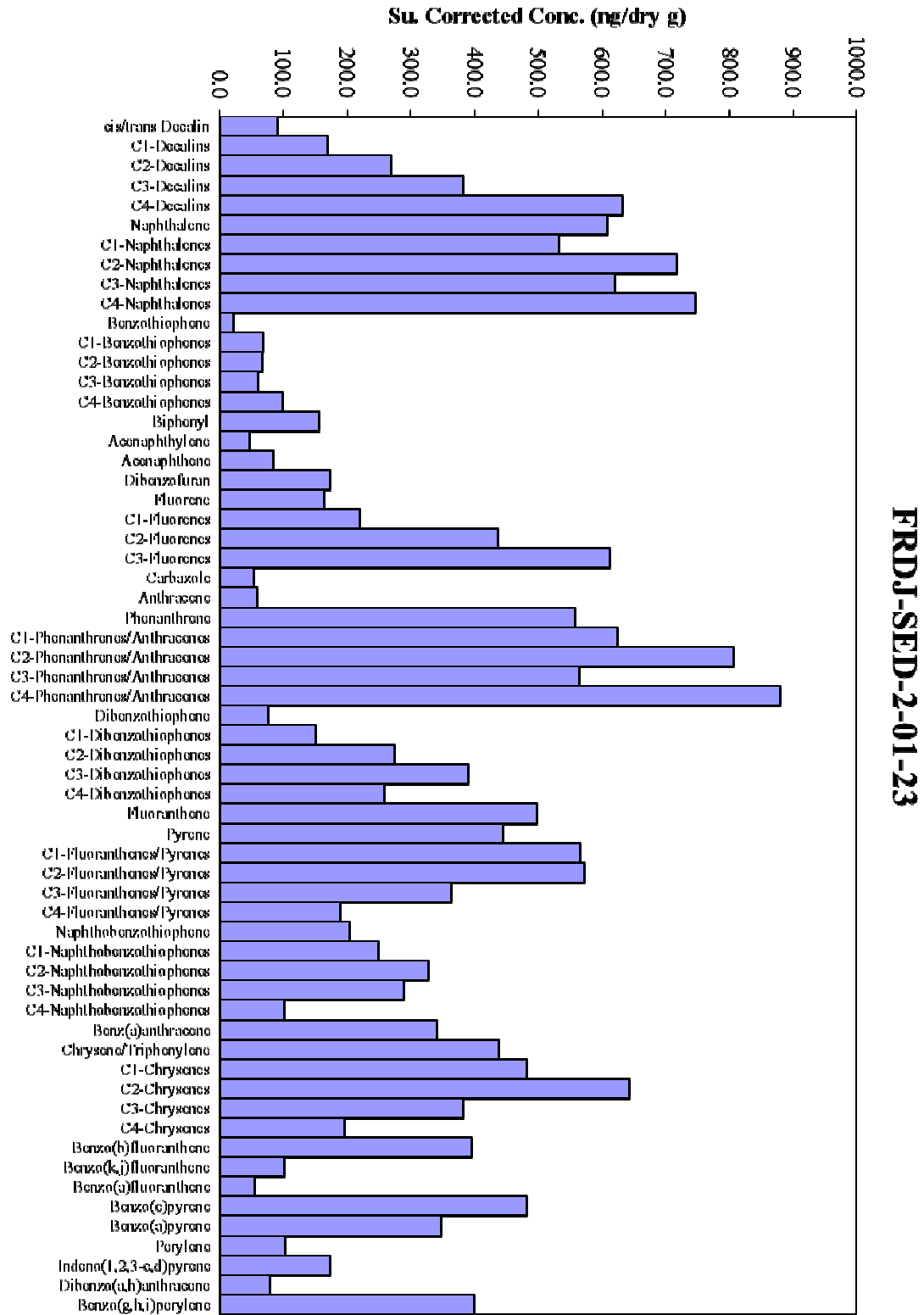


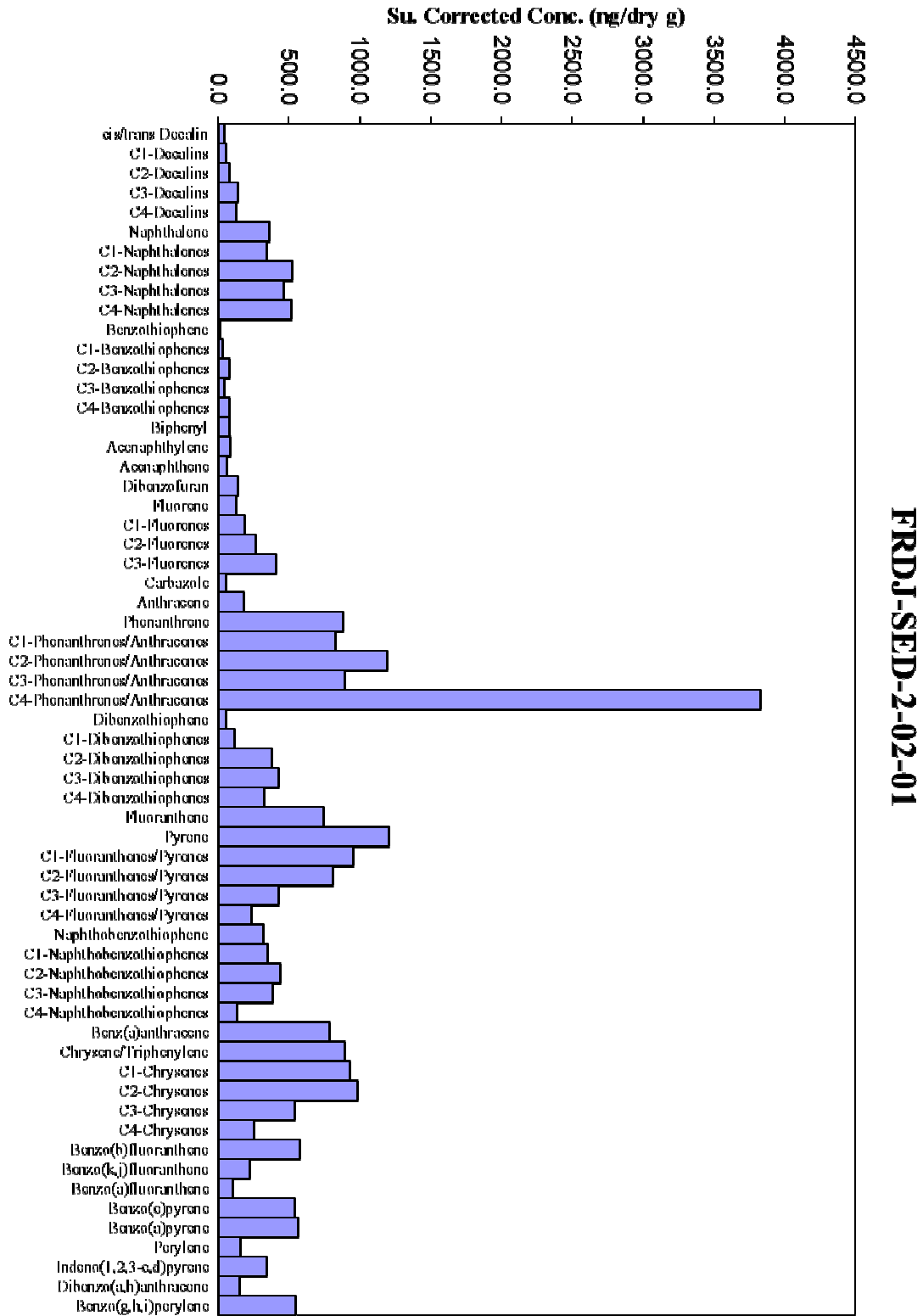
FRDJ-SED-1-03-12

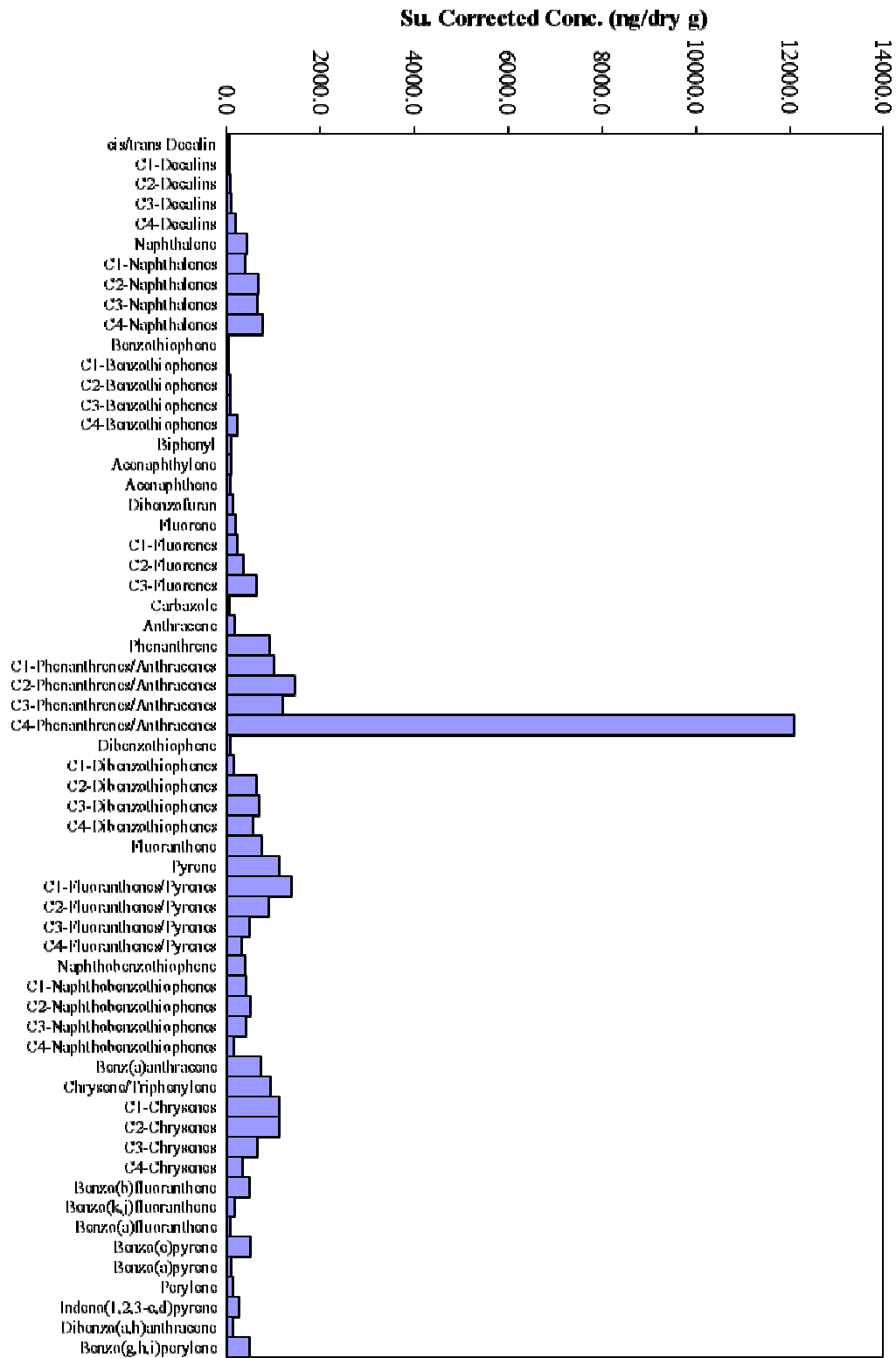




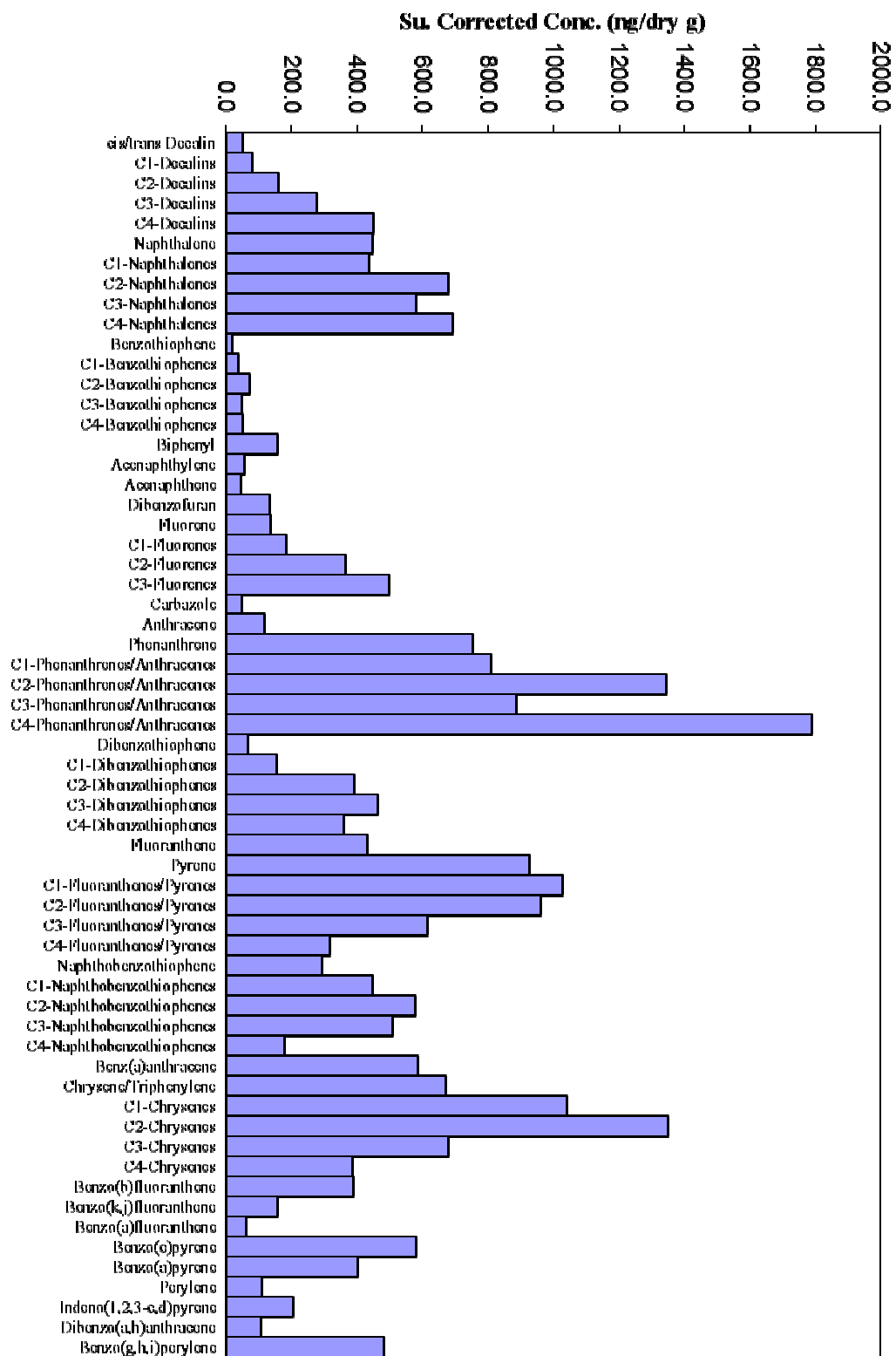




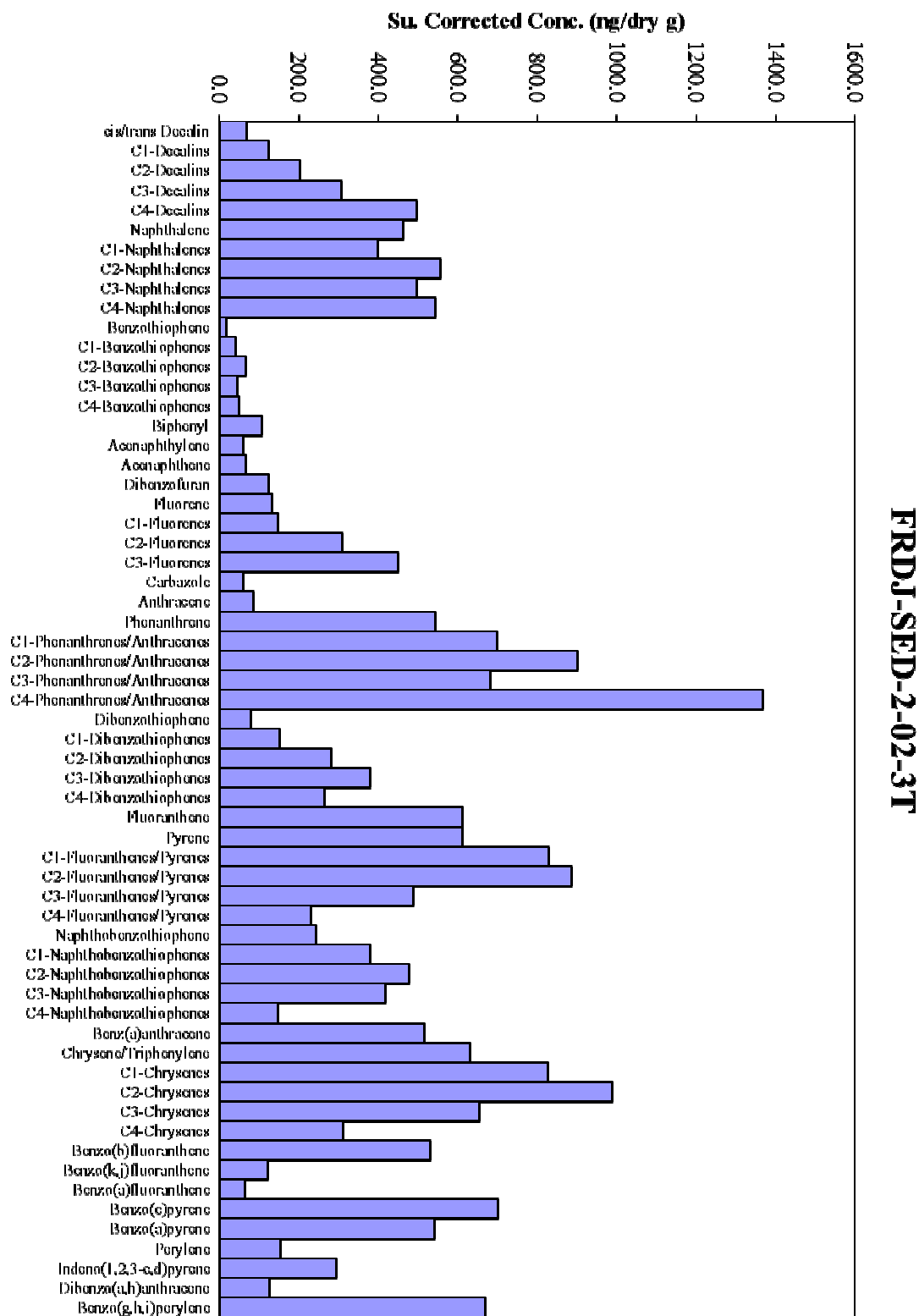


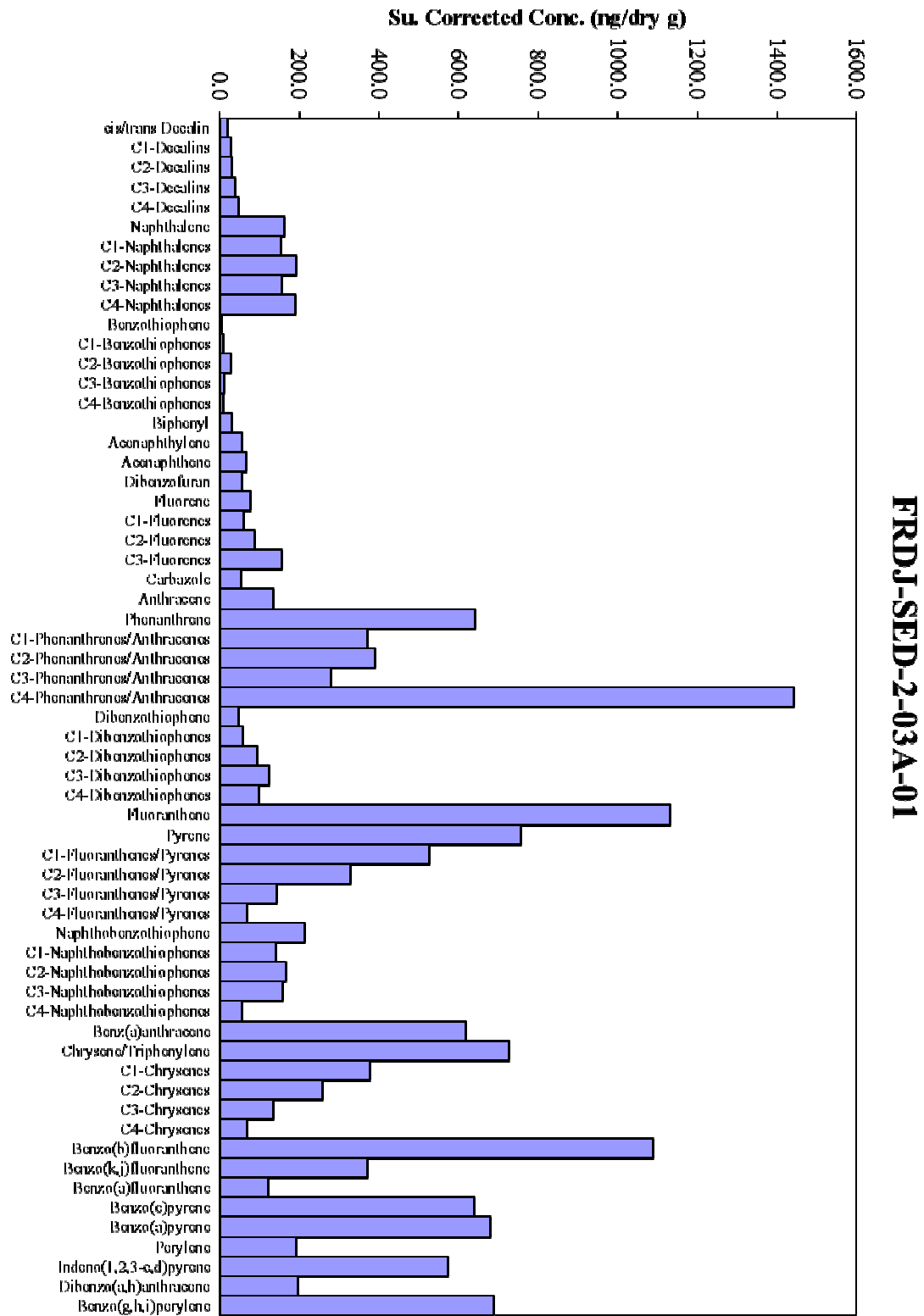


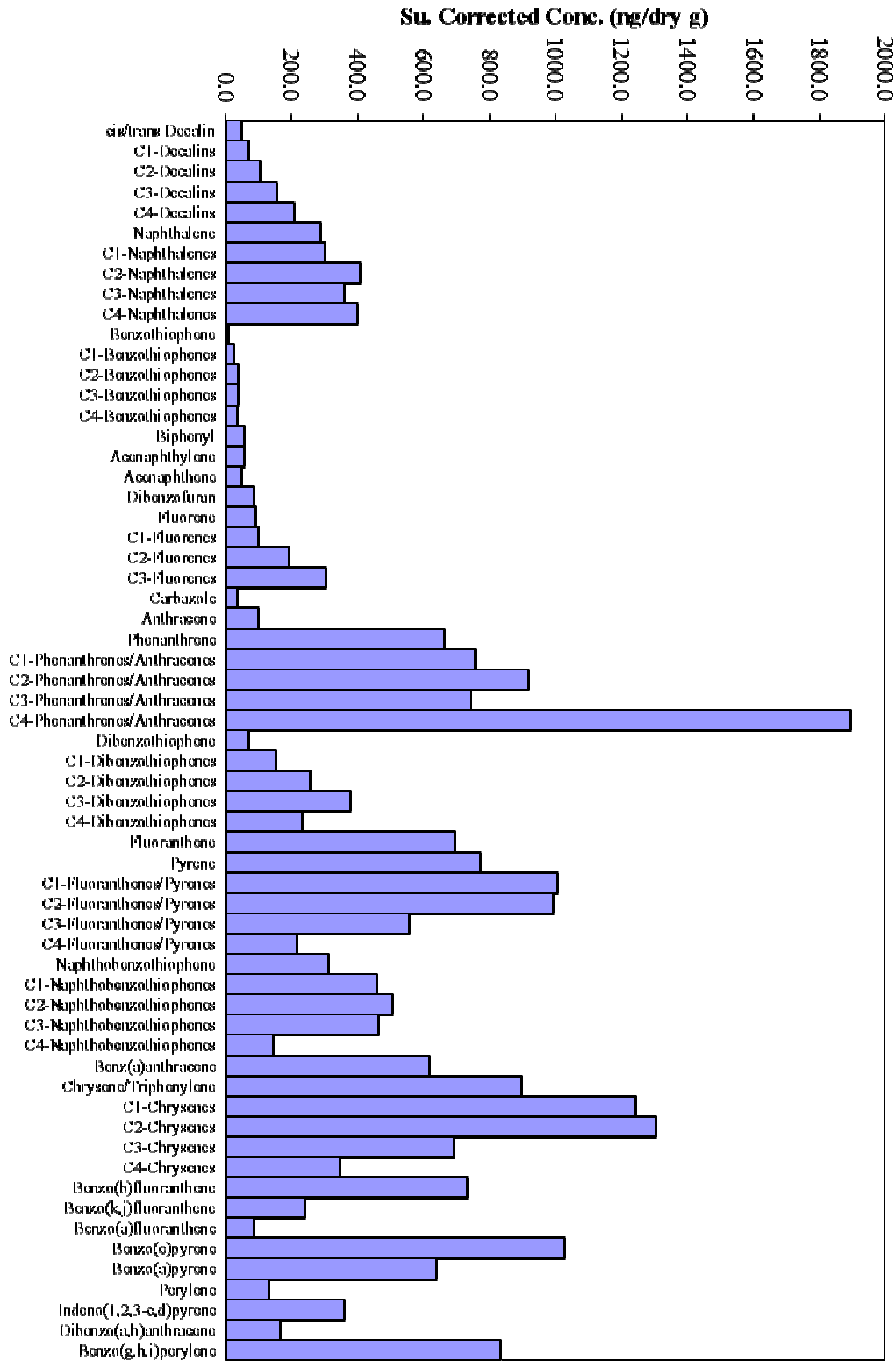
FRDJ-SED-2-02-12



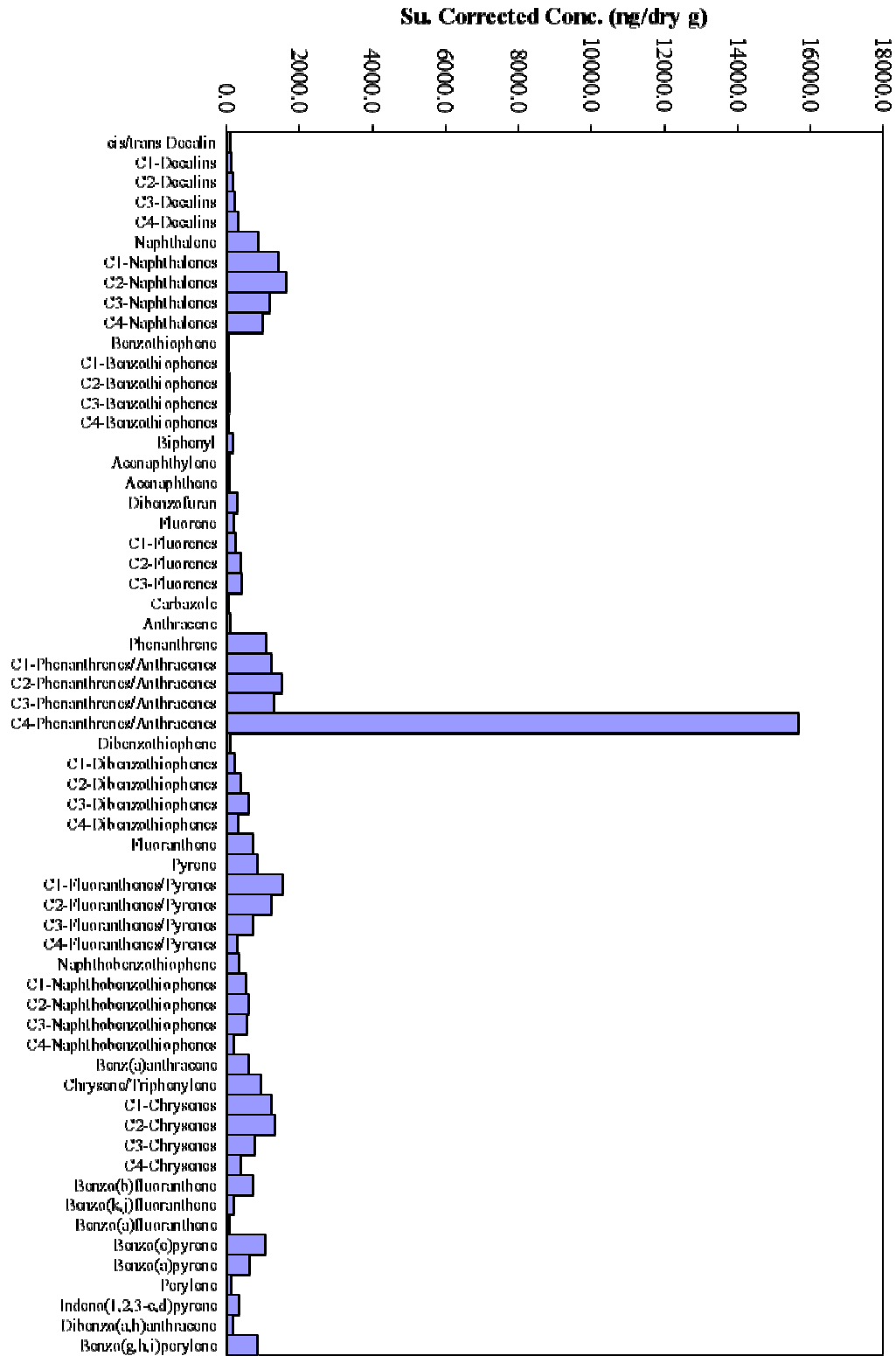
FRDJ-SED-2-02-23



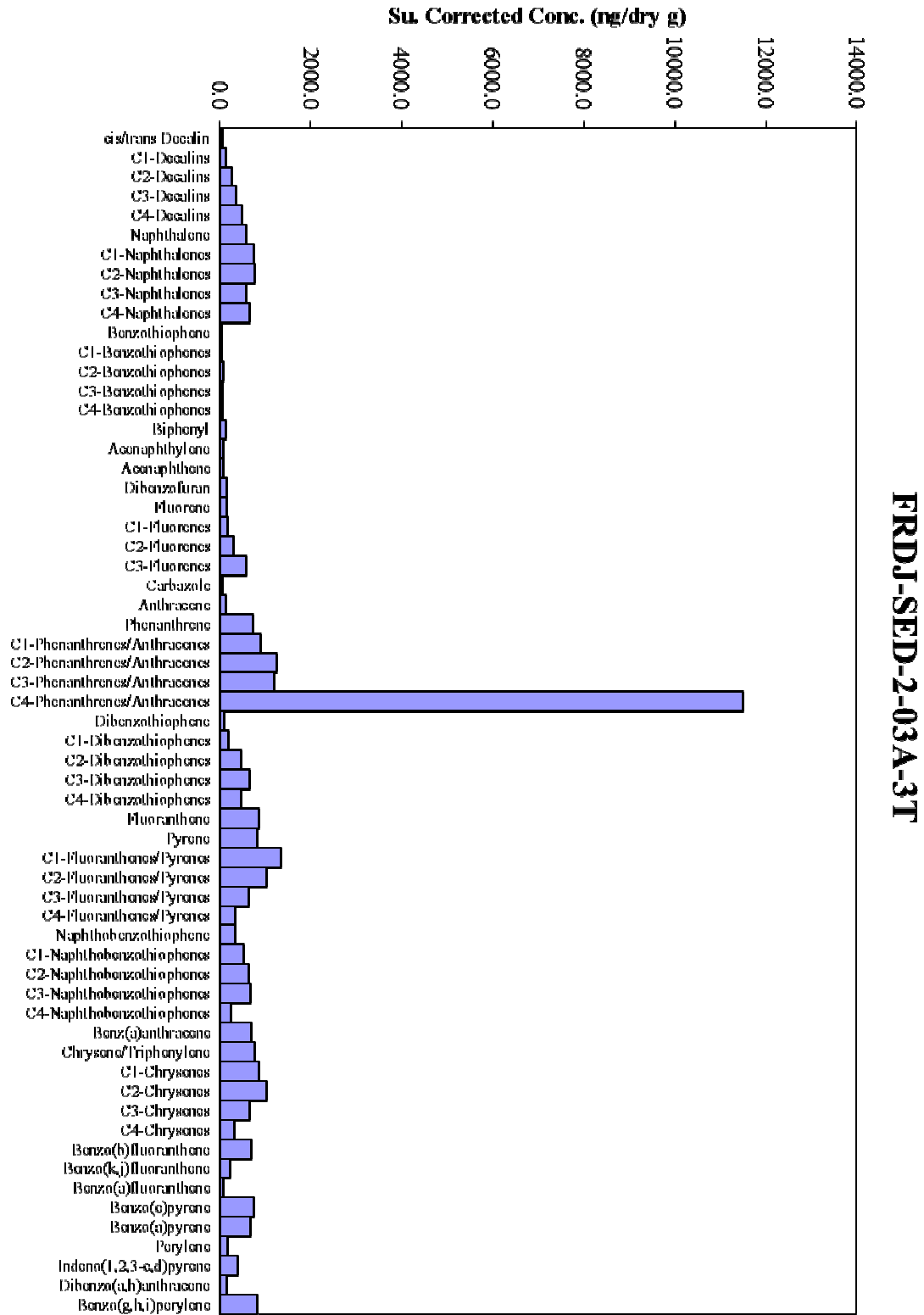


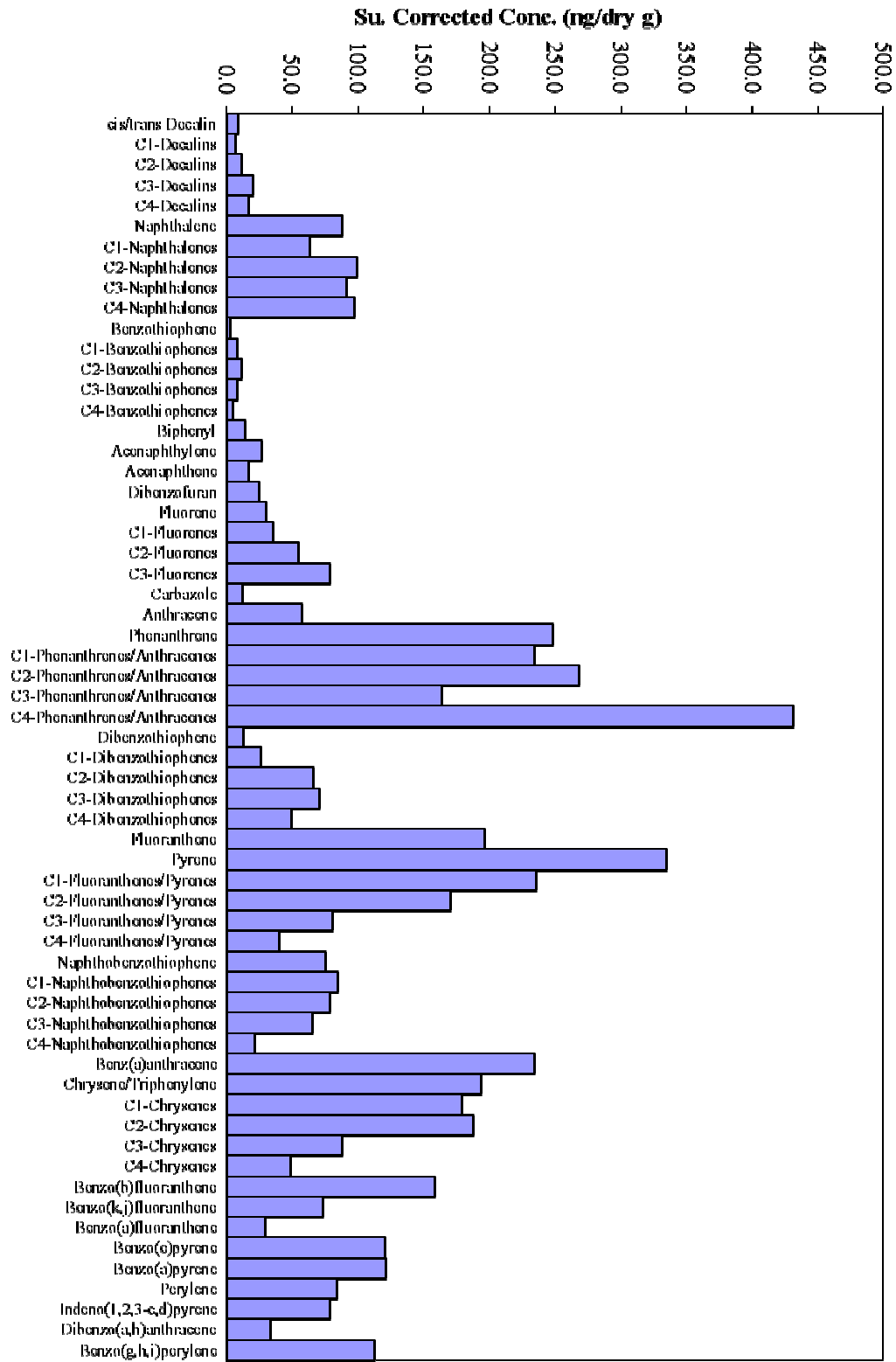


FRDJ-SED-2-03A-12

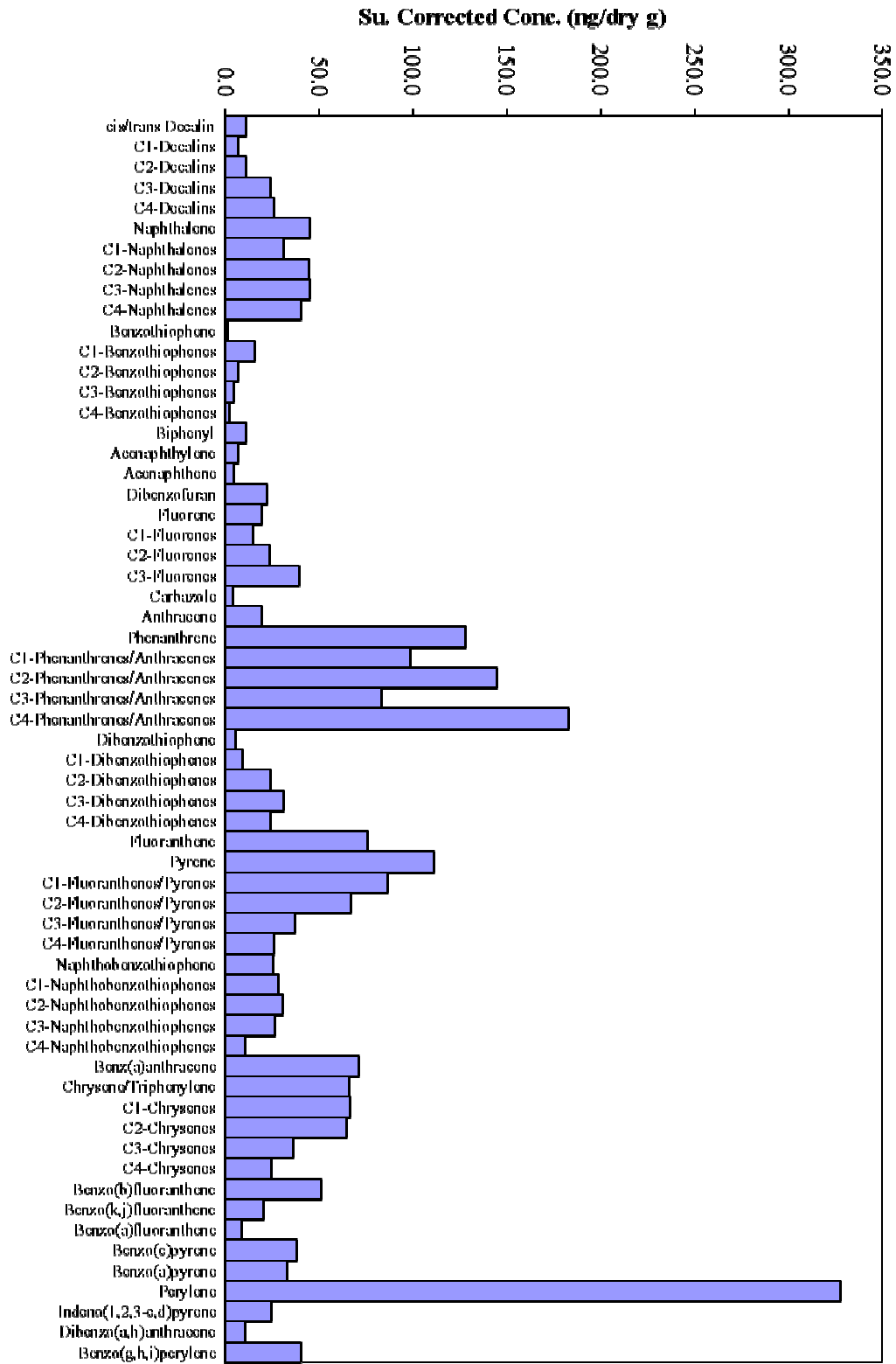


FRDJ-SED-2-03A-23

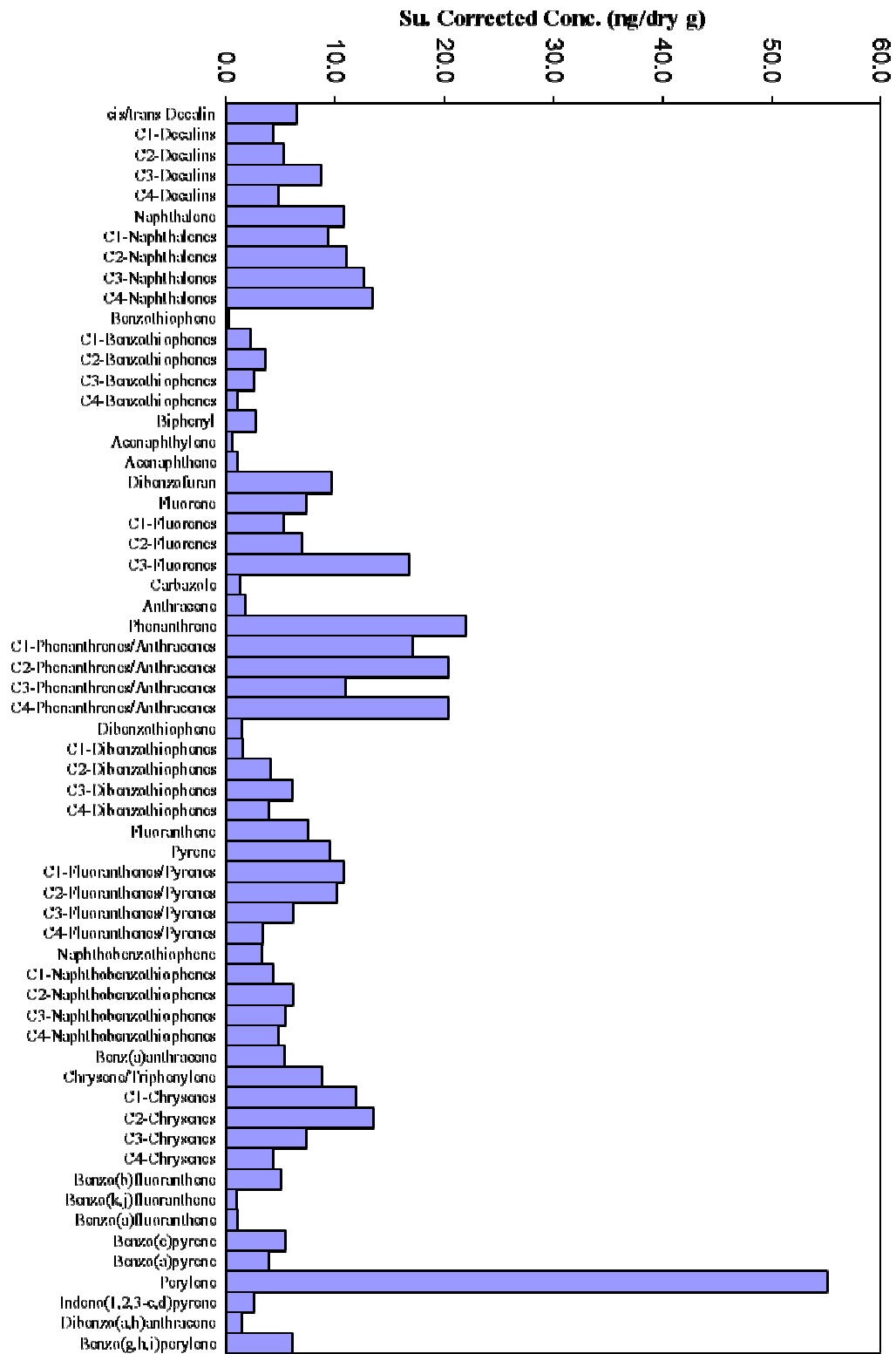




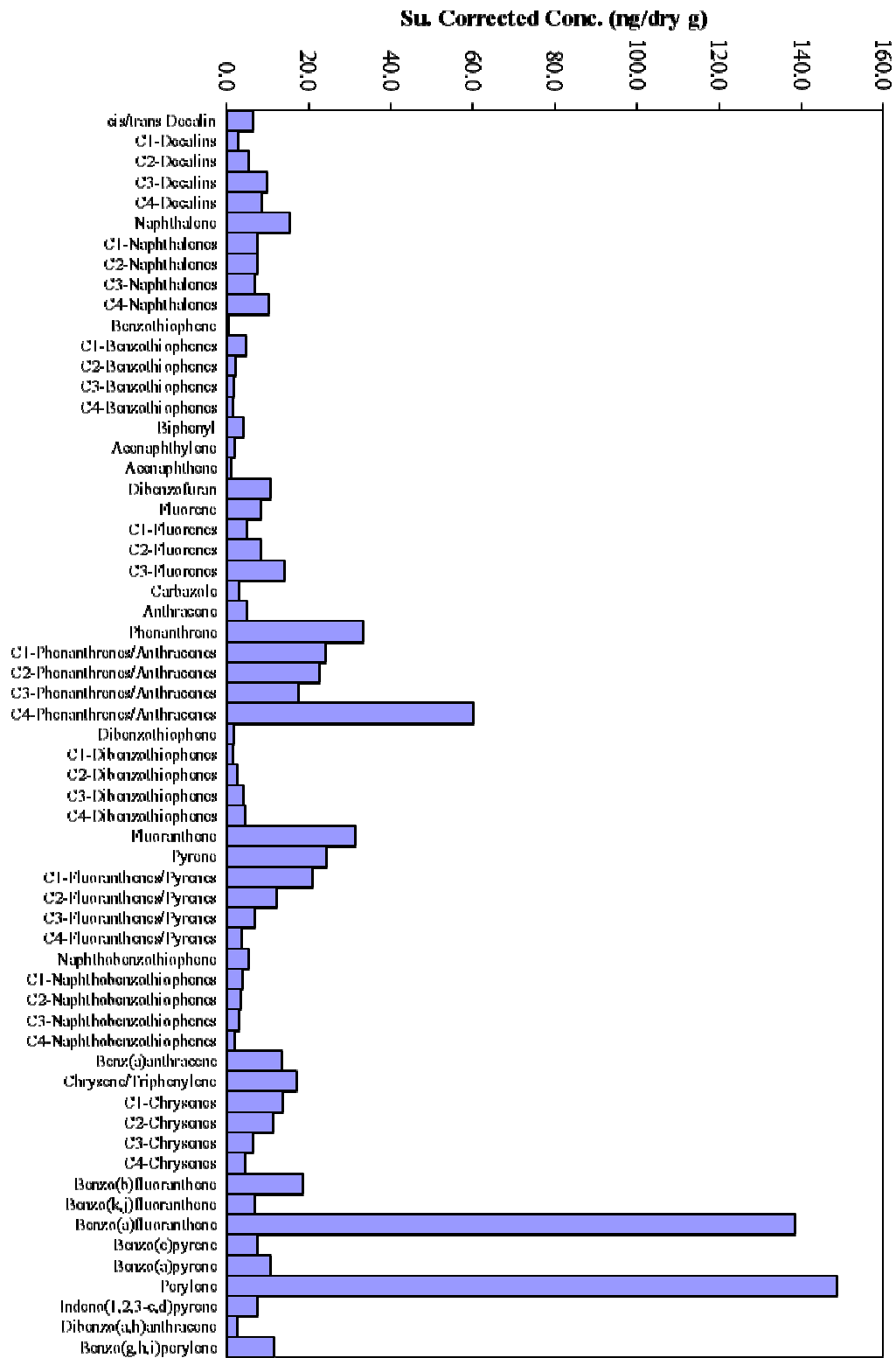
FRDJ-SED-3-01-01



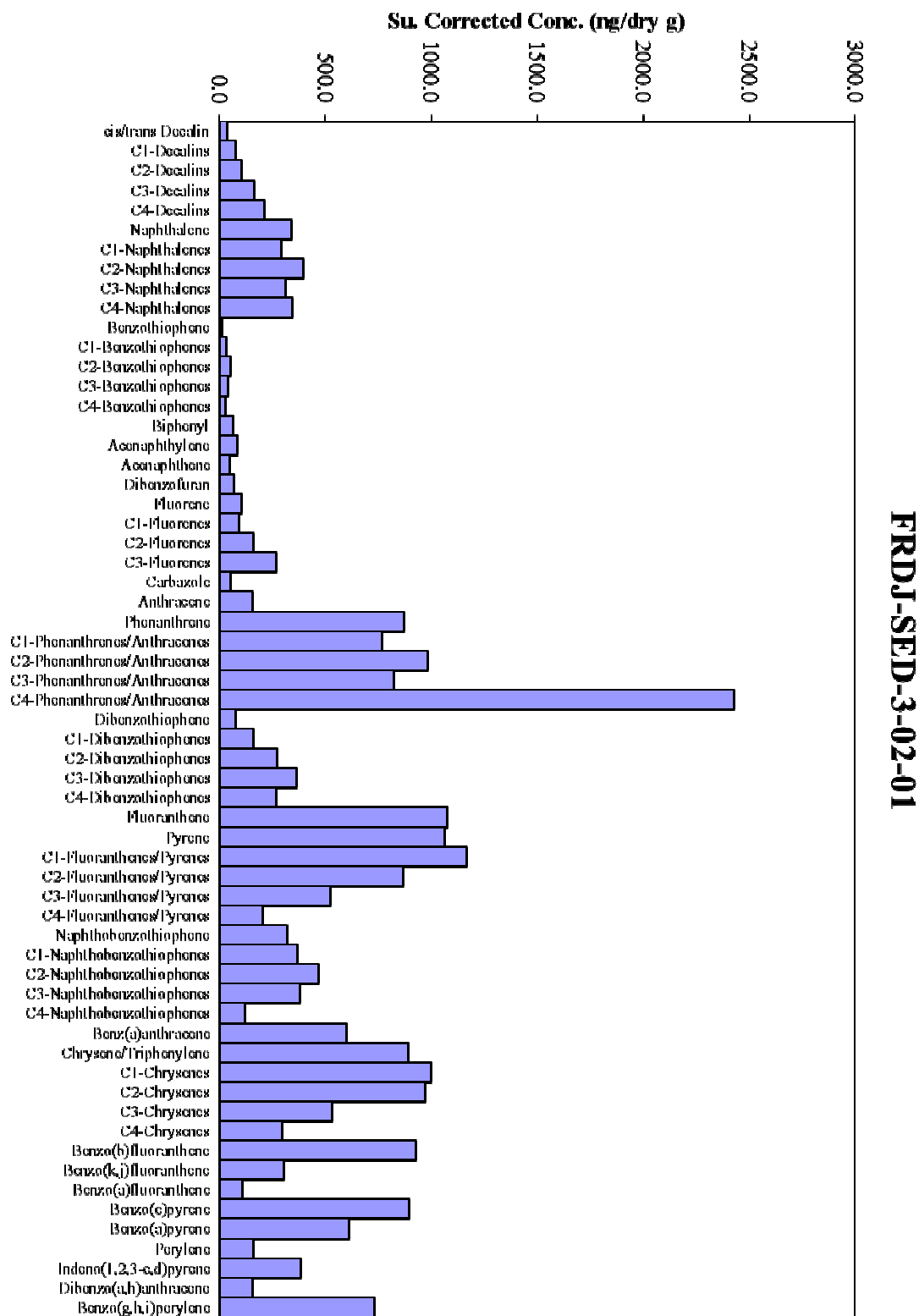
FRDJ-SED-3-01-12

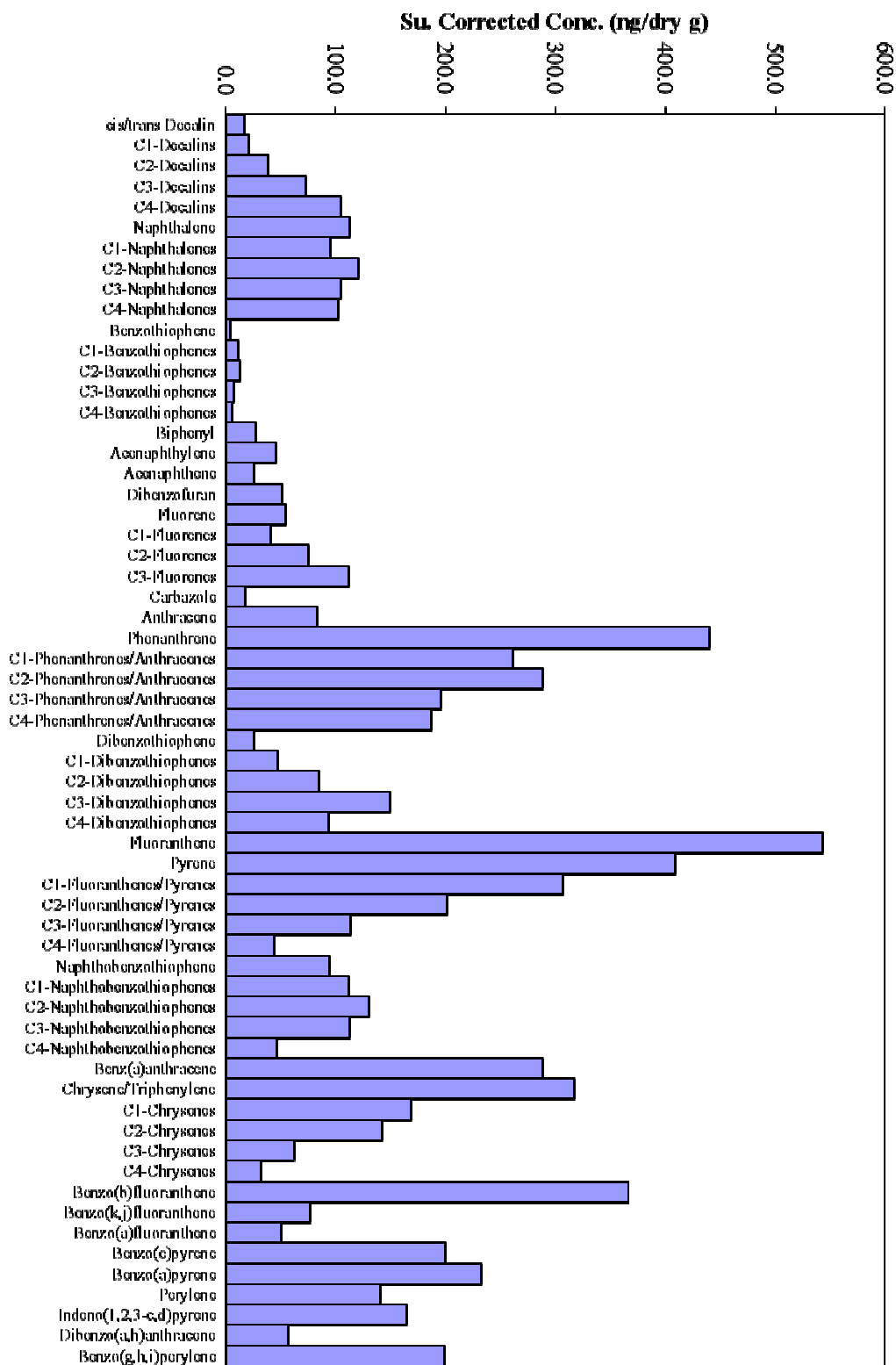


FRDJ-SED-3-01-23

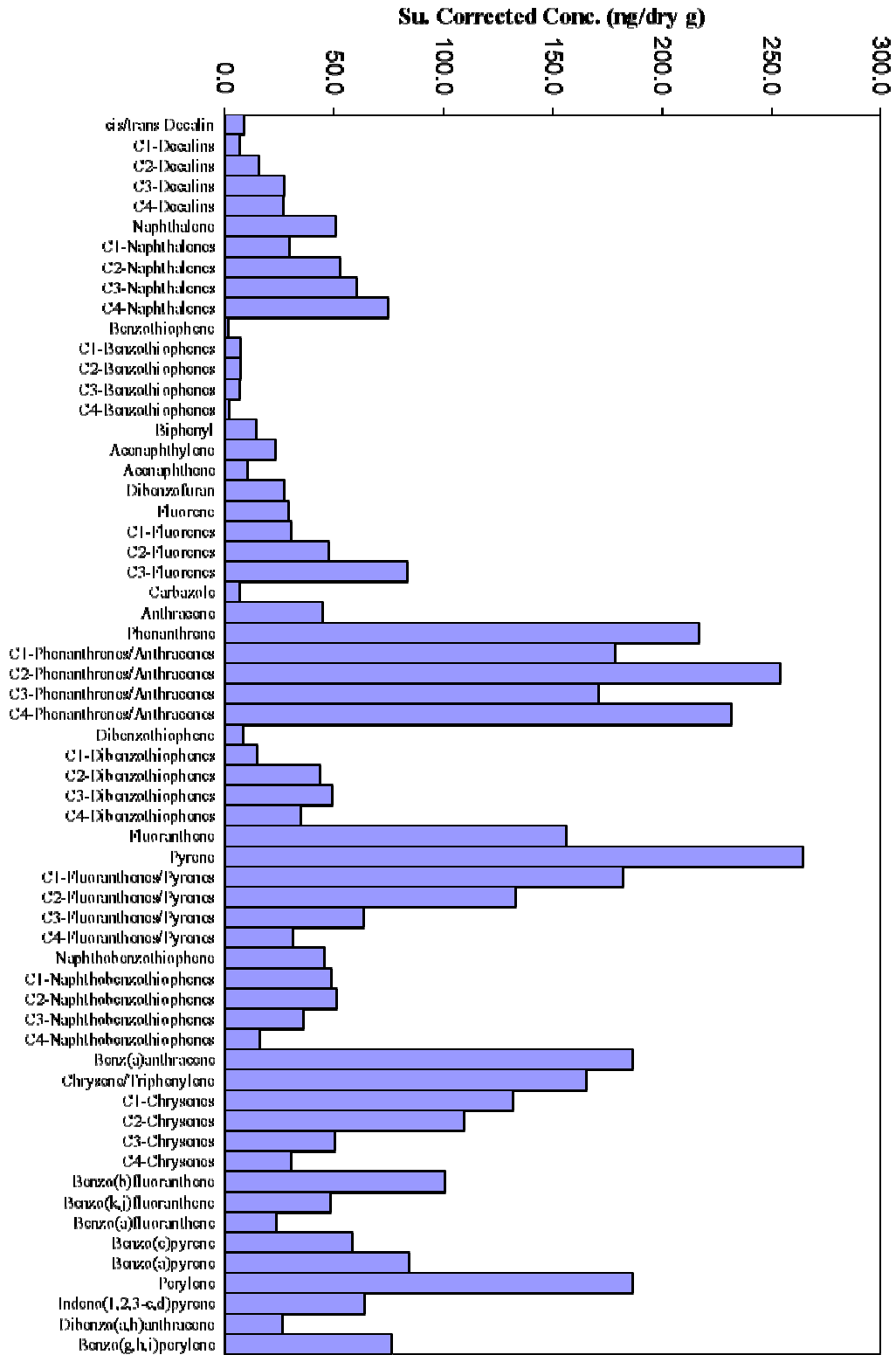


FRDJ-SED-3-01-3T

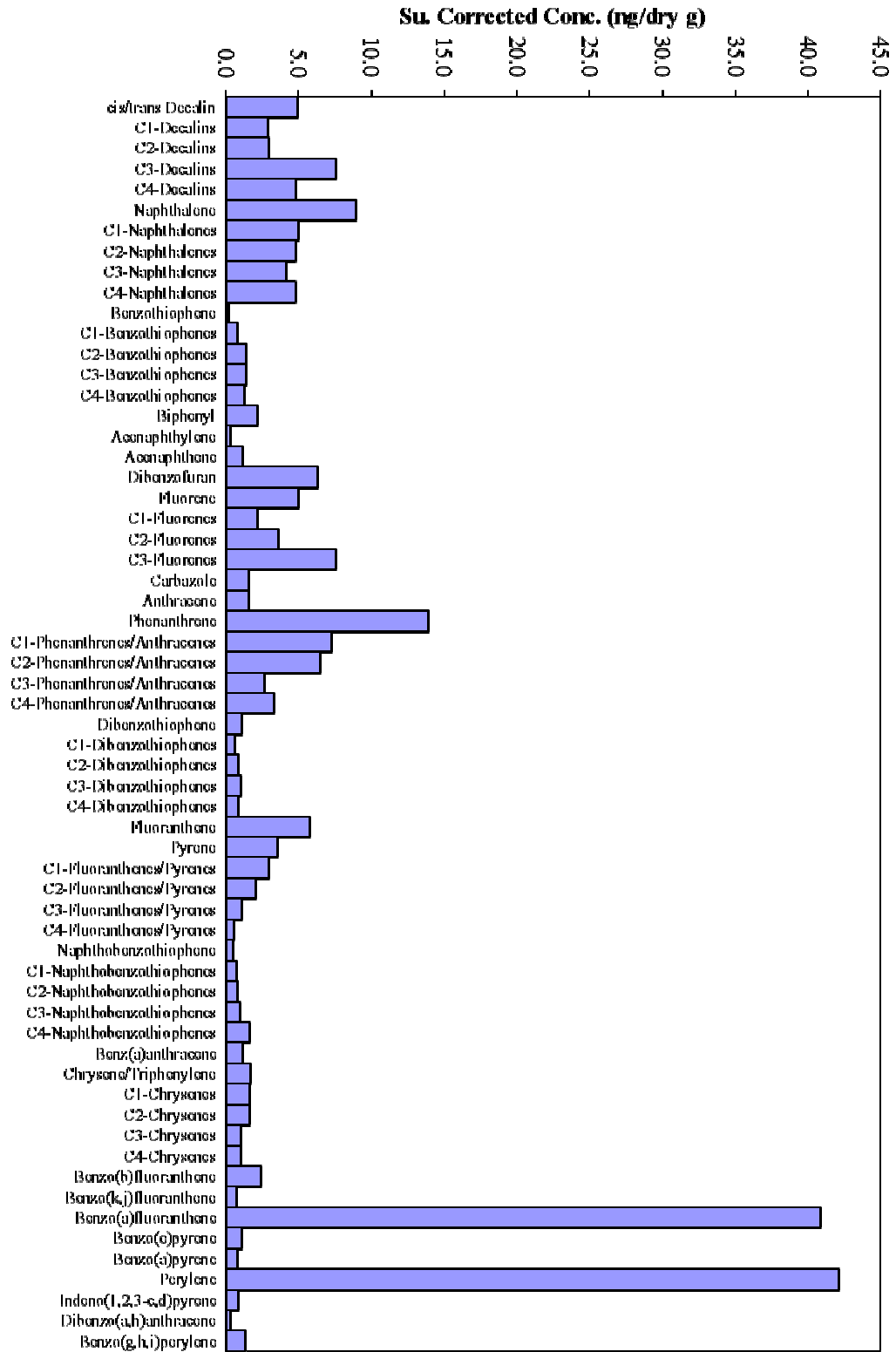




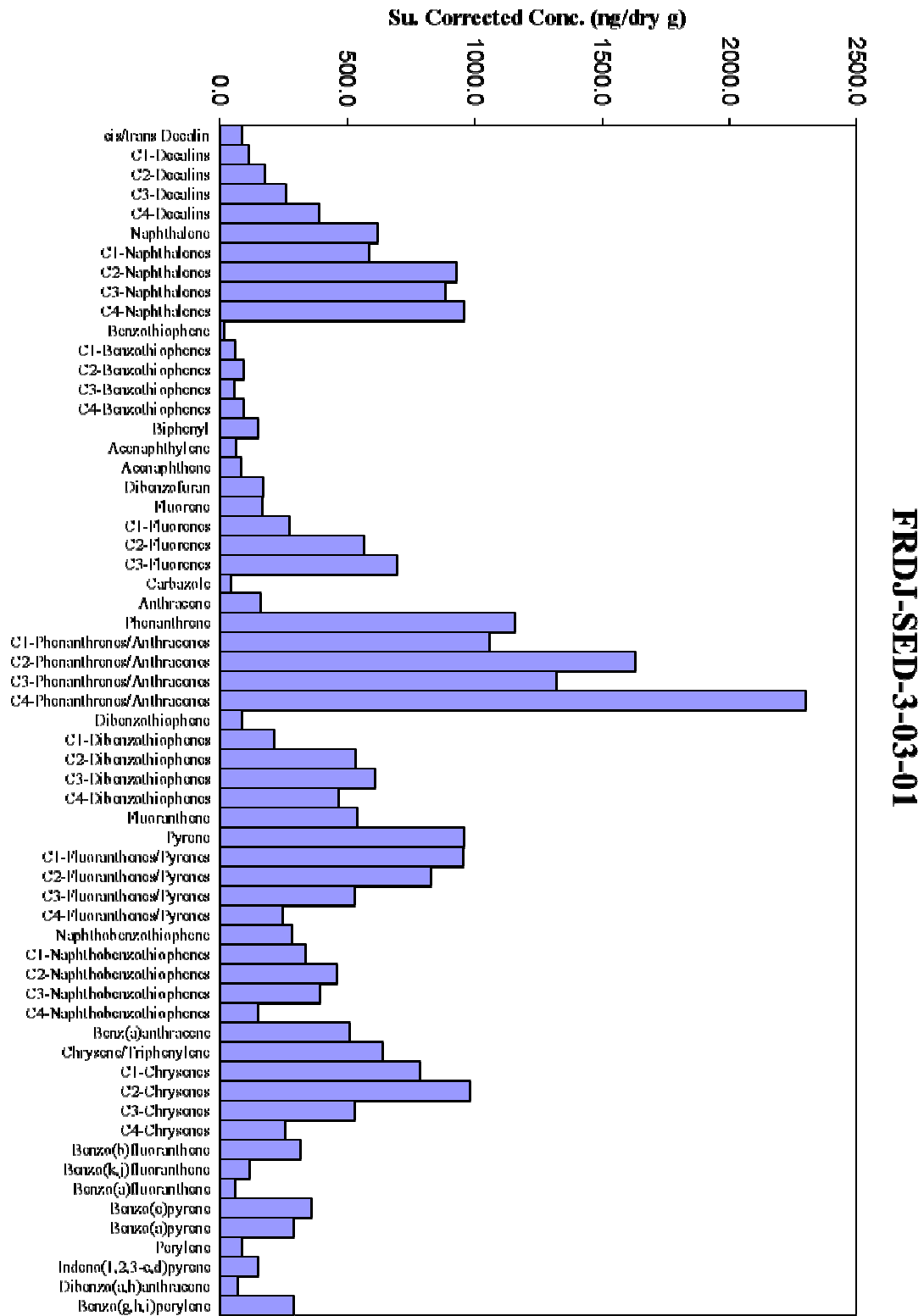
FRDJ-SED-3-02-12

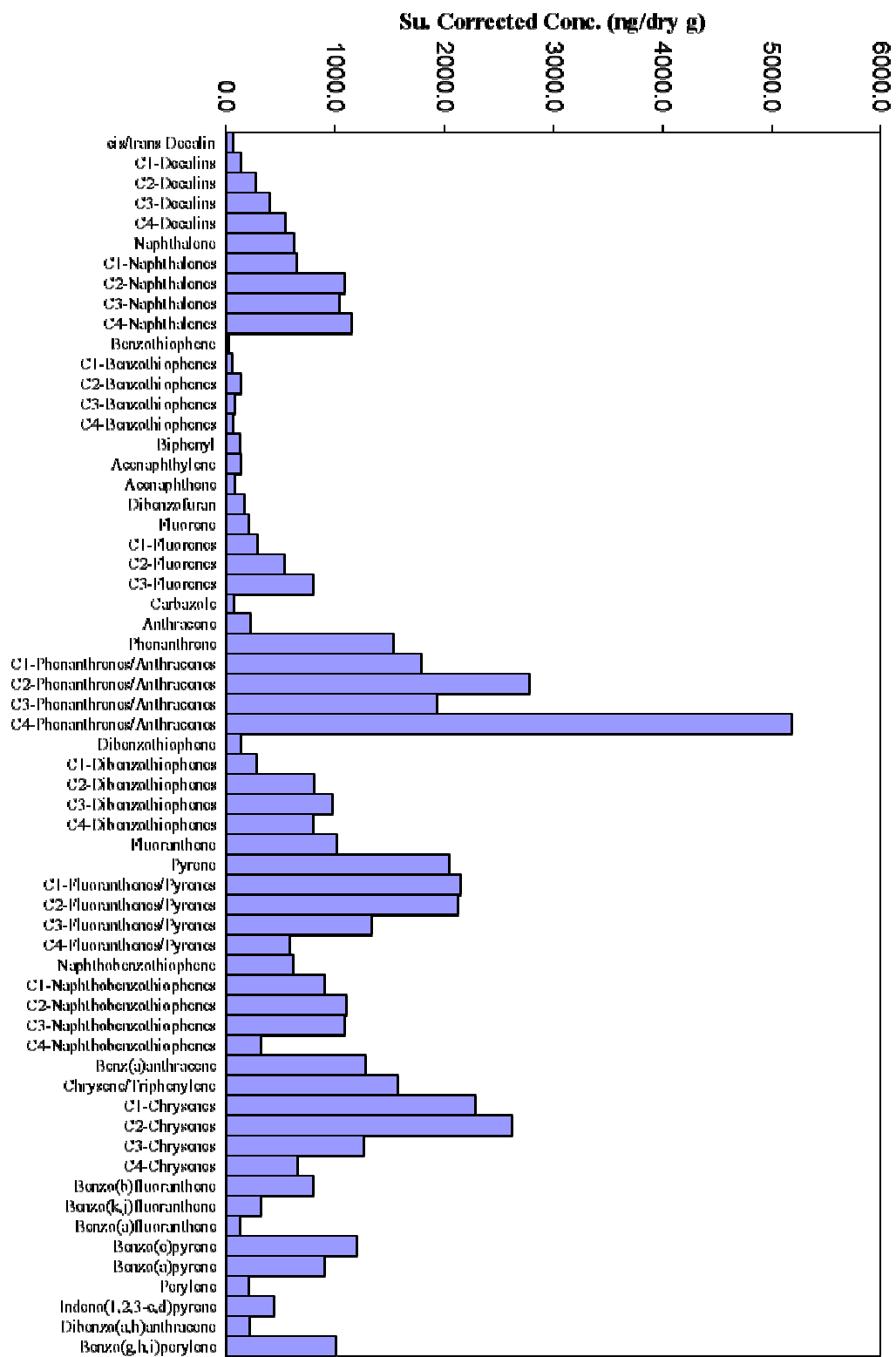


FRDJ-SED-3-02-23

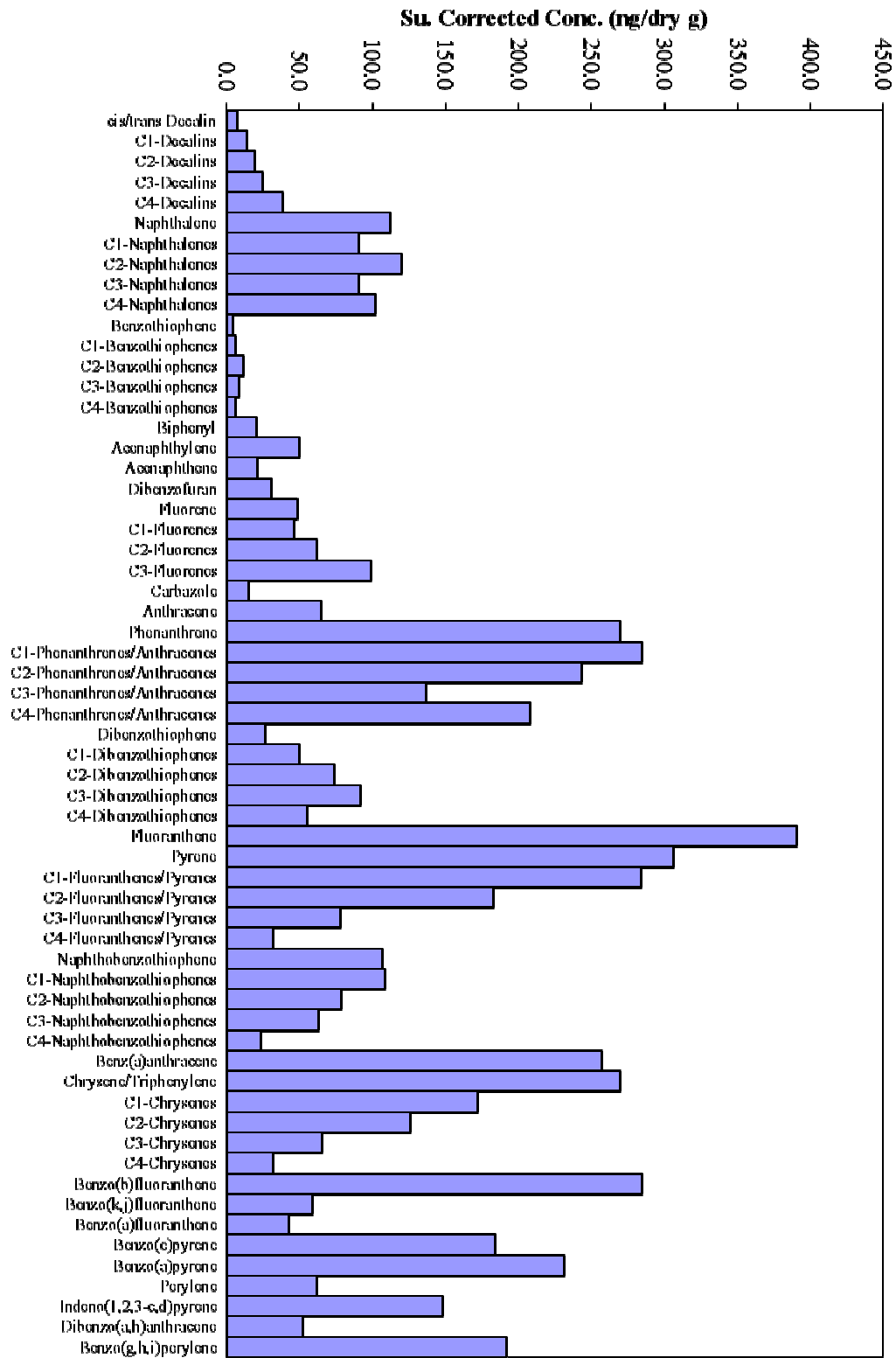


FRDJ-SED-3-02-3T

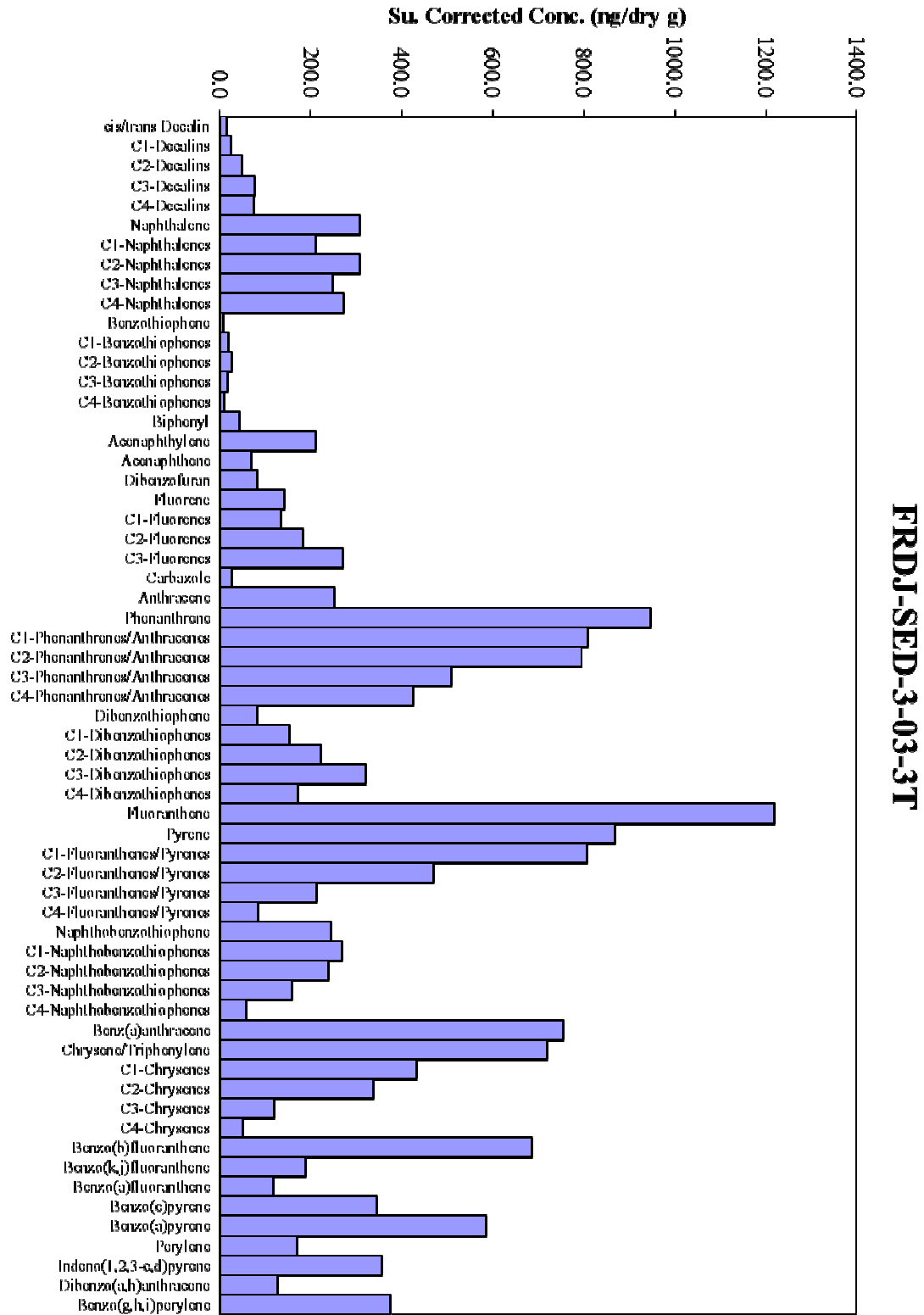


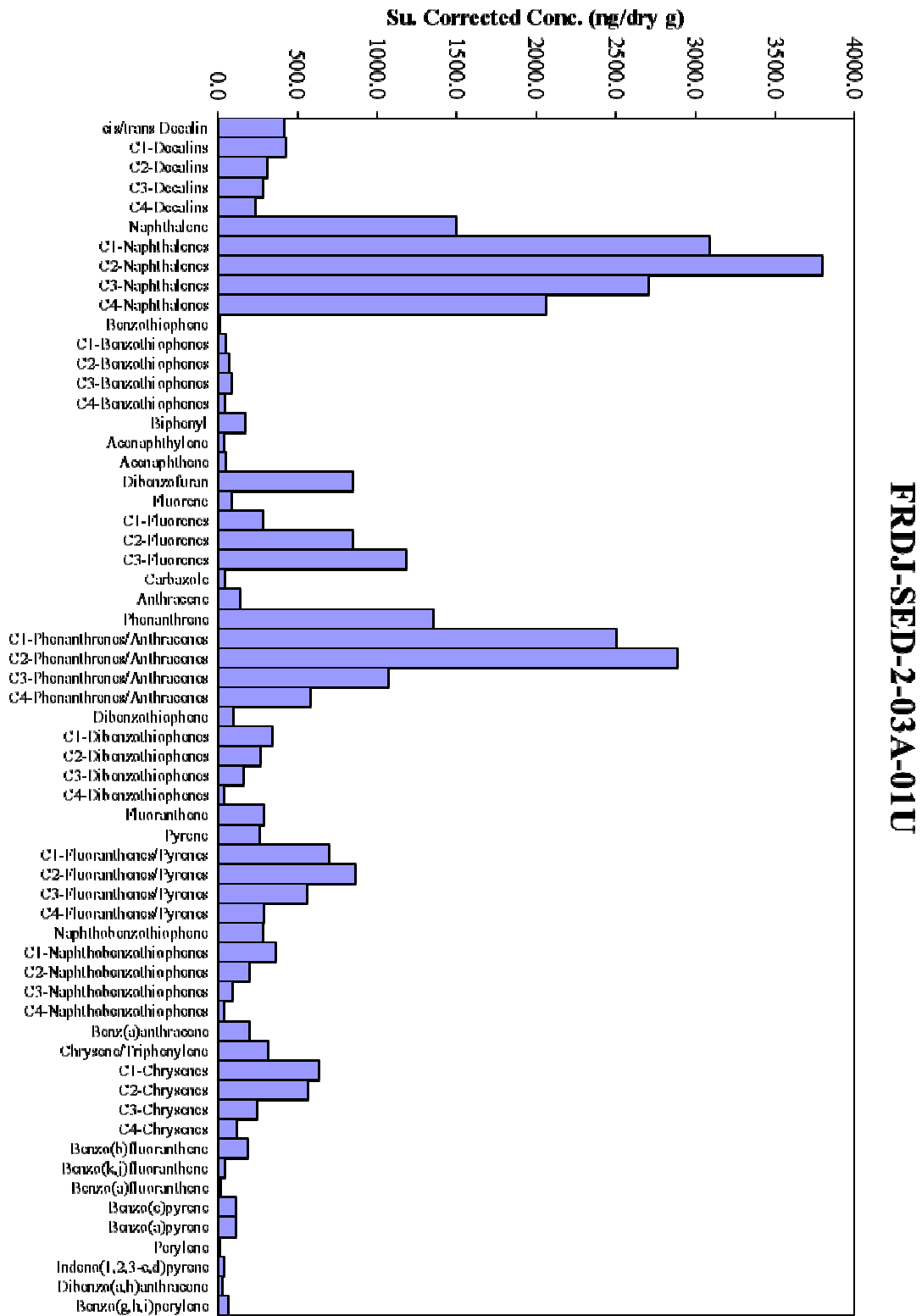


FRDJ-SED-3-03-12



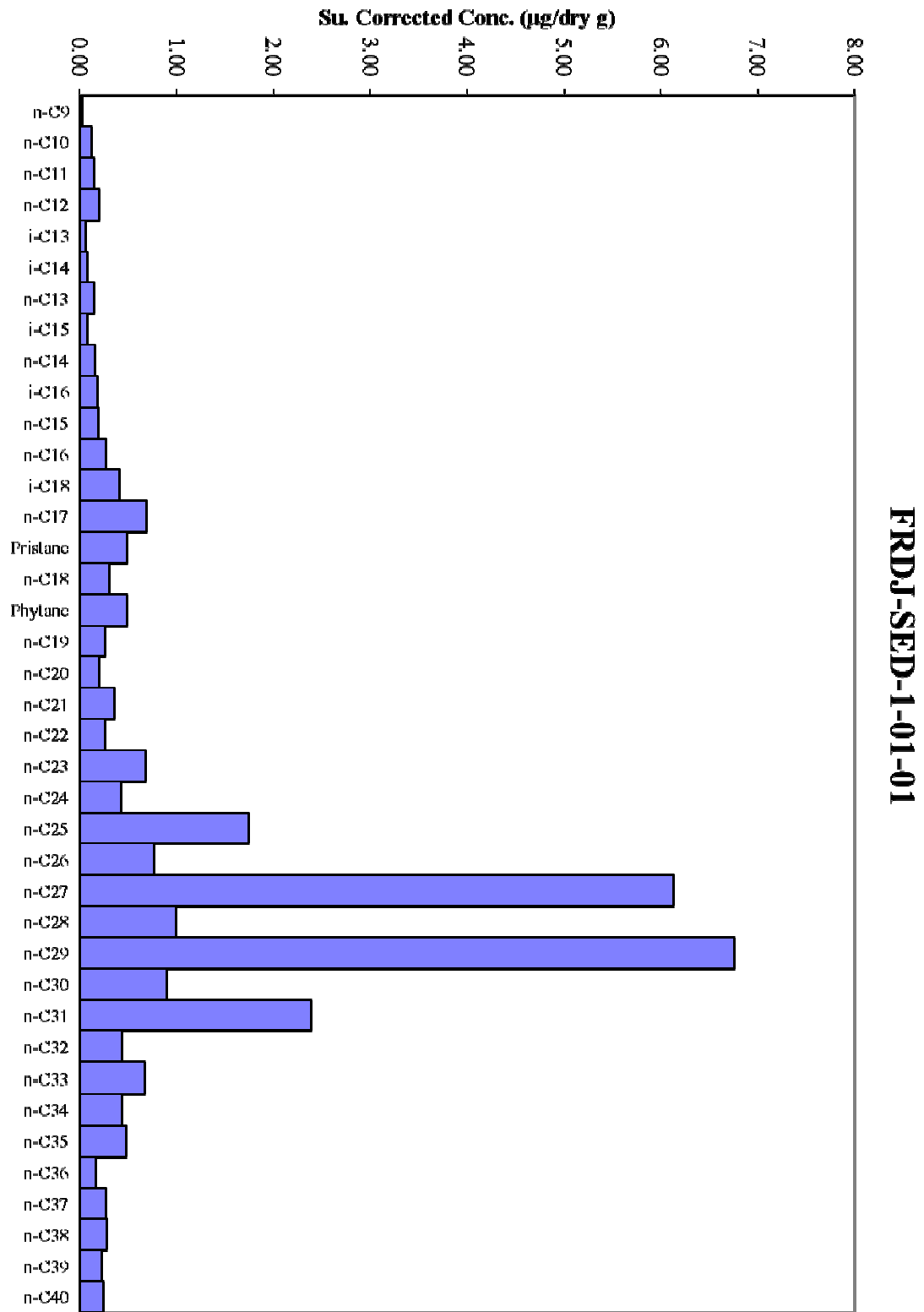
FRDJ-SED-3-03-23



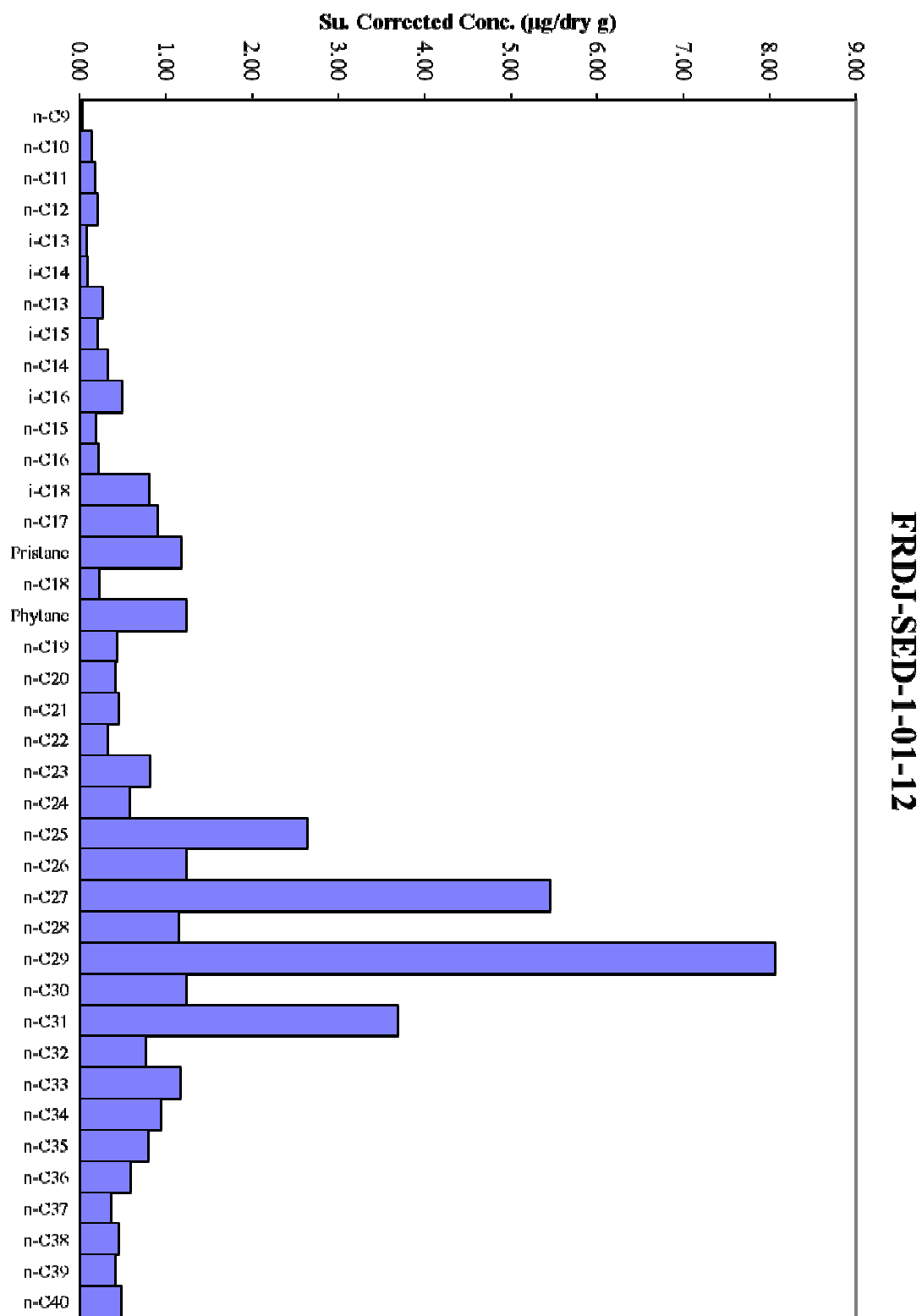


APPENDIX B

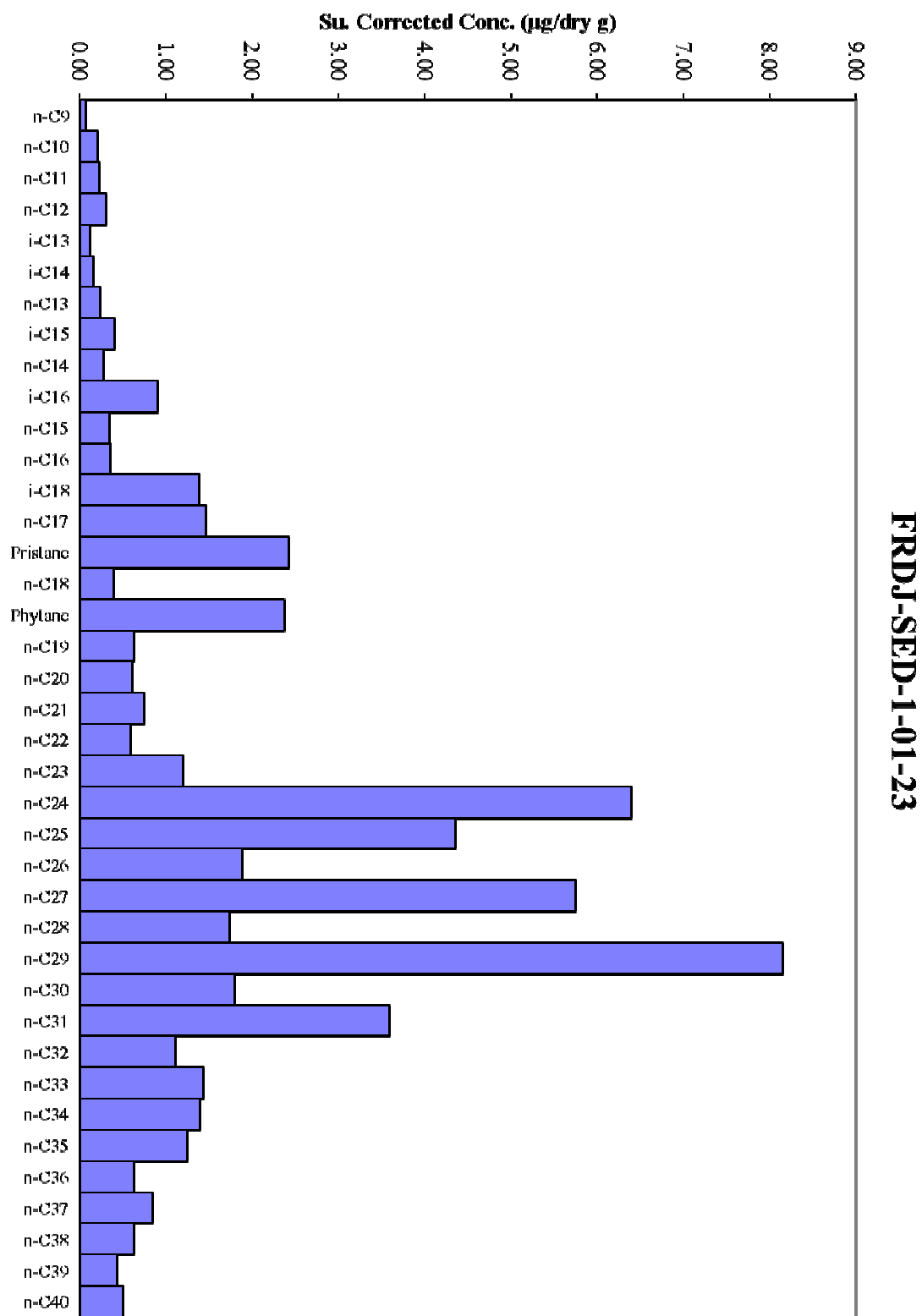
B-1



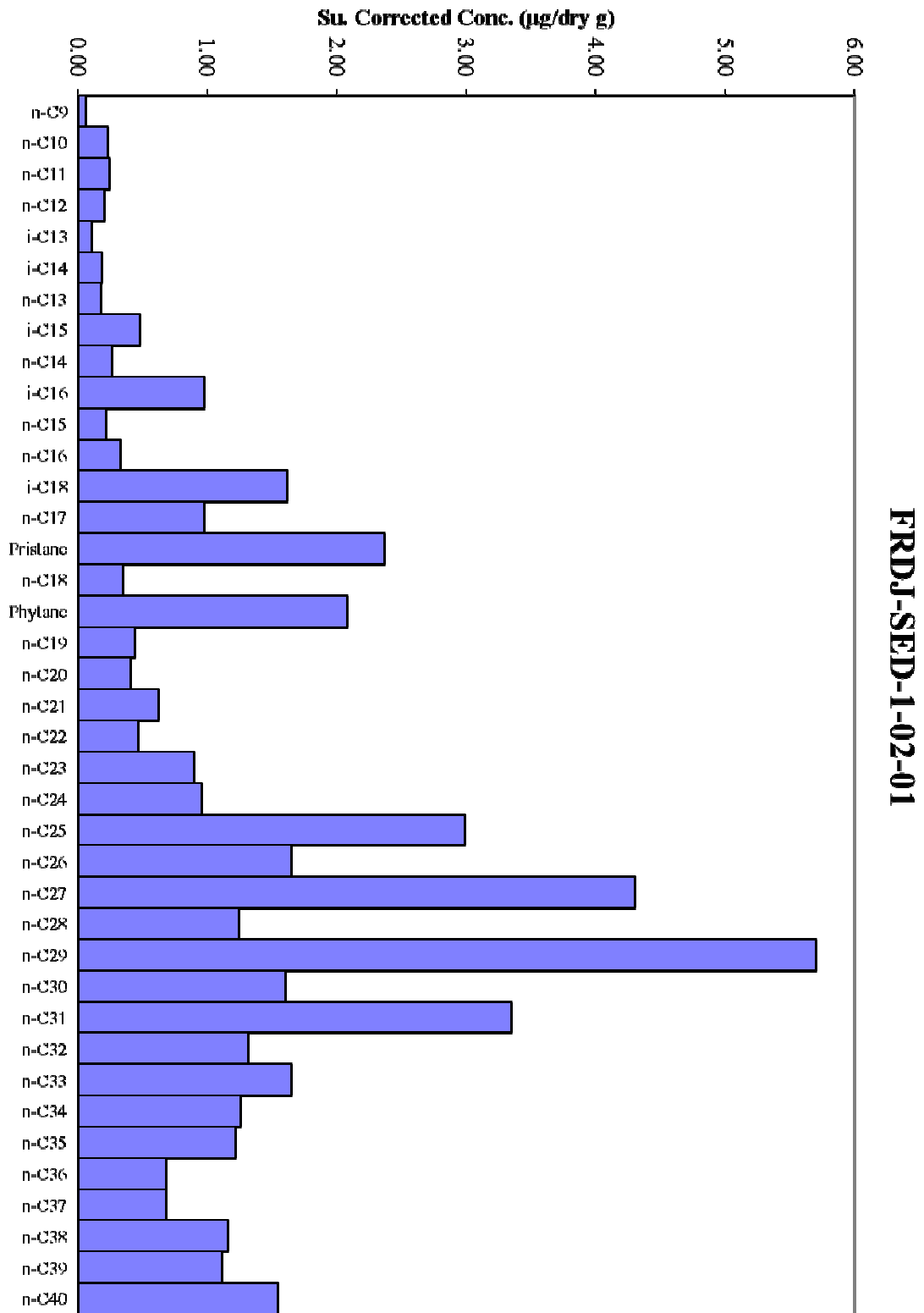
B-2



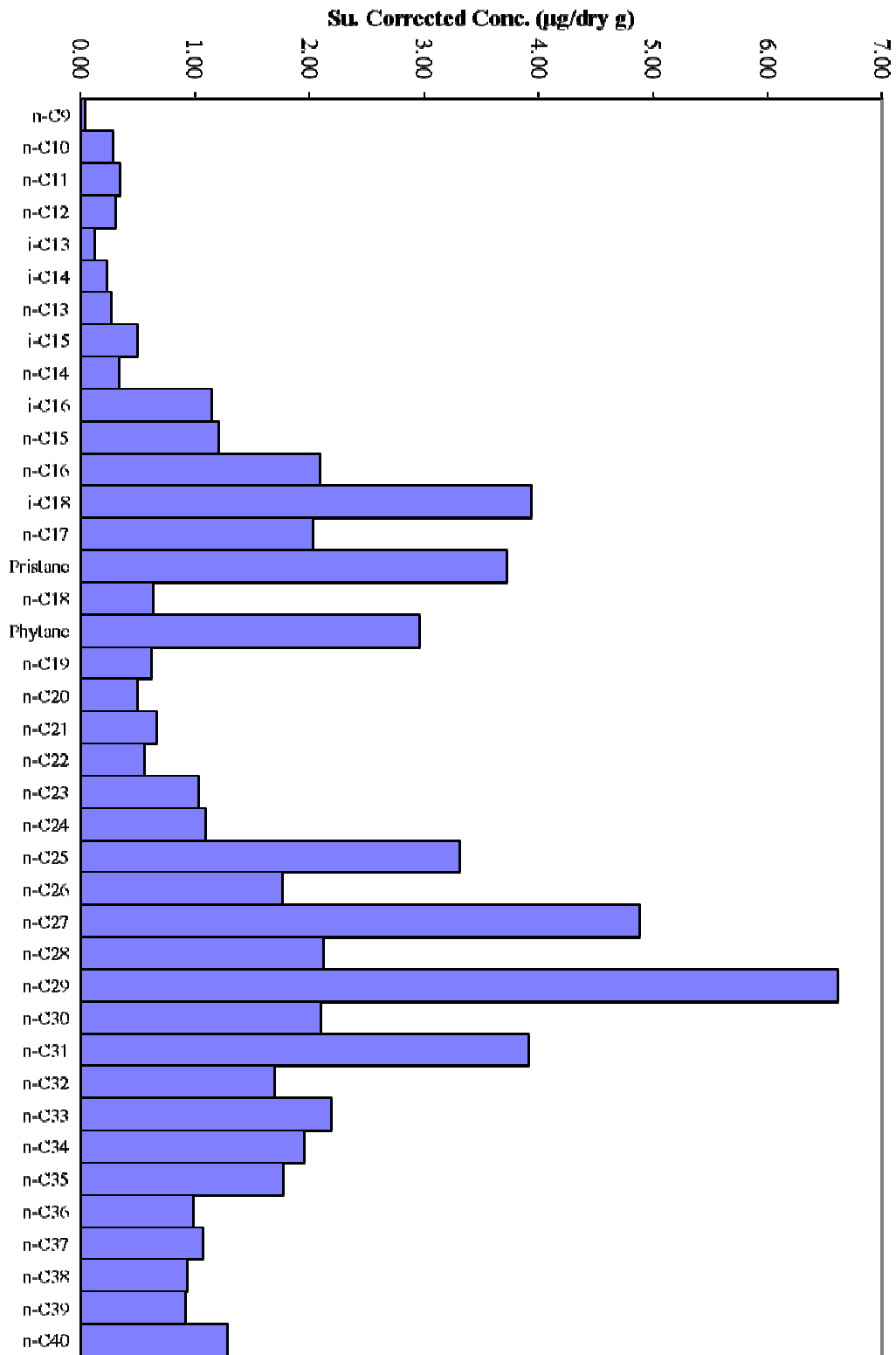
B-3



B-4

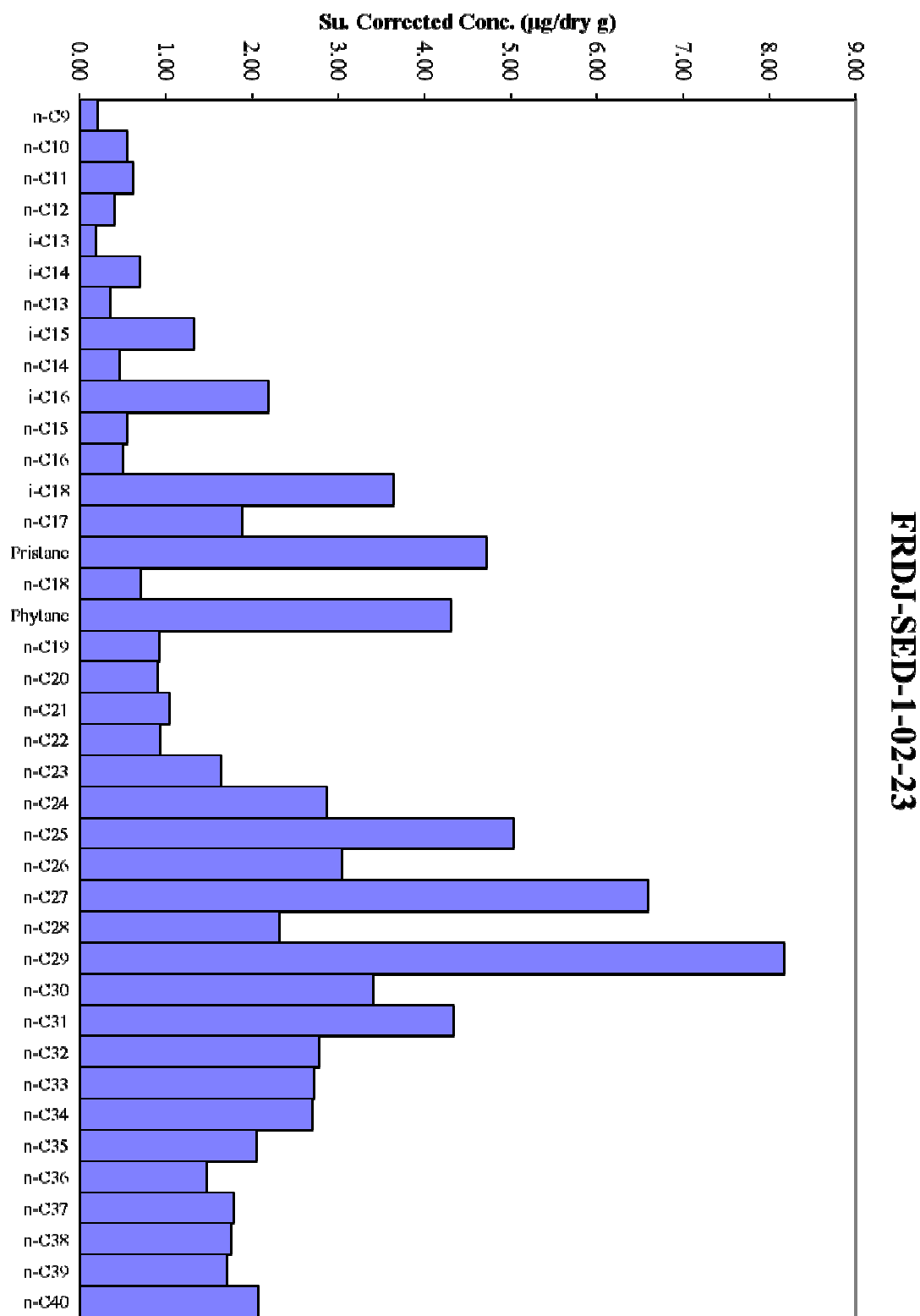


B-5

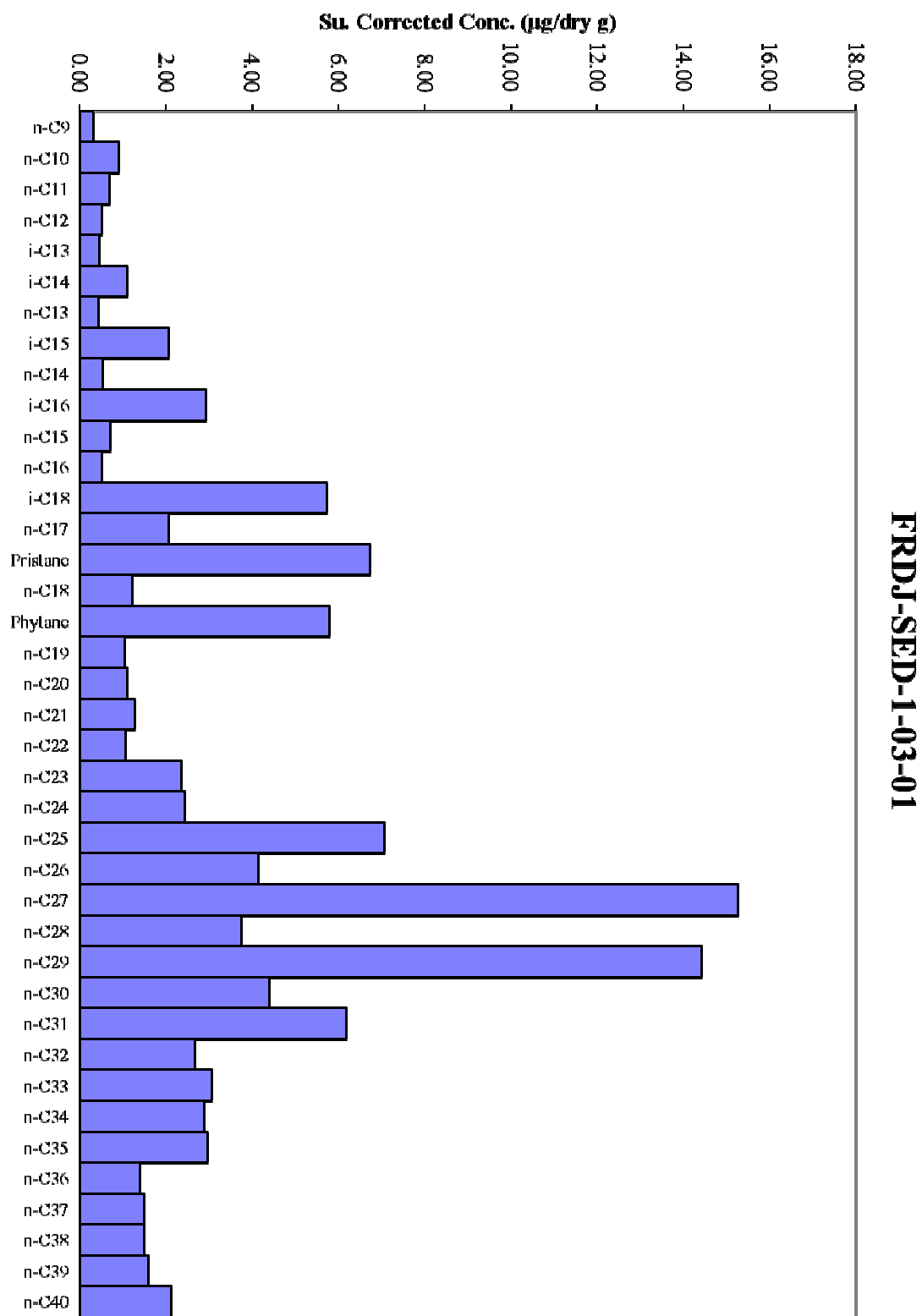


FRDJ-SED-1-02-12

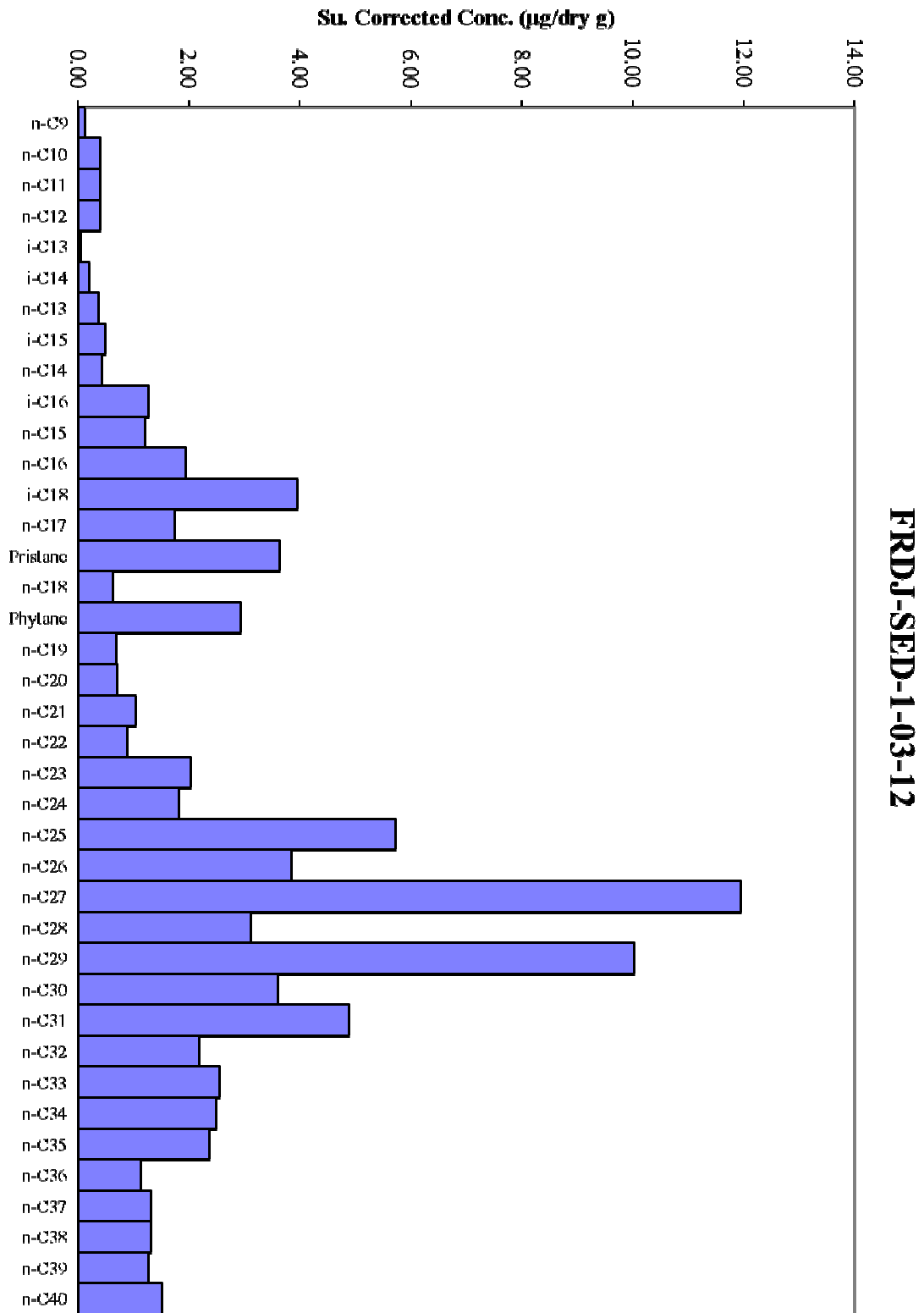
B-6



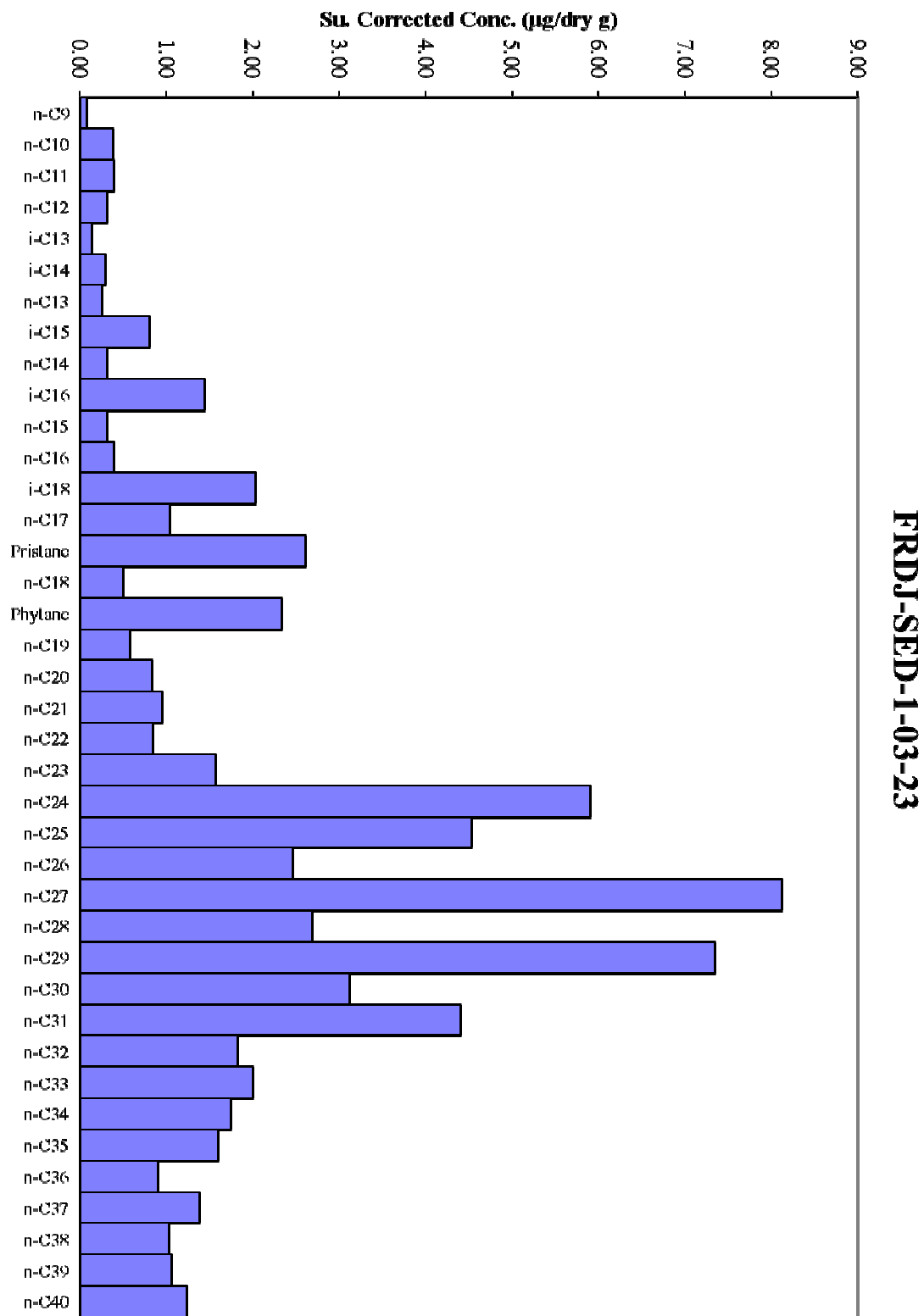
B-7



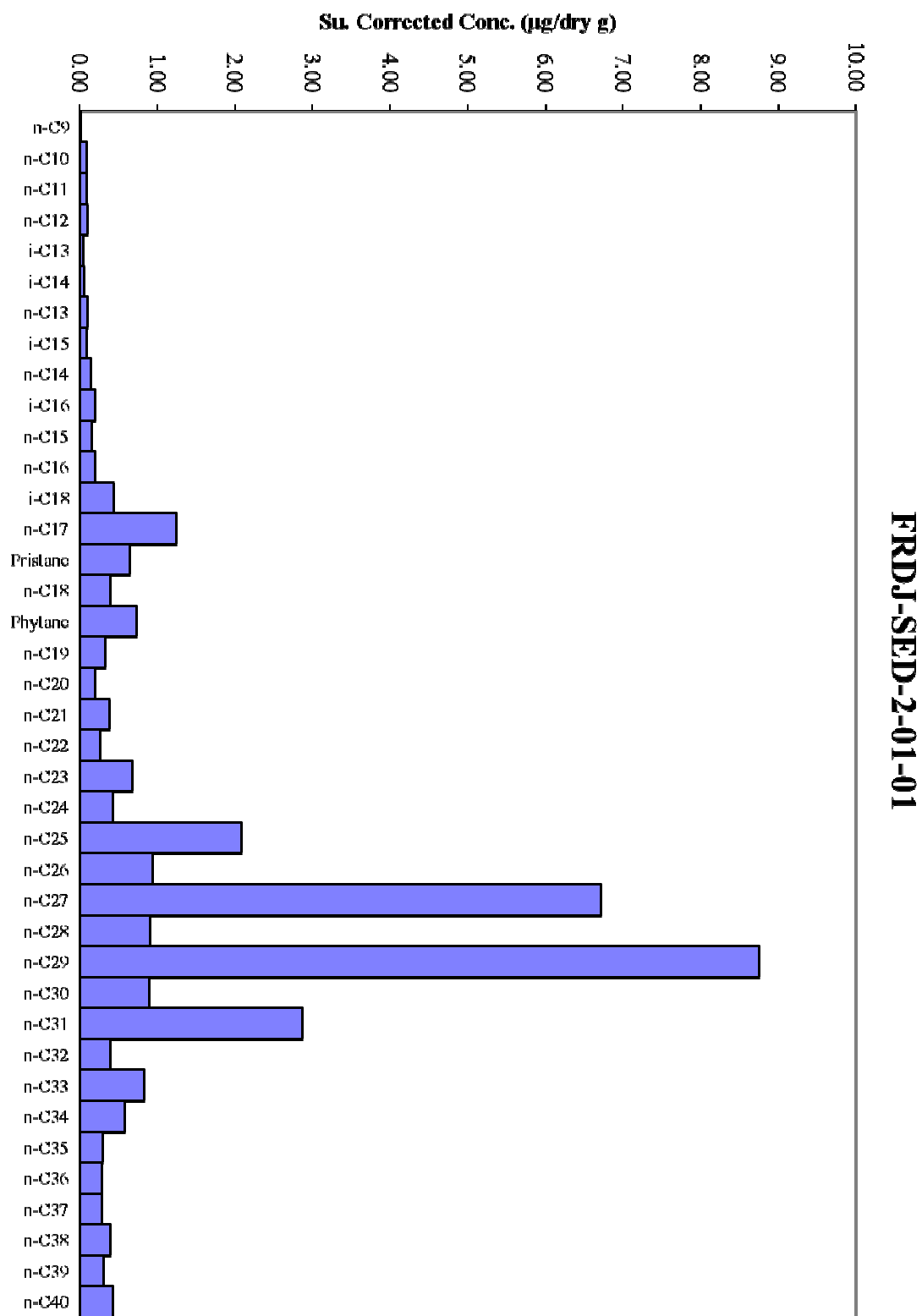
B-8



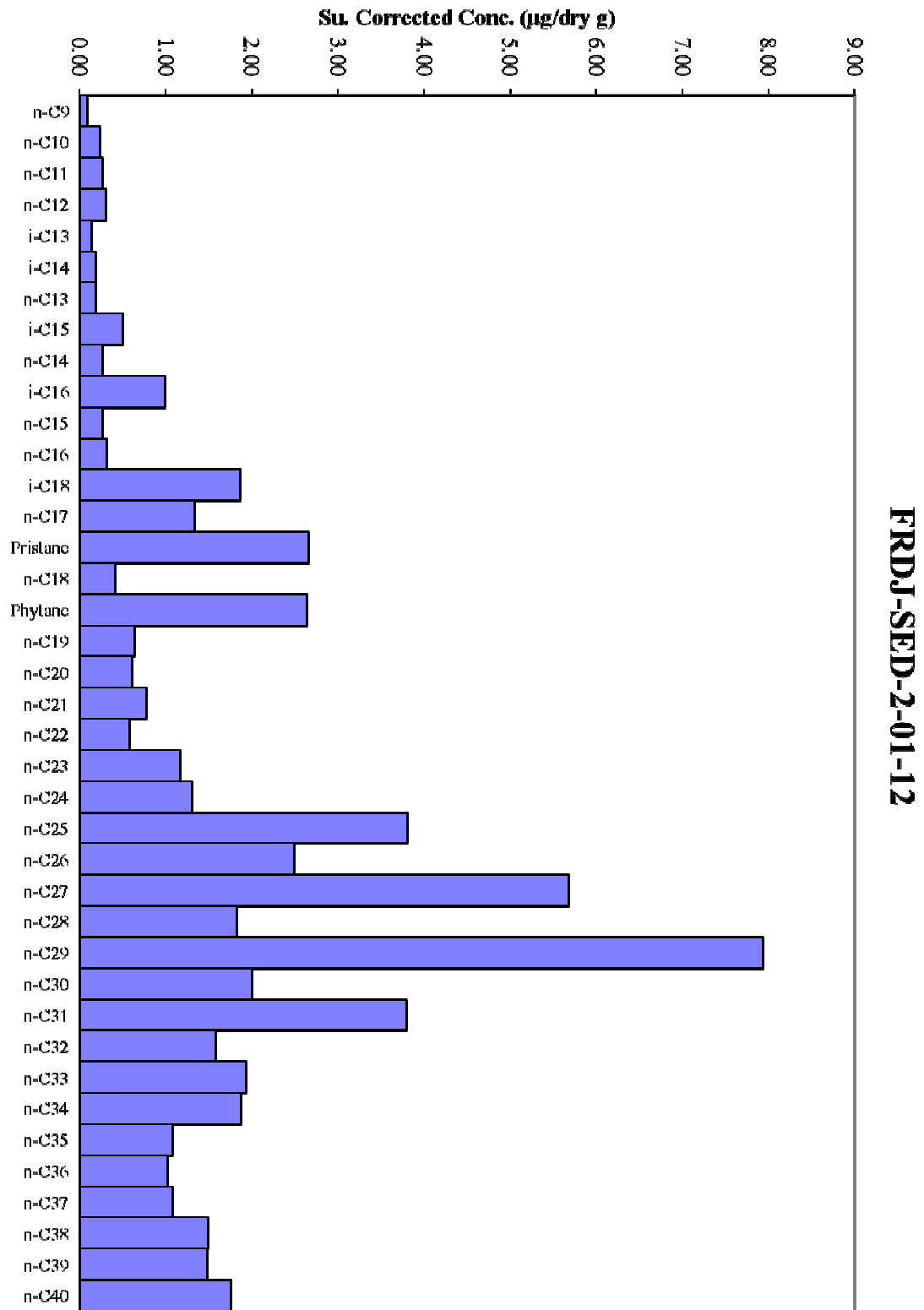
B-9



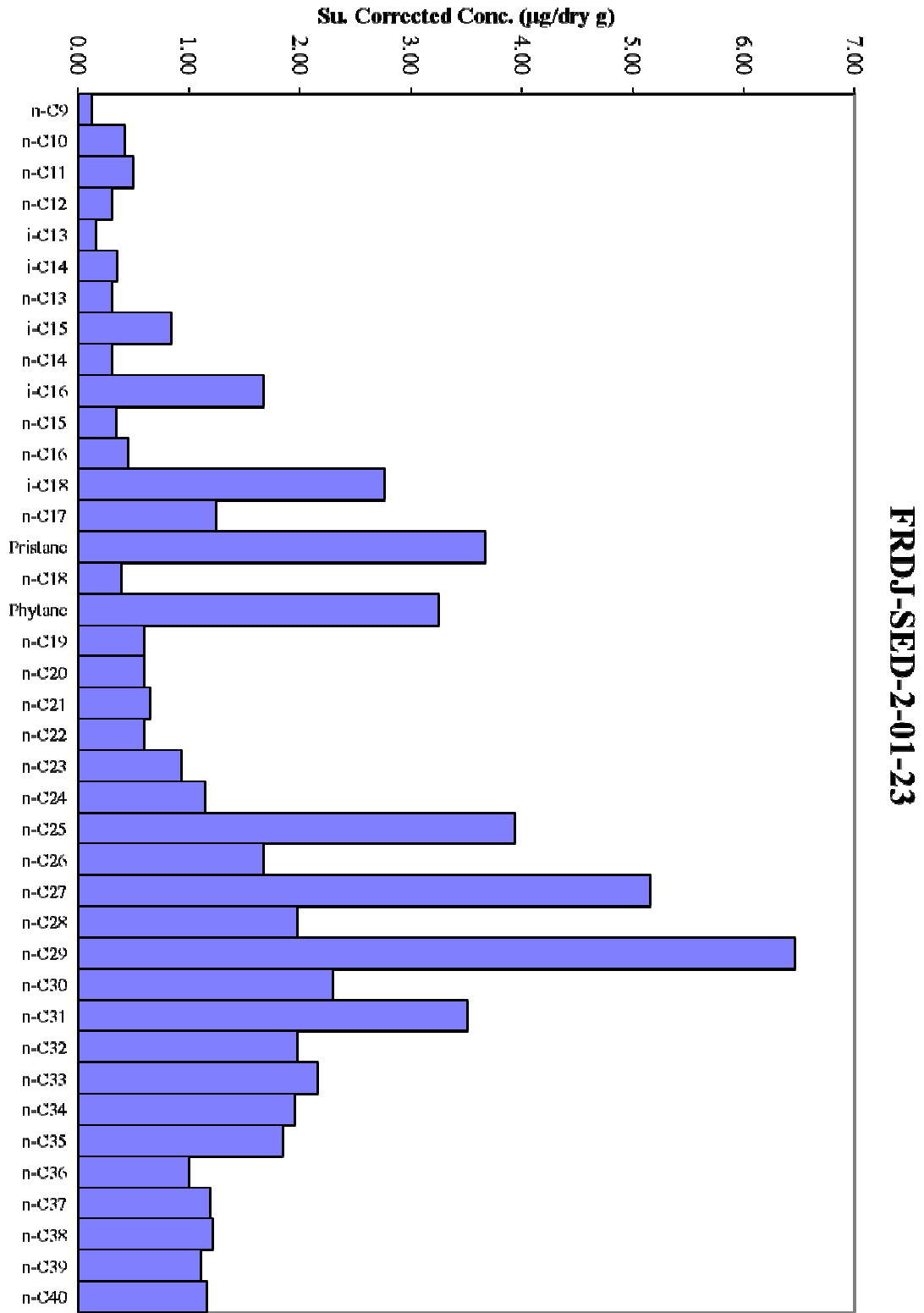
B-10



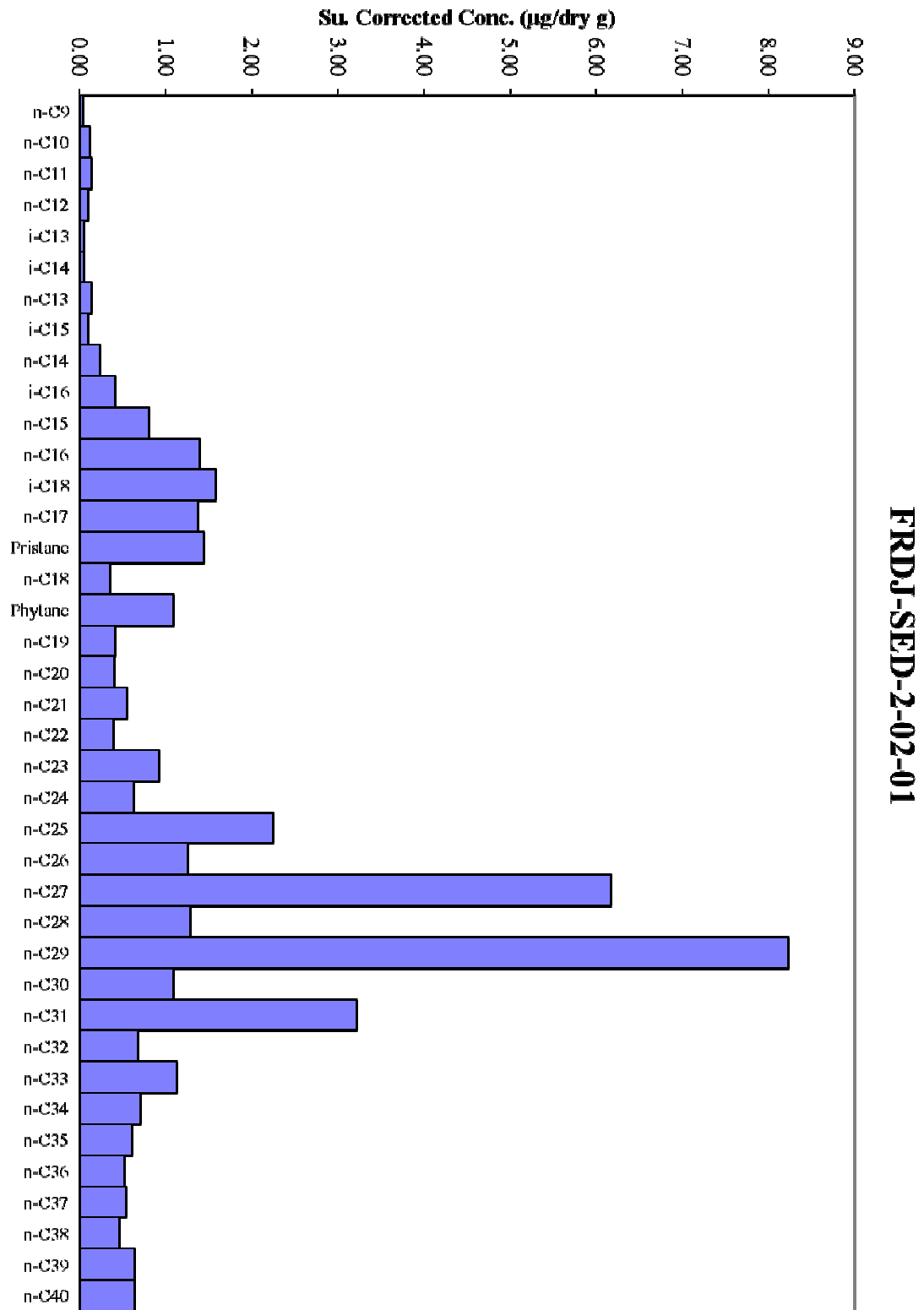
B-11



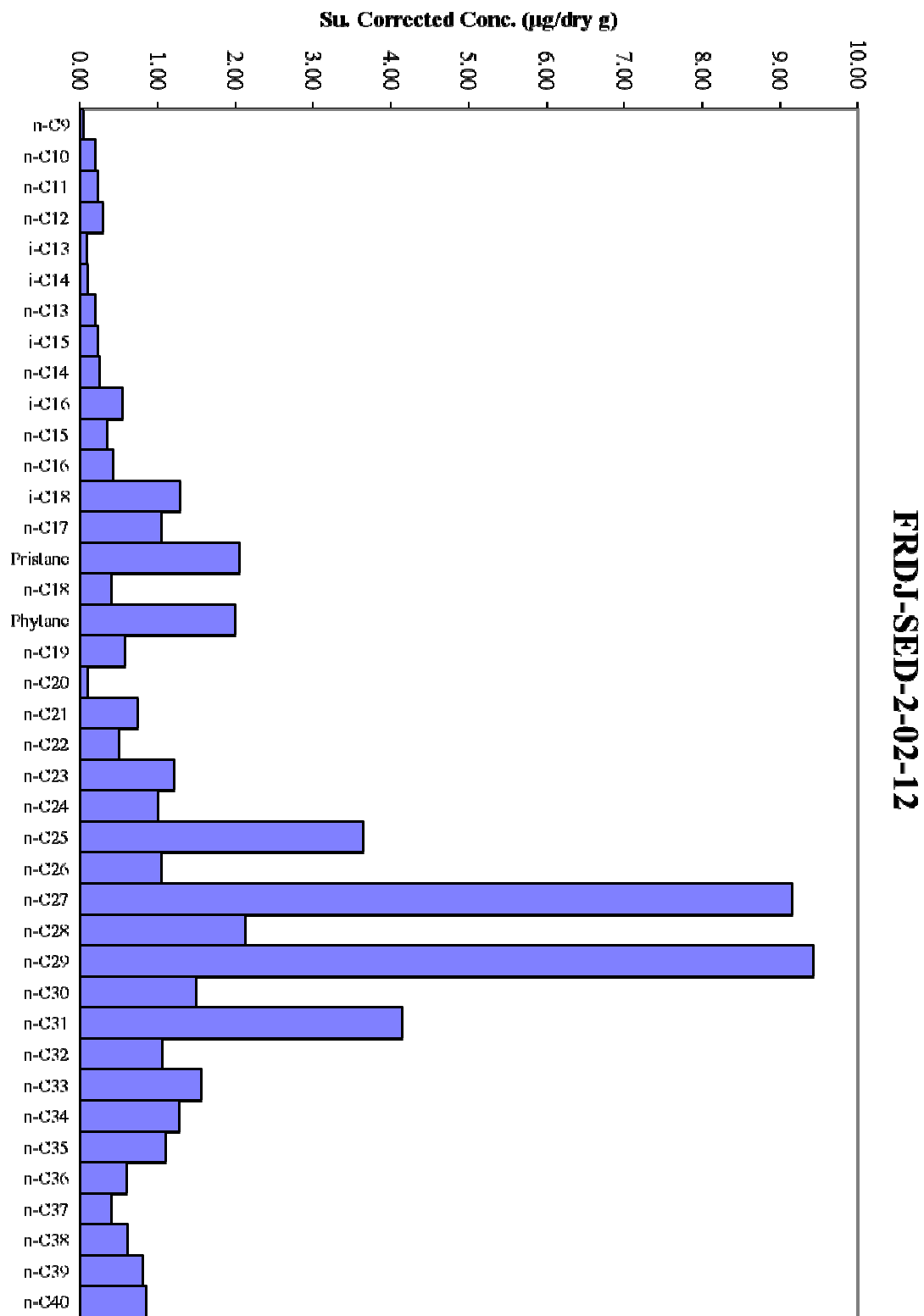
B-12



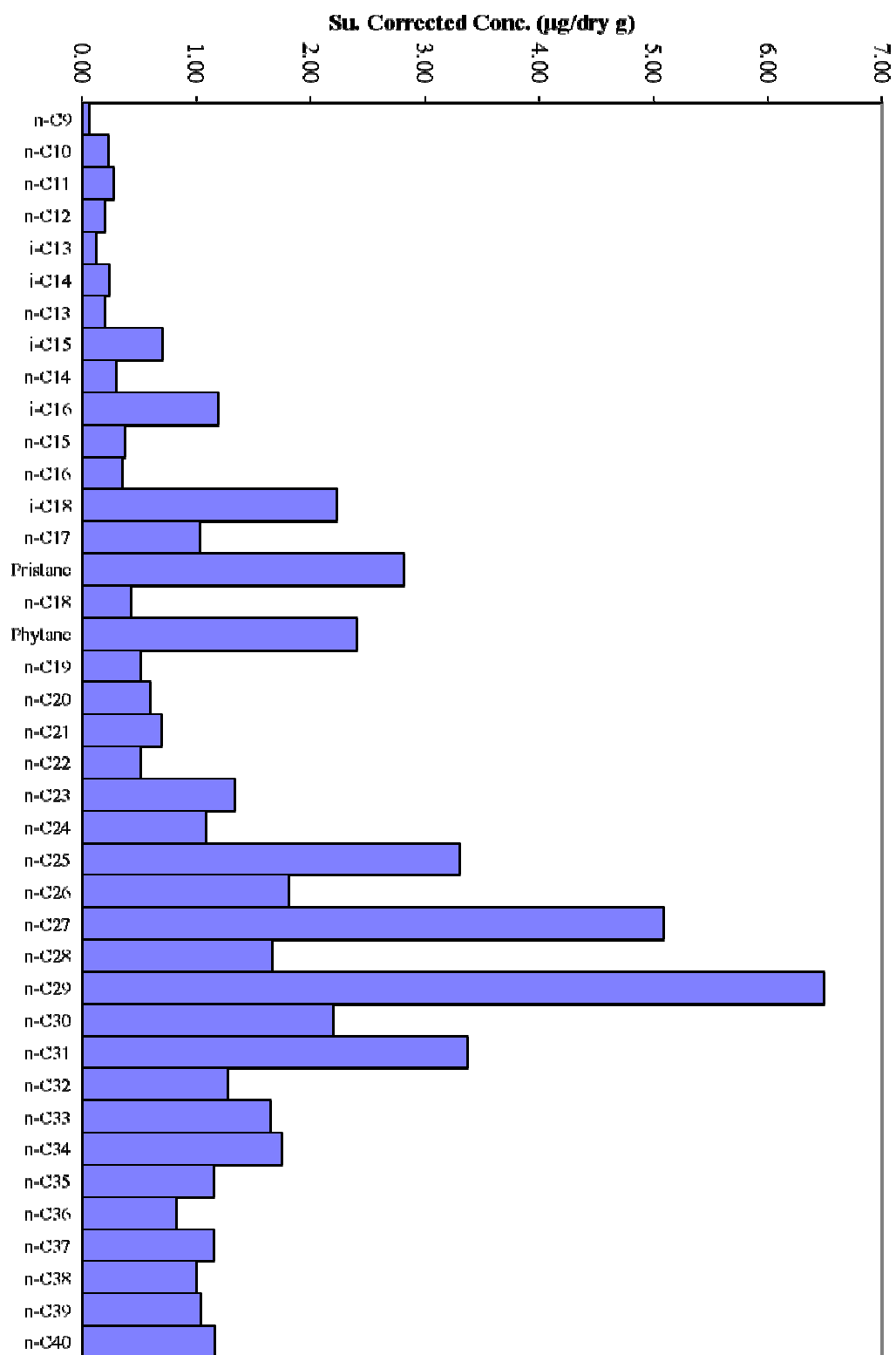
B-13



B-14

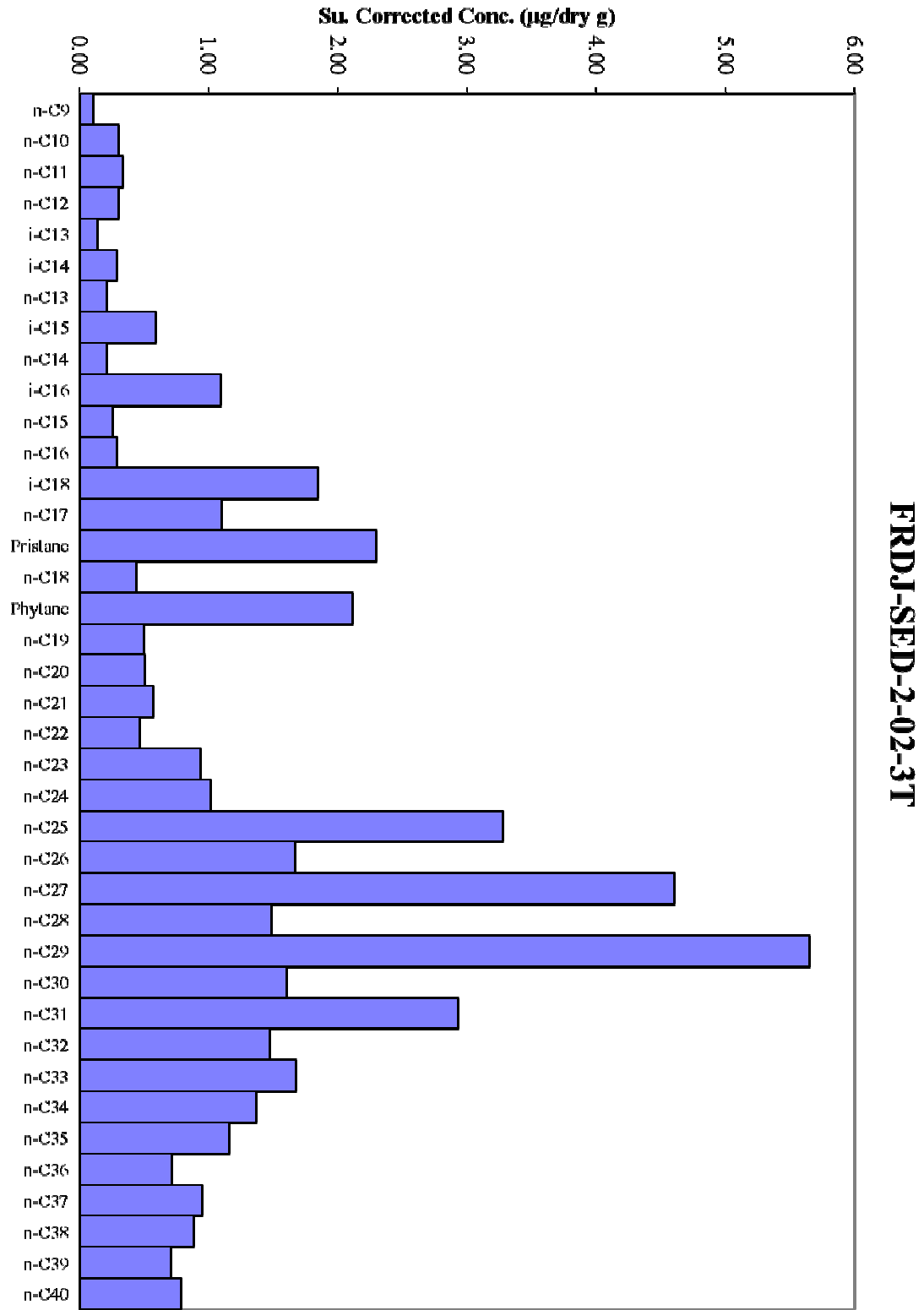


B-15

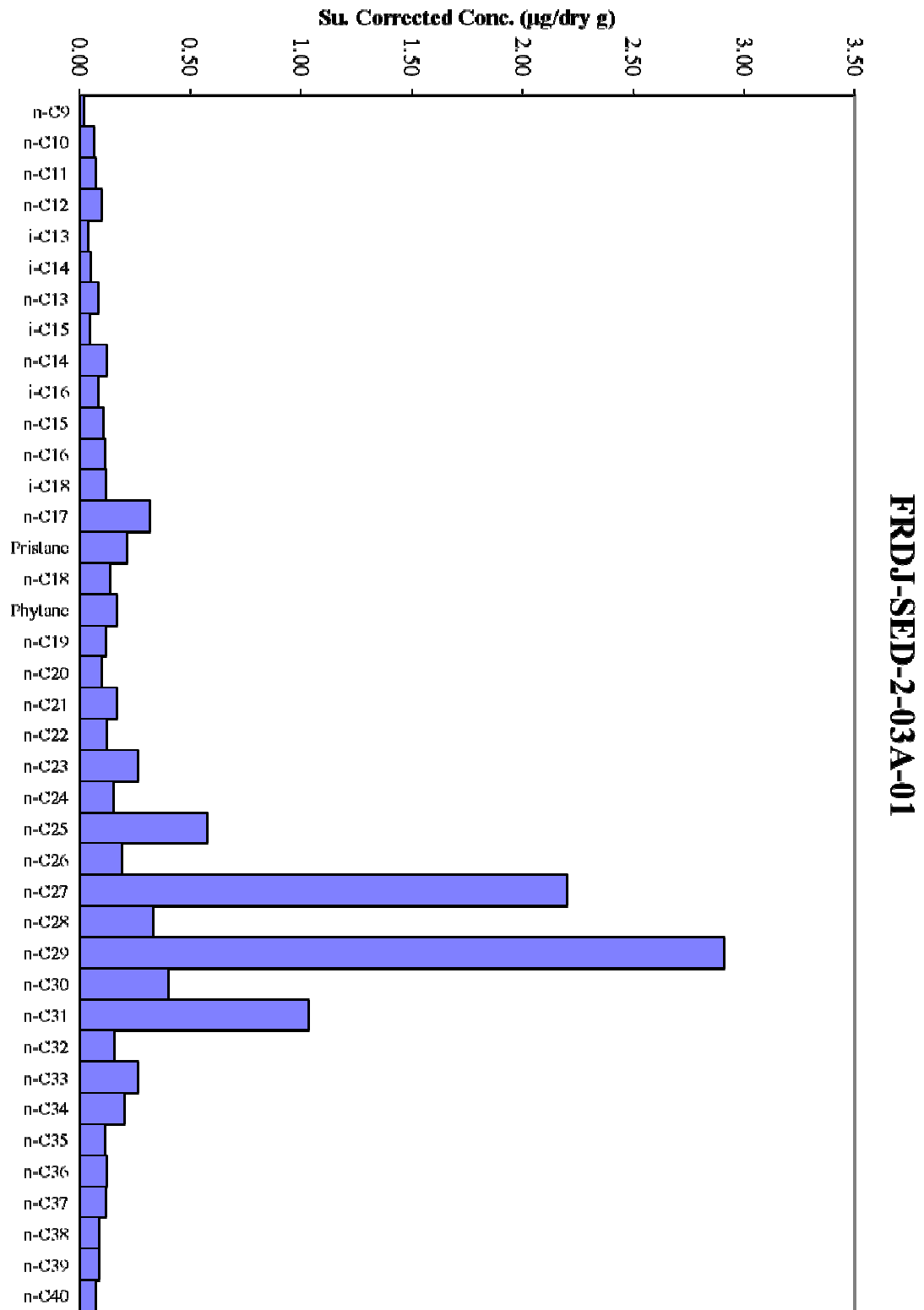


FRDJ-SED-2-02-23

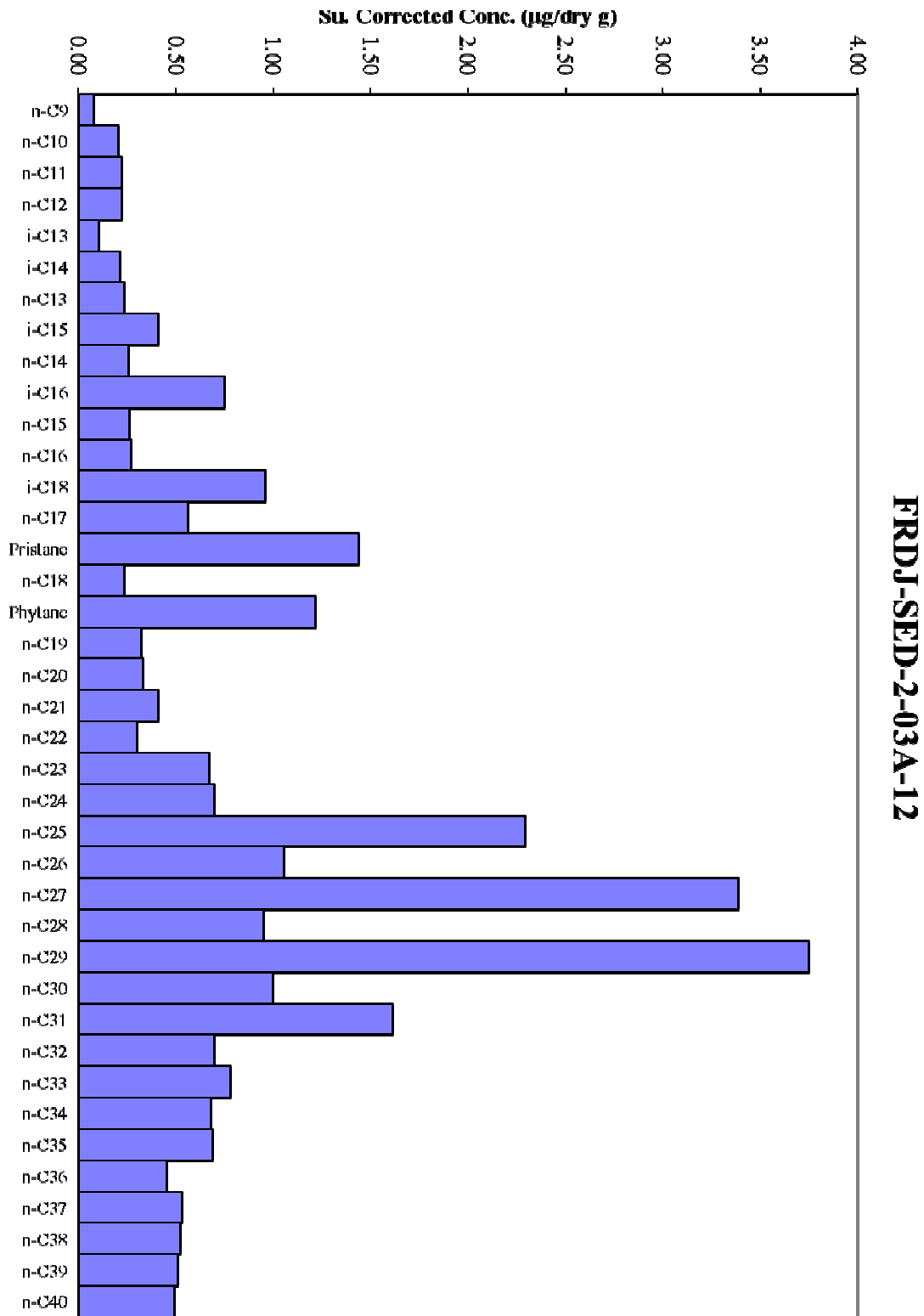
B-16



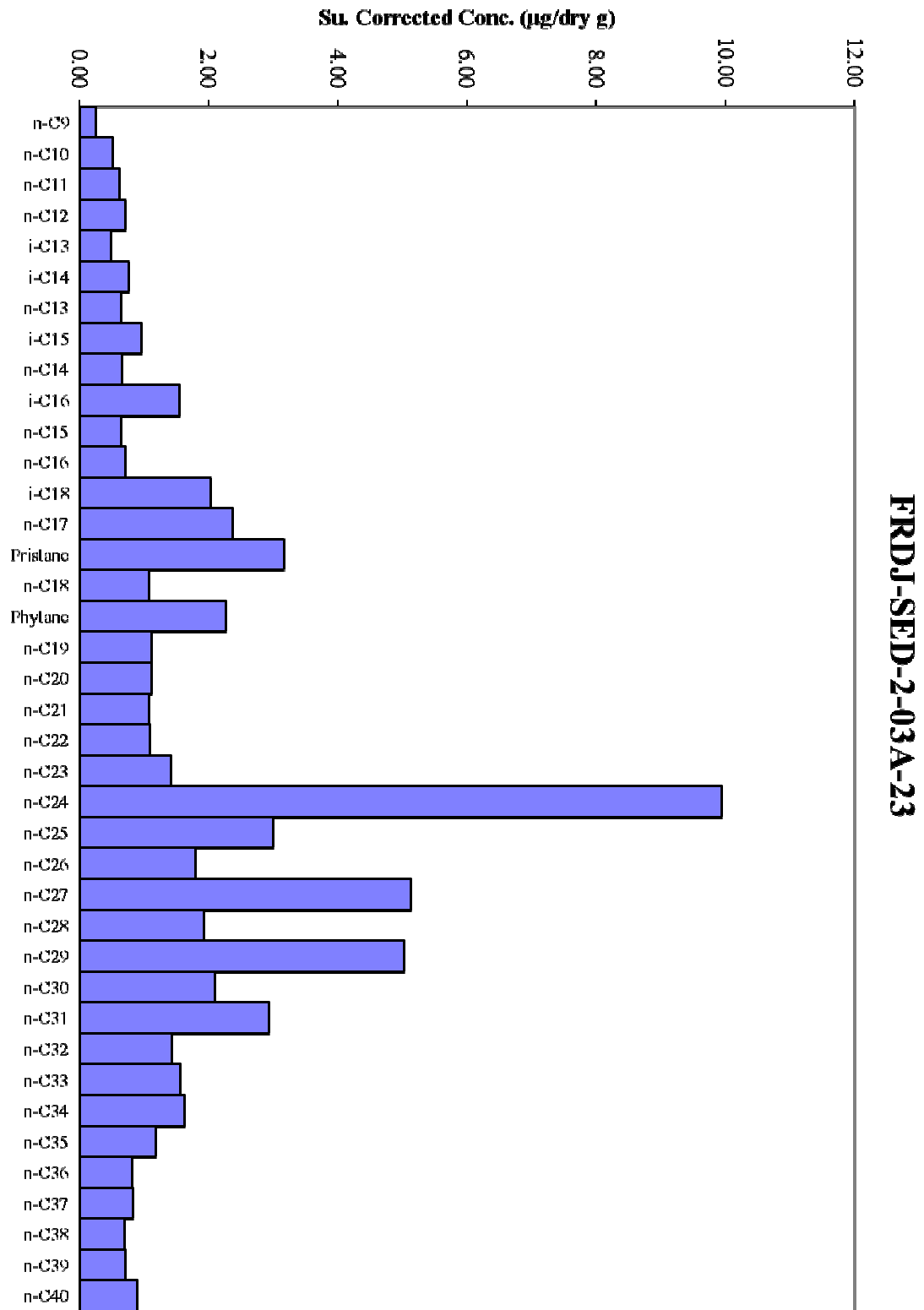
B-17



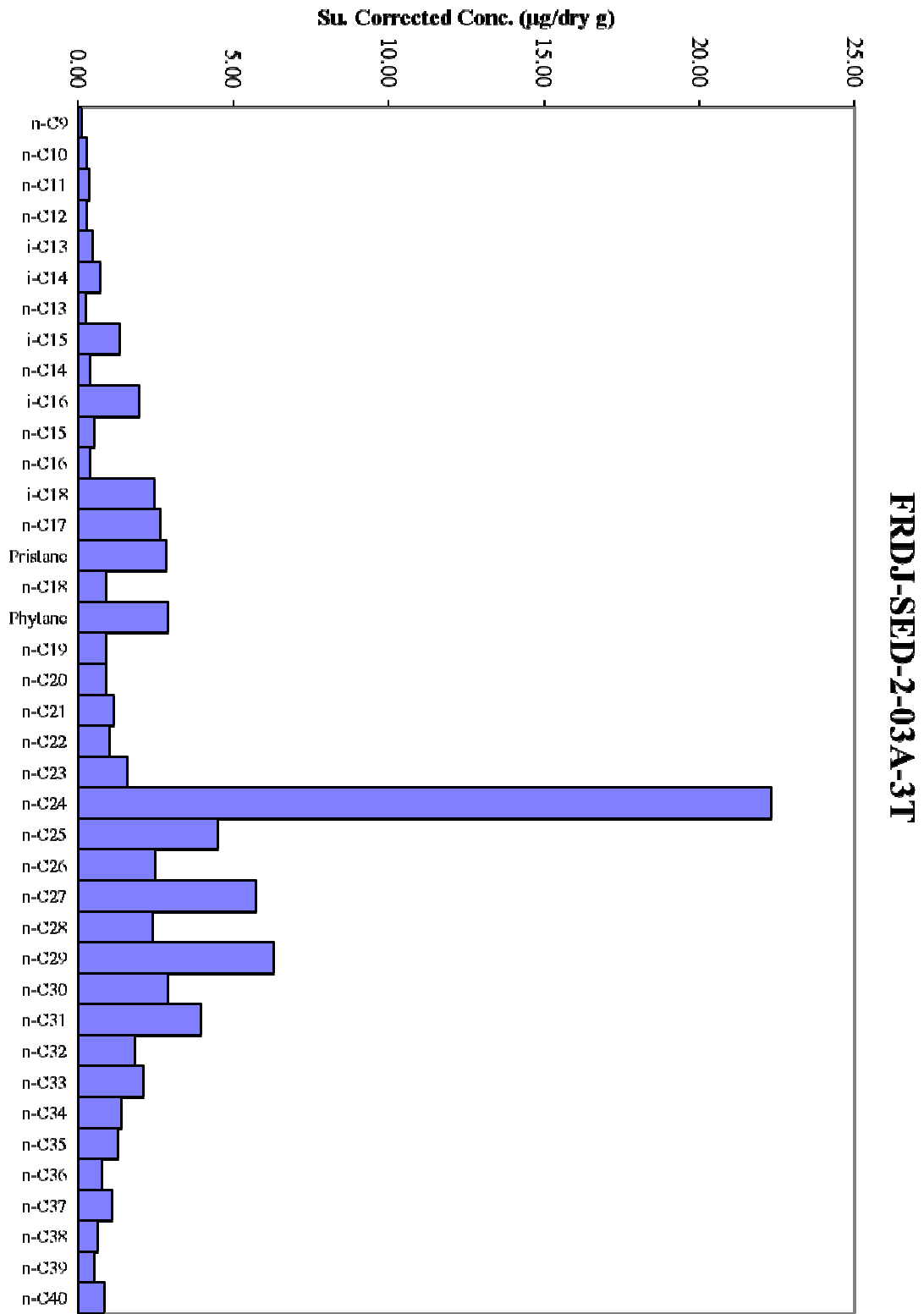
B-18



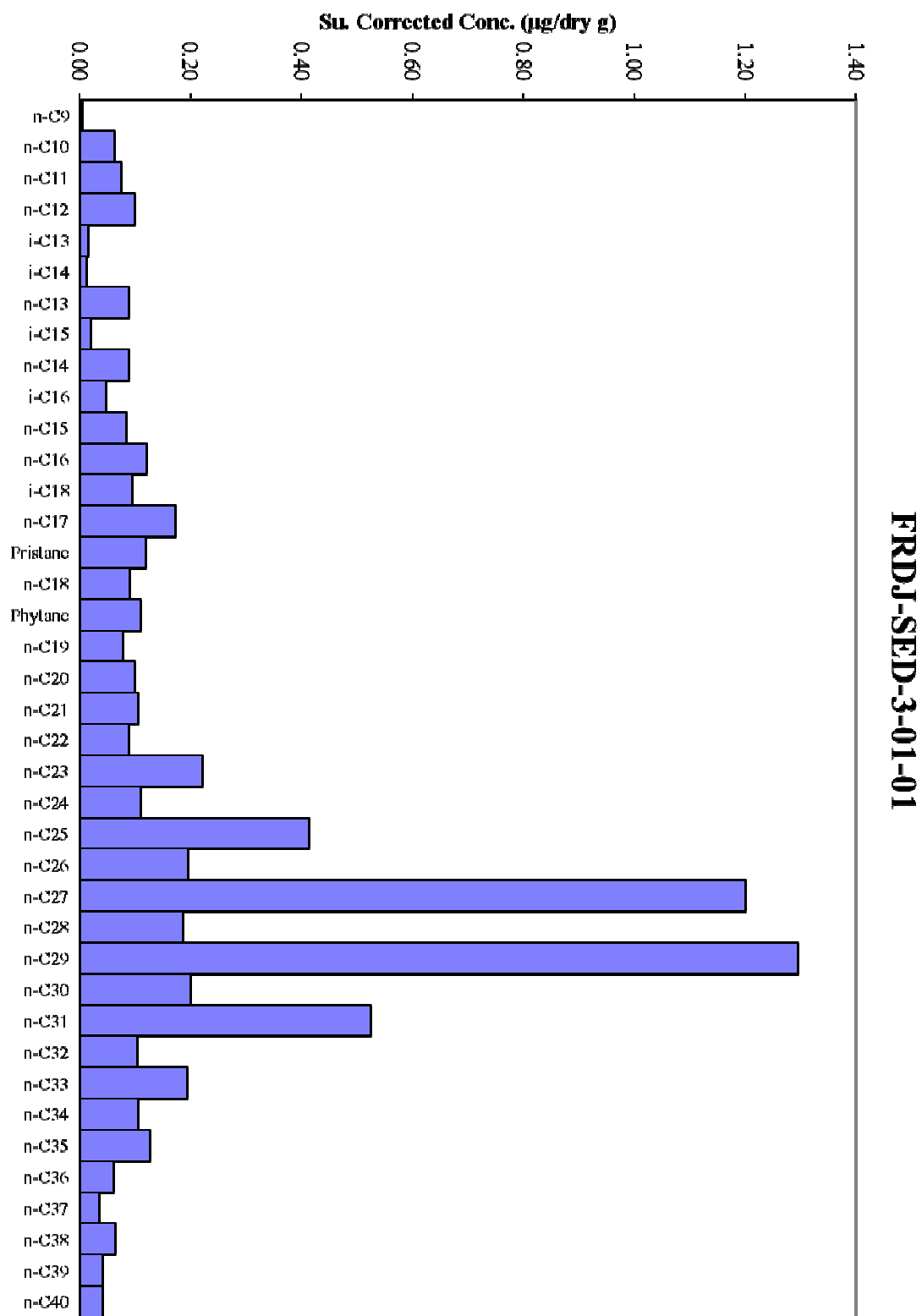
B-19



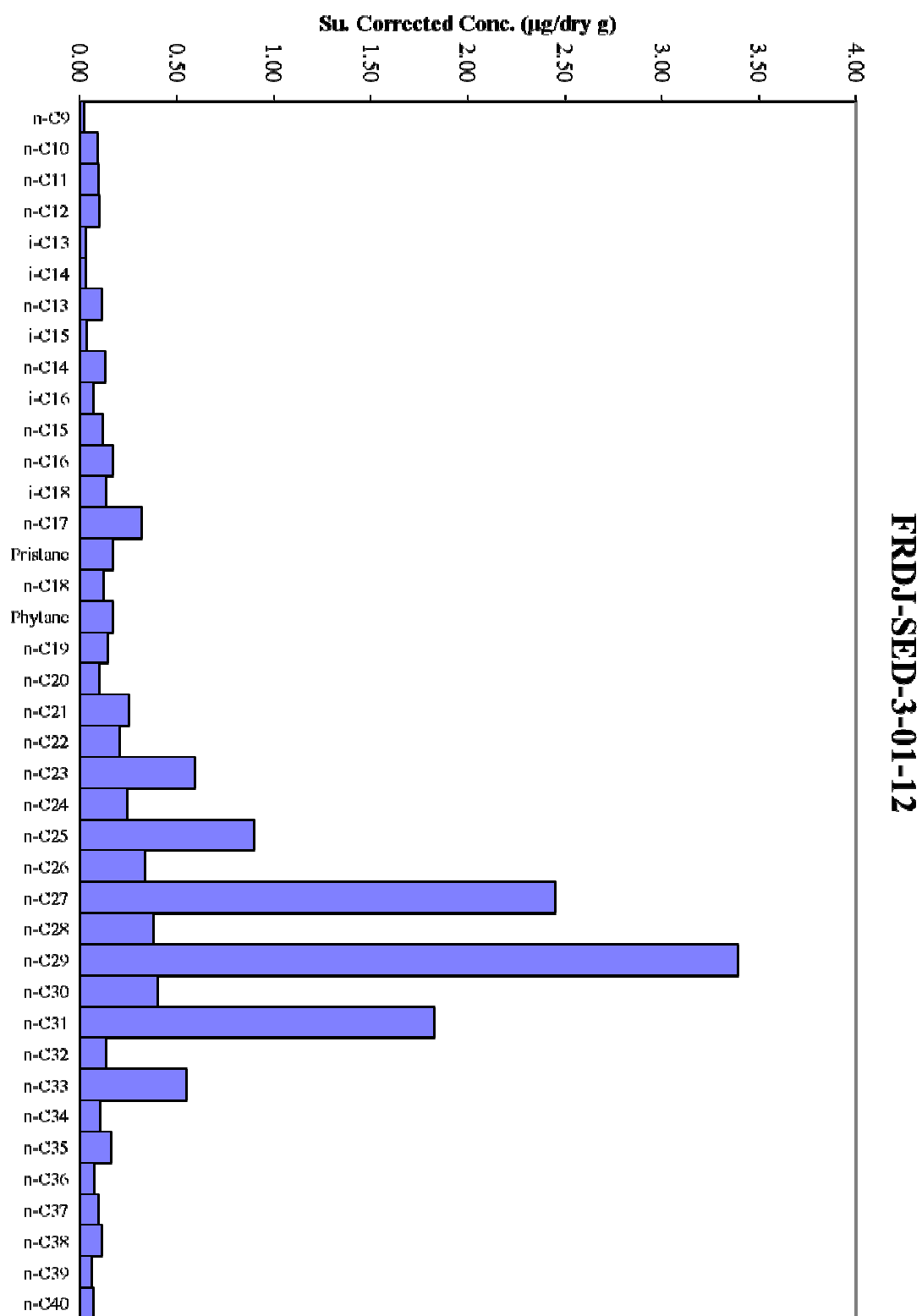
B-20



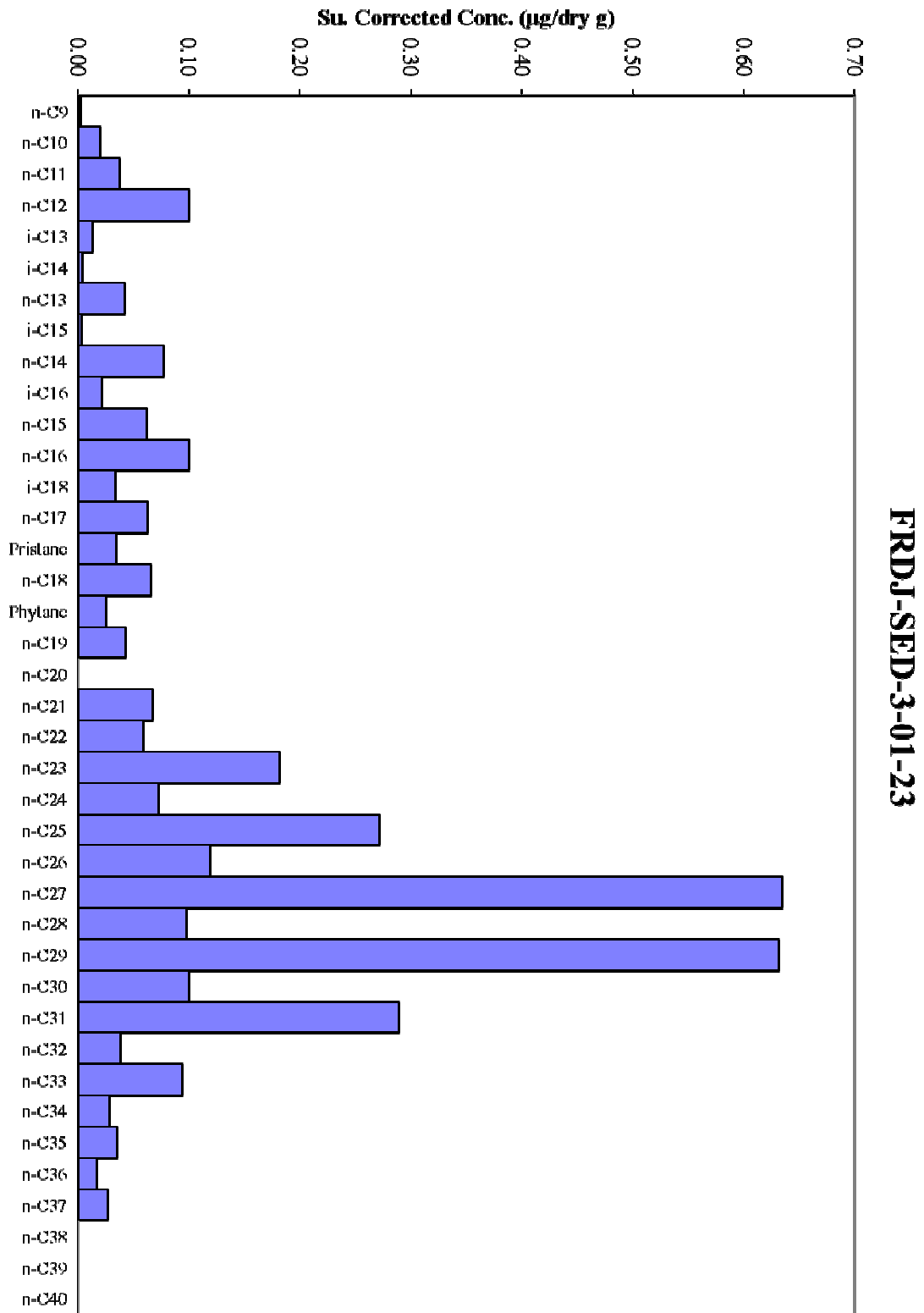
B-21



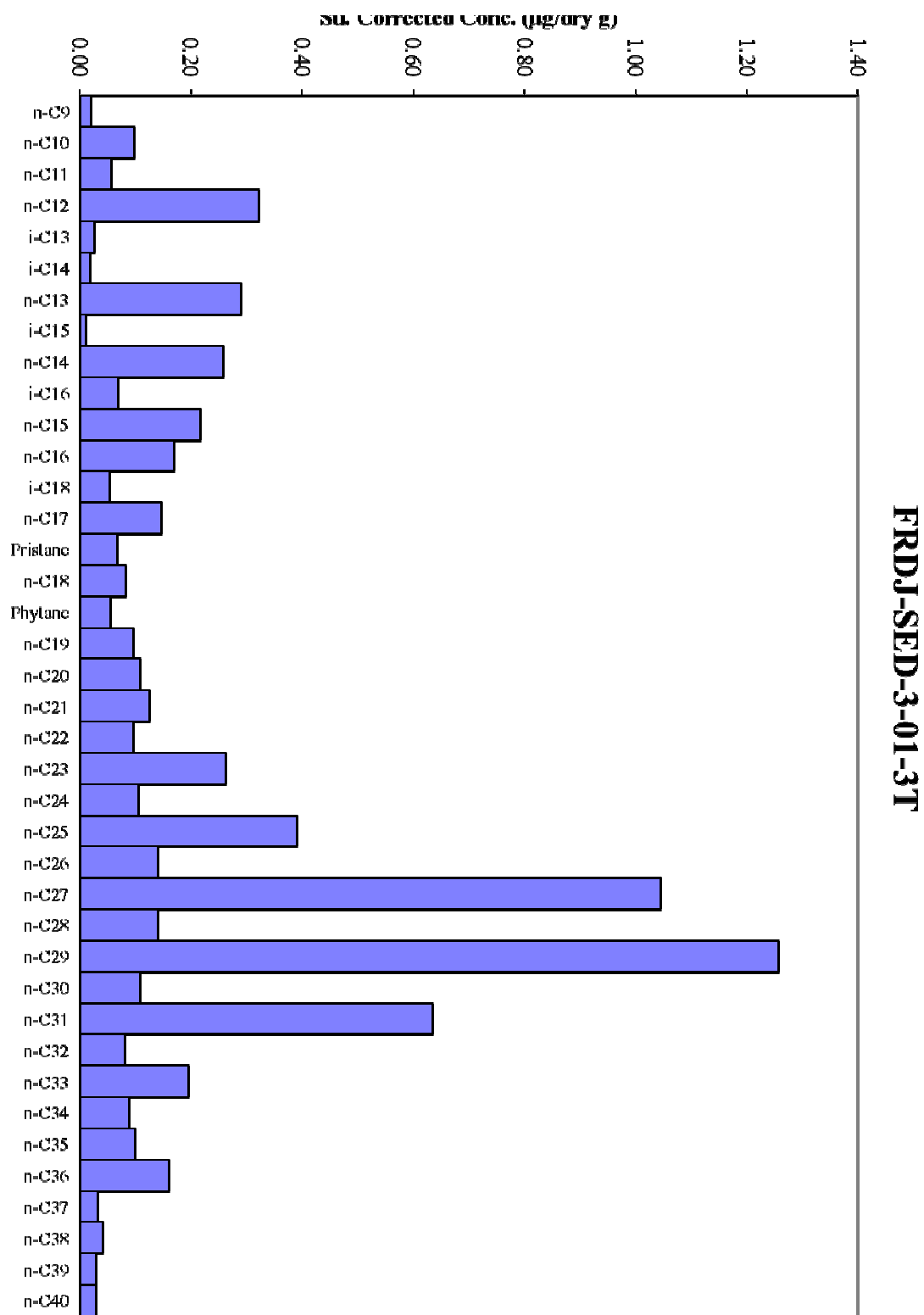
B-22



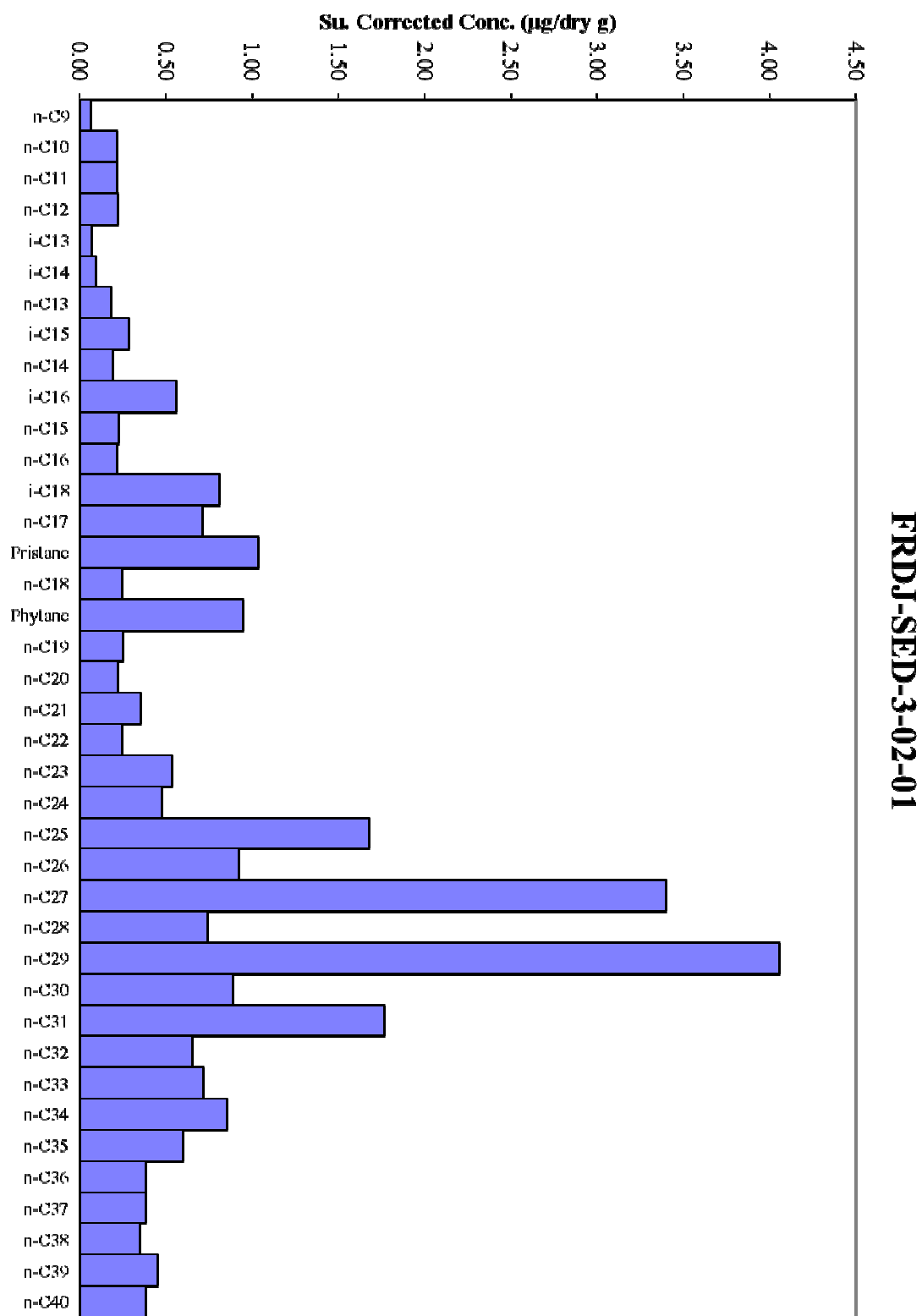
B-23



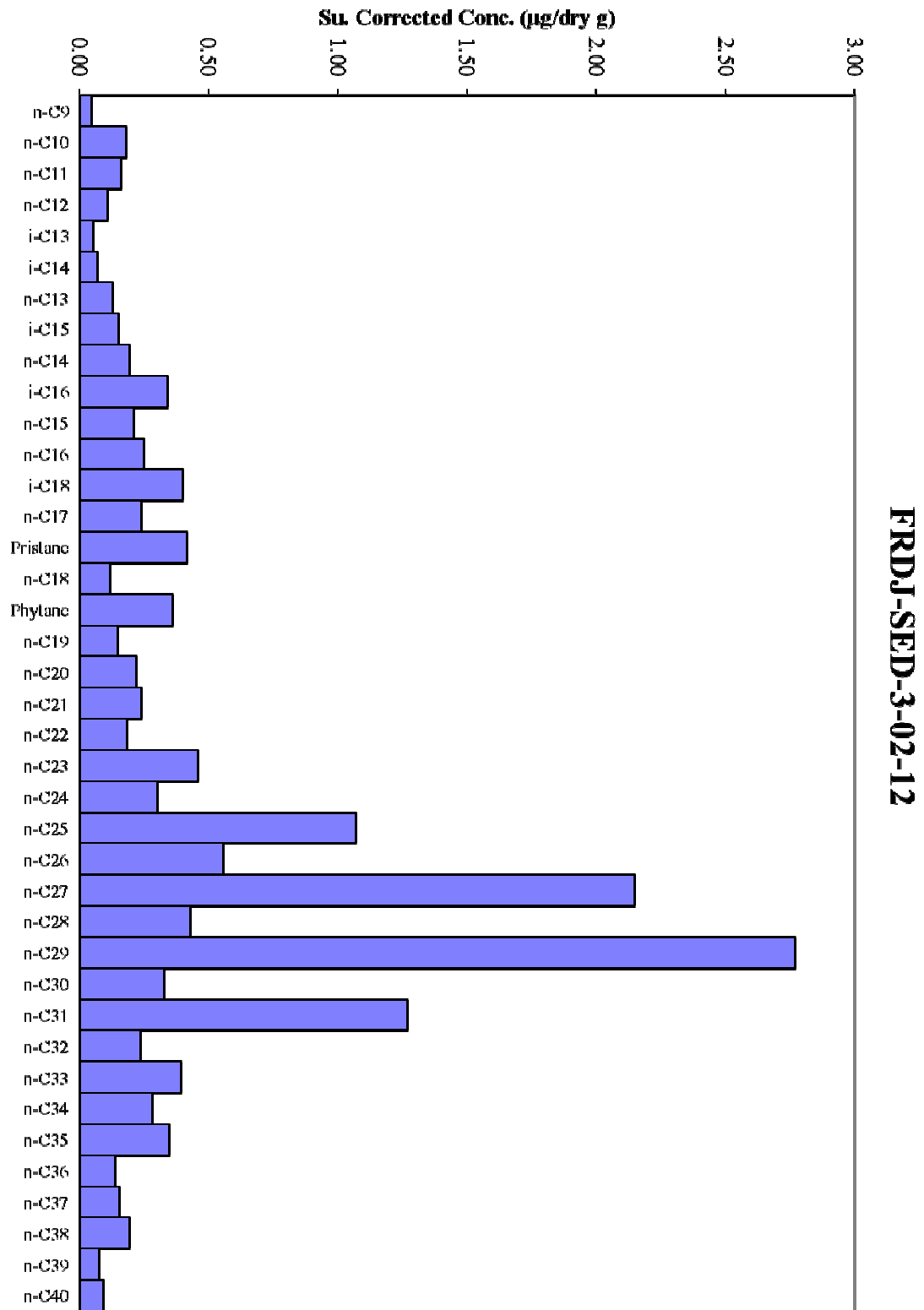
B-24



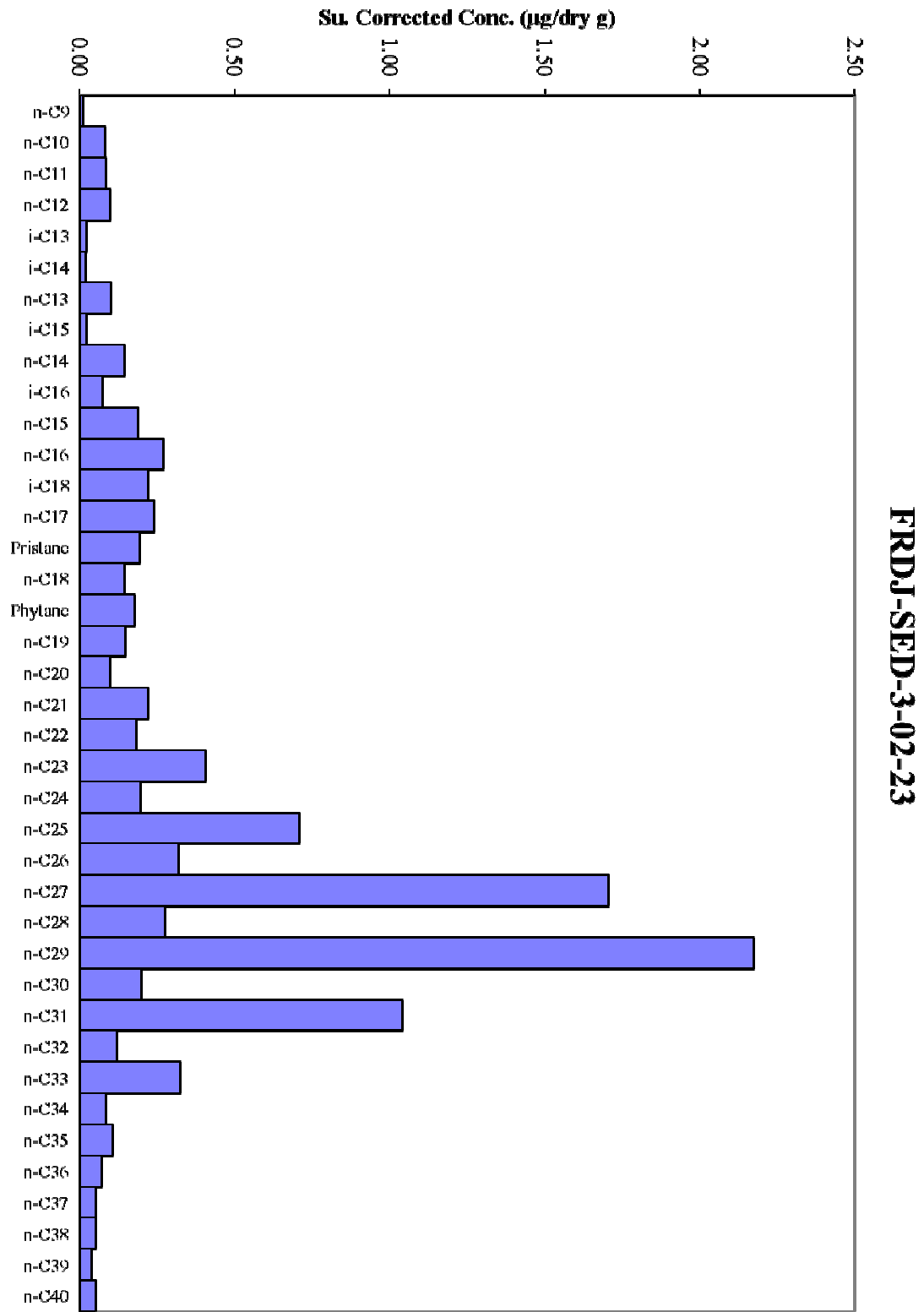
B-25



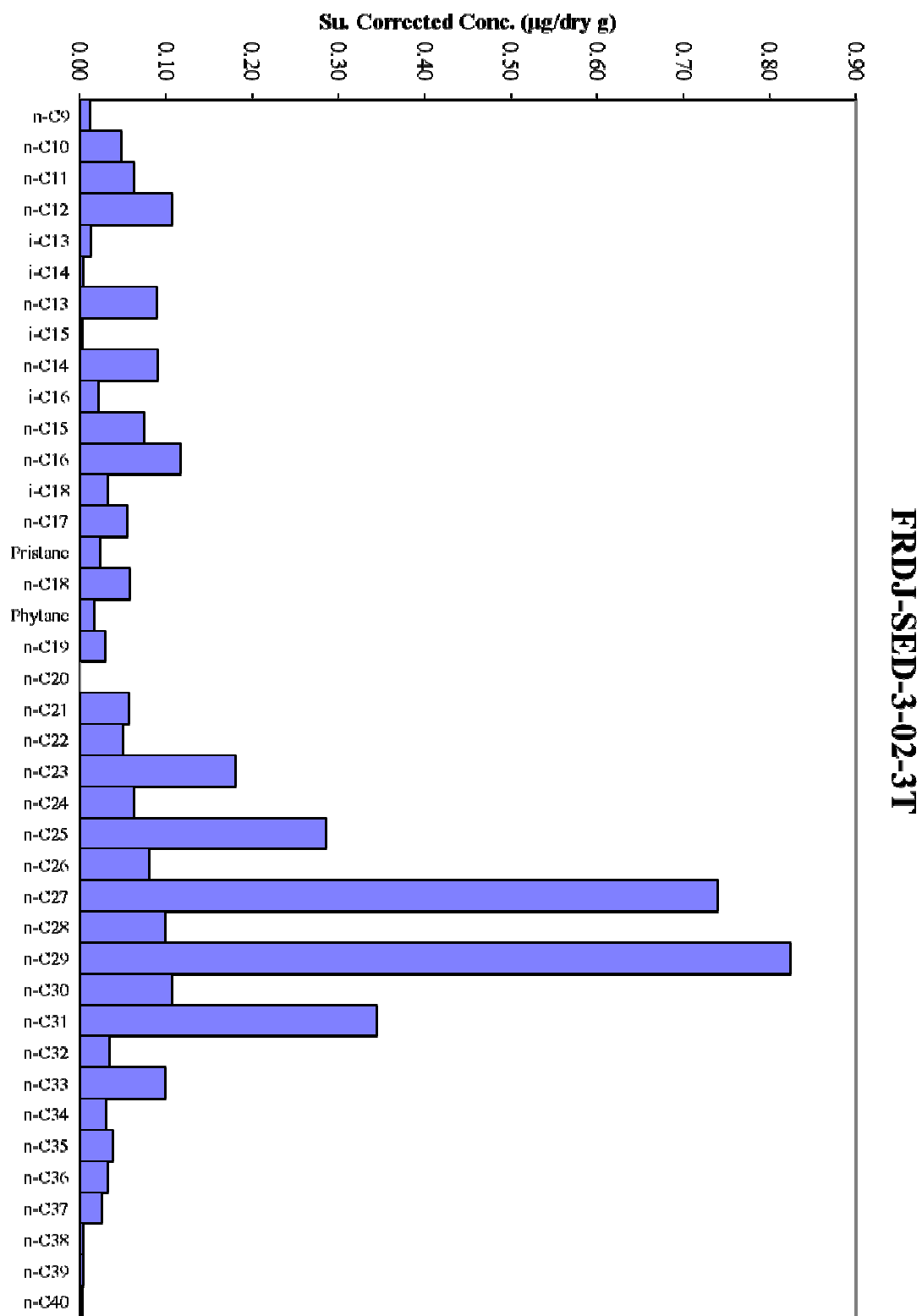
B-26



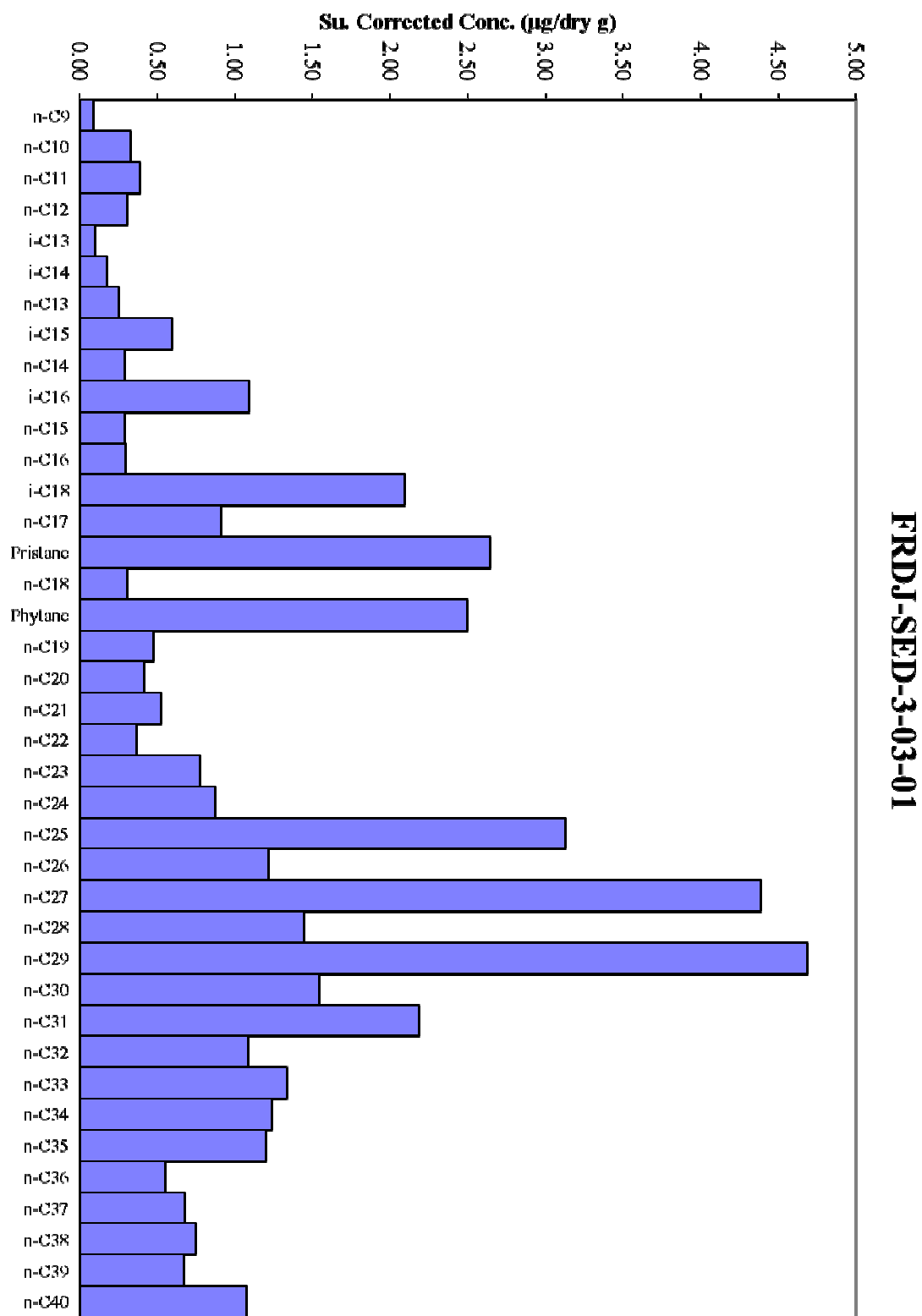
B-27



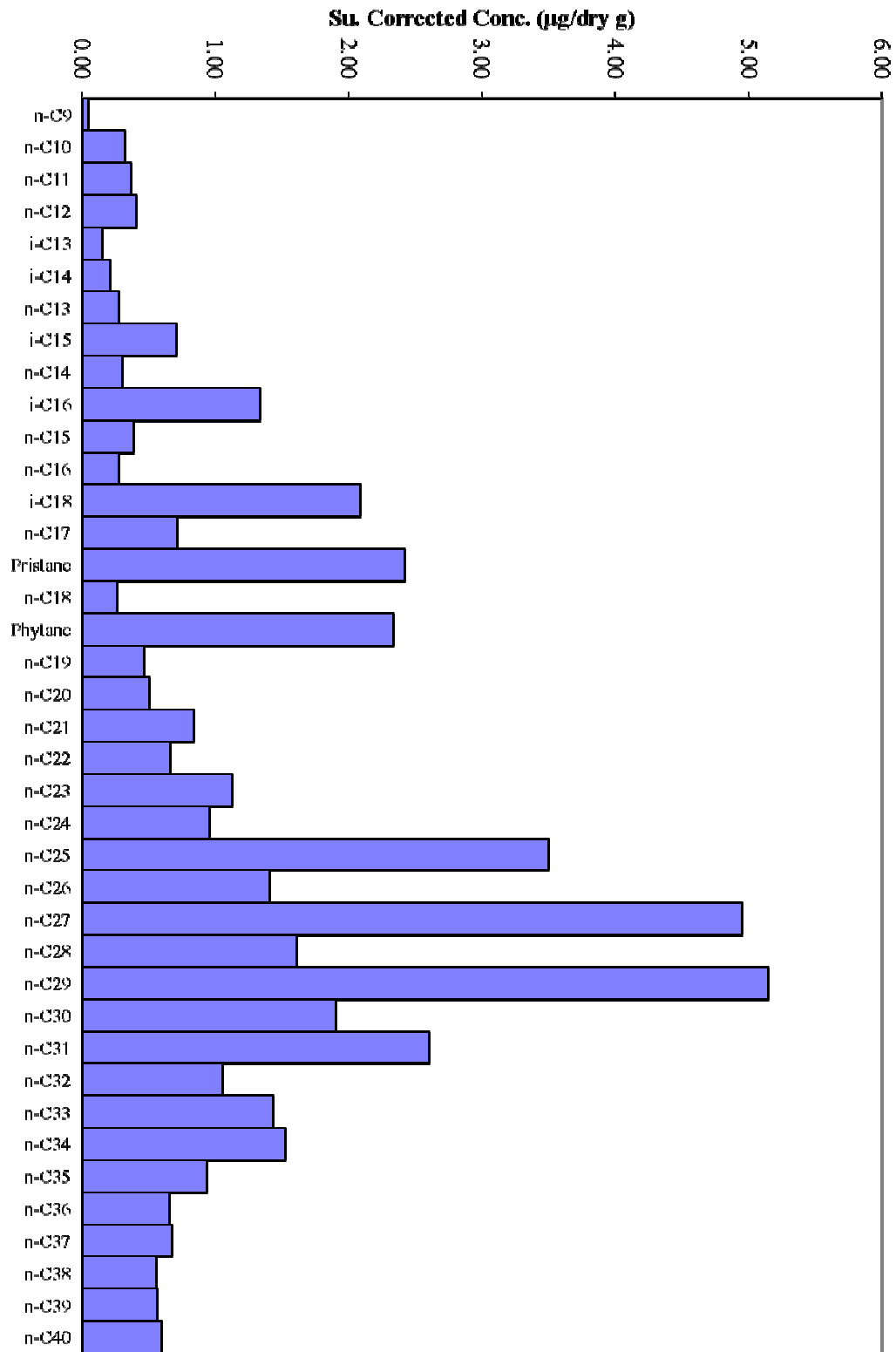
B-28



B-29

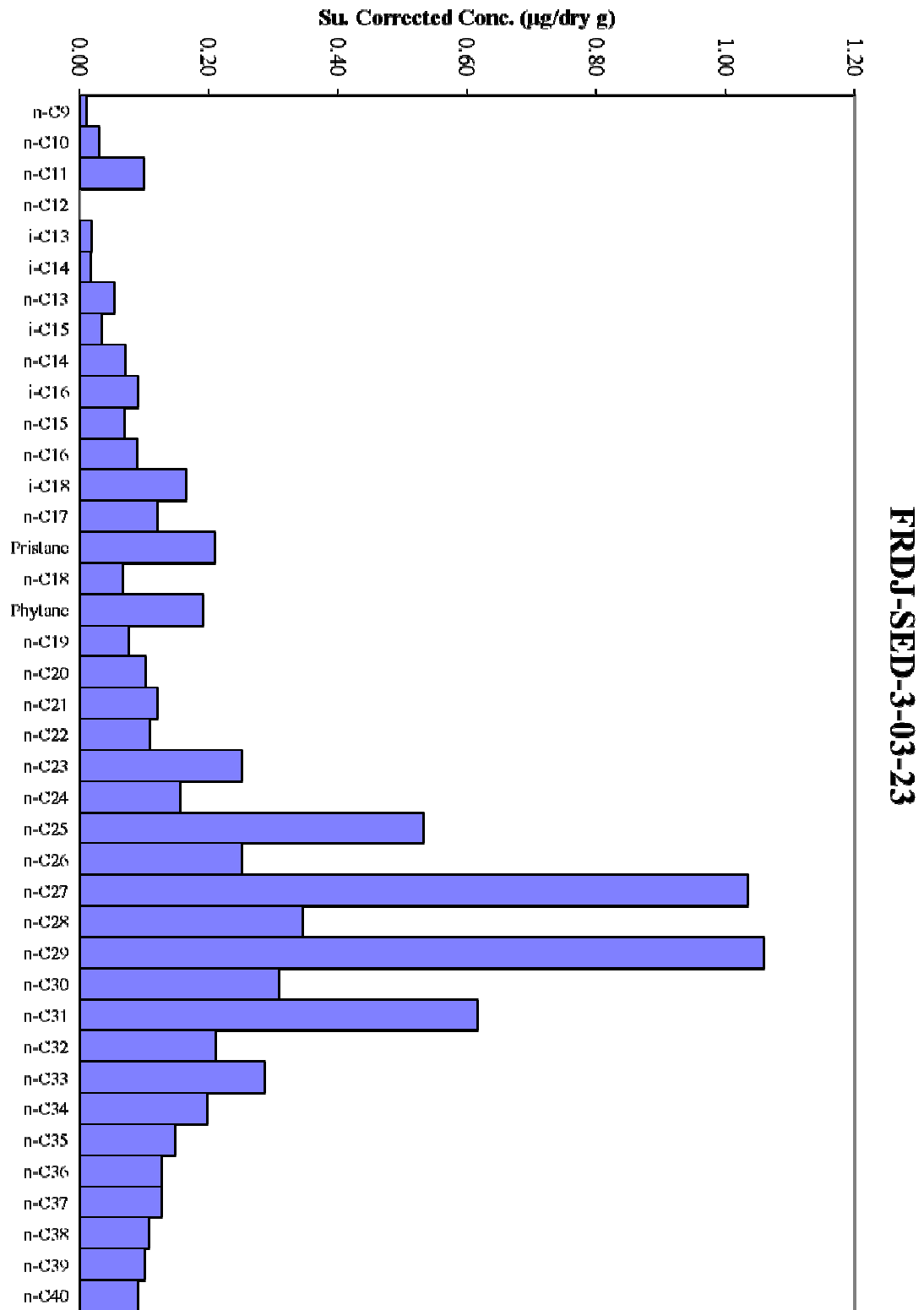


B-30

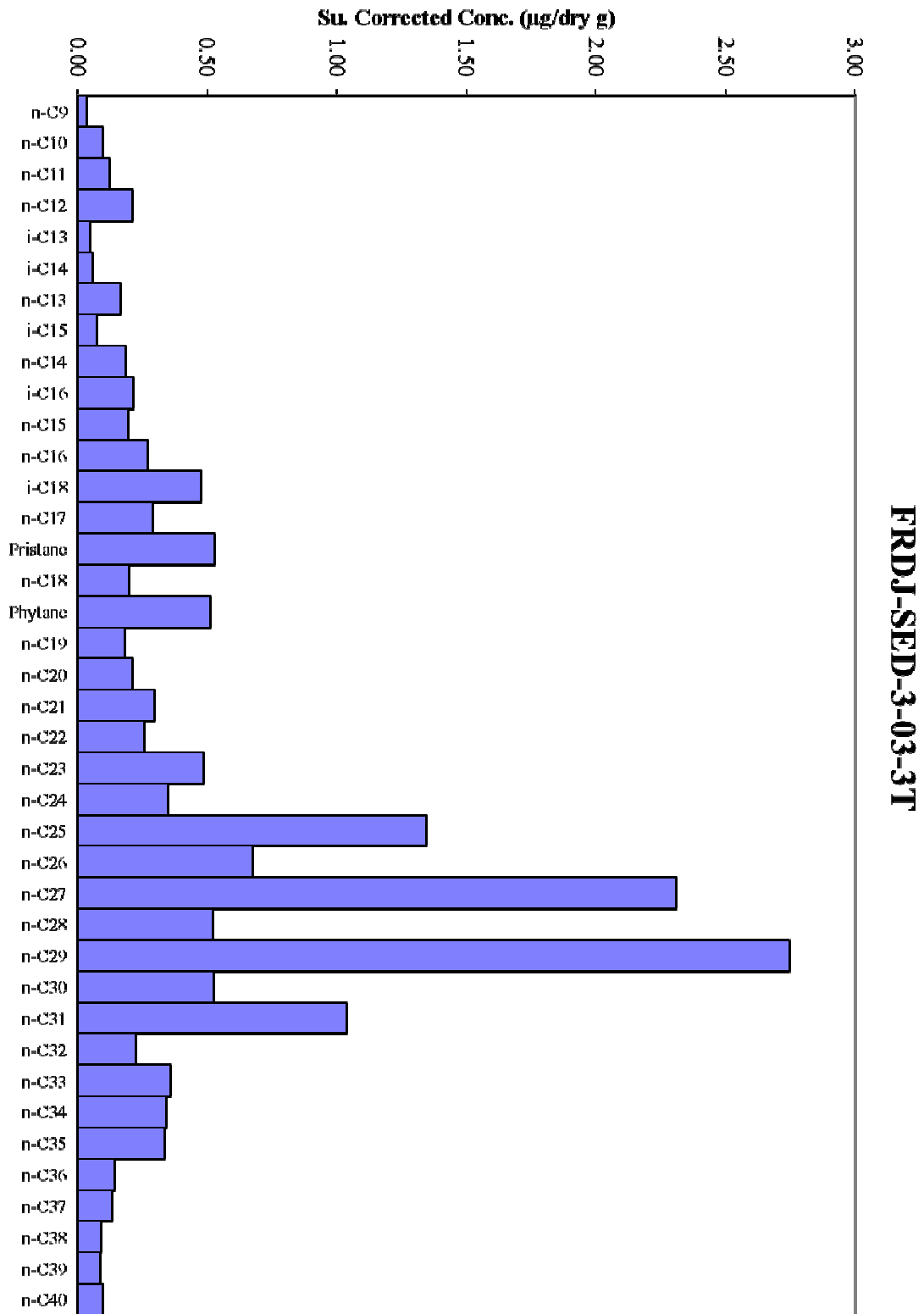


FRDJ-SED-3-03-12

B-31



B-32



B-33

